

Raman Optical Activity in the Ultraviolet Spectral Region

Philip J. Stephens Award Address

Josef Kapitán, Laurence D. Barron, Lutz Hecht



Palacký University
Olomouc



5th International Conference
on Vibrational Optical Activity

September 11-16, 2016

Overview of Raman scattering signal origin and instrumentation

DUV ROA spectrometer

Measurement of non-resonant and pre-resonant spectra
and their interpretation

Outlook for further development of DUV ROA spectrometer

Origin of Raman scattering signal

1. Raman scattering from a single molecule:
 - wavenumber of scattered radiation
 - geometry of scattering
 - polarization of excitation and scattered radiation
 - molecular properties

2. Raman scattering from a bulk sample - volume source of radiation

3. Properties of spectral analyzers:
 - optical throughput, étendue
 - spectral resolution
 - spectral range
 - efficiency (transmittance)
 - signal/noise, sources of noise

4. Optics for transfer of scattered radiation to spectral analyser

1. Raman scattering from a single molecule

Radiant intensity of Raman scattering from single molecule:

$$I \equiv \frac{d\Phi}{d\Omega} = \beta E_0$$

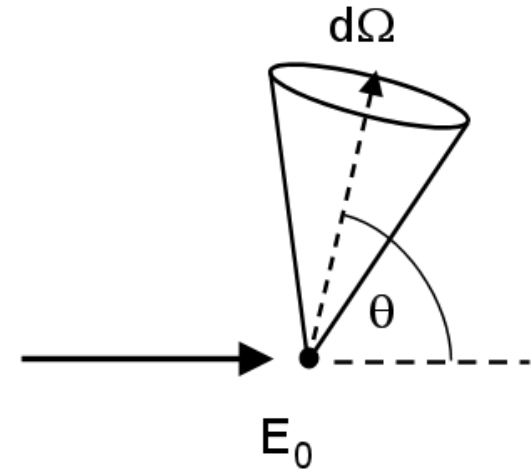
[W sr⁻¹] Irradiance [W cm⁻²]

Differential Raman scattering cross-section:

$$\beta \equiv \frac{d\sigma}{d\Omega} = k_{\nu} \tilde{\nu}_s^4 F(\theta, p_i, p_s, T_{fi})$$

[cm² sr⁻¹ molecule⁻¹]

also wavenumber dependent



$$\tilde{\alpha}_{\alpha\beta}(\omega_0) = \frac{1}{\hbar} \sum_{j \neq m, n} \left[\frac{\langle m | \hat{\mu}_{\alpha} | j \rangle \langle j | \hat{\mu}_{\beta} | n \rangle}{\omega_{jn} - \omega_0 - i\Gamma_j} + \frac{\langle m | \hat{\mu}_{\beta} | j \rangle \langle j | \hat{\mu}_{\alpha} | n \rangle}{\omega_{jm} + \omega_s + i\Gamma_j} \right]$$

$$\tilde{G}_{\alpha\beta}(\omega_0) = \frac{1}{\hbar} \sum_{j \neq m, n} \left[\frac{\langle m | \hat{\mu}_{\alpha} | j \rangle \langle j | \hat{m}_{\beta} | n \rangle}{\omega_{jn} - \omega_0 - i\Gamma_j} + \frac{\langle m | \hat{m}_{\beta} | j \rangle \langle j | \hat{\mu}_{\alpha} | n \rangle}{\omega_{jn} + \omega_s + i\Gamma_j} \right]$$

$$\tilde{A}_{\alpha, \beta\gamma}(\omega_0) = \frac{1}{\hbar} \sum_{j \neq m, n} \left[\frac{\langle m | \hat{\mu}_{\alpha} | j \rangle \langle j | \hat{\Theta}_{\beta\gamma} | n \rangle}{\omega_{jn} - \omega_0 - i\Gamma_j} + \frac{\langle m | \hat{\Theta}_{\beta\gamma} | j \rangle \langle j | \hat{\mu}_{\alpha} | n \rangle}{\omega_{jn} + \omega_s + i\Gamma_j} \right]$$

1. Raman scattering from a single molecule

Radiant intensity of Raman scattering from single molecule:

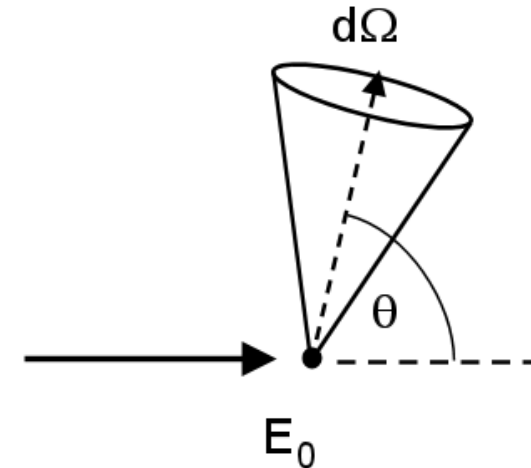
$$I \equiv \frac{d\Phi}{d\Omega} = \beta E_0$$

[W sr⁻¹] Irradiance [W cm⁻²]

Differential Raman scattering cross-section:

$$\beta \equiv \frac{d\sigma}{d\Omega} = k_{\tilde{\nu}} \tilde{\nu}_s^4 F(\theta, p_i, p_s, T_{fi})$$

[cm² sr⁻¹ molecule⁻¹]



But: detected signal proportional to detected photons.s⁻¹ (in UV and VIS, NIR spectral regions)

$$I_p \equiv \frac{d\Phi_p}{d\Omega} = \frac{\beta E_0}{h c \tilde{\nu}_s} = \beta' E_0$$

[photons s⁻¹ sr] Irradiance [W cm⁻²]

$$\beta' = \frac{d\sigma'}{d\Omega} = \frac{k_{\tilde{\nu}} \tilde{\nu}_s^3}{h c} F$$

2. Raman scattering from a bulk sample - volume source of radiation

Radiant emissivity (radiant flux from unit volume into unit solid angle):

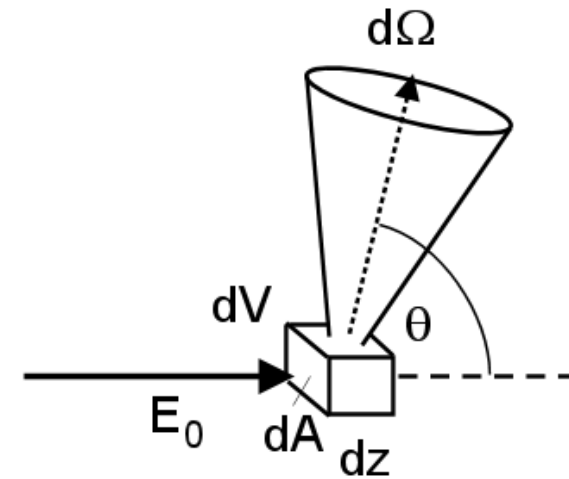
$$J \equiv \frac{d^2\Phi_s}{d\Omega dV} = D \beta' E_0$$

concentration of molecules [molecule cm⁻³]

Radiant flux of Raman scattering:

$$d^3\Phi_s = J T dA dz d\Omega = D \beta' T d\Phi_0 dz d\Omega$$

transmission factor



Radiance from a thin sample:

$$B_s \equiv \frac{d^2\Phi_s}{d\Omega dA \cos \theta}$$

$$dB_s = \frac{J dz}{\cos \theta}$$

2. Raman scattering from a bulk sample - volume source of radiation

Radiant emissivity (radiant flux from unit volume into unit solid angle):

$$J \equiv \frac{d^2\Phi_s}{d\Omega dV} = D \beta' E_0$$

\uparrow
 concentration of molecules [molecule cm⁻³]

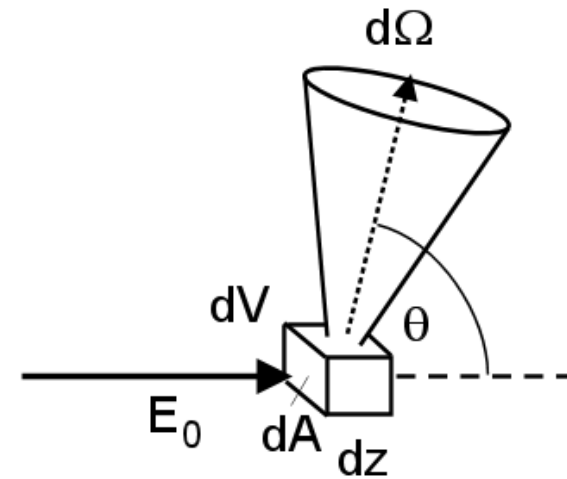
Radiant flux of Raman scattering:

$$d^3\Phi_s = J T dA dz d\Omega = D \beta' T d\Phi_0 dz d\Omega$$

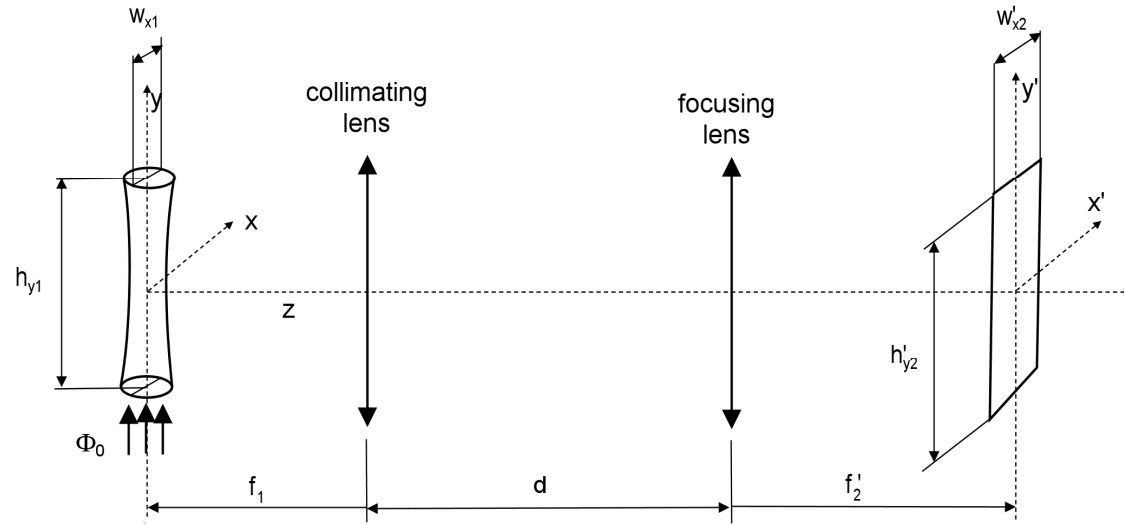
\uparrow
 transmission factor

often possible to evaluate as:

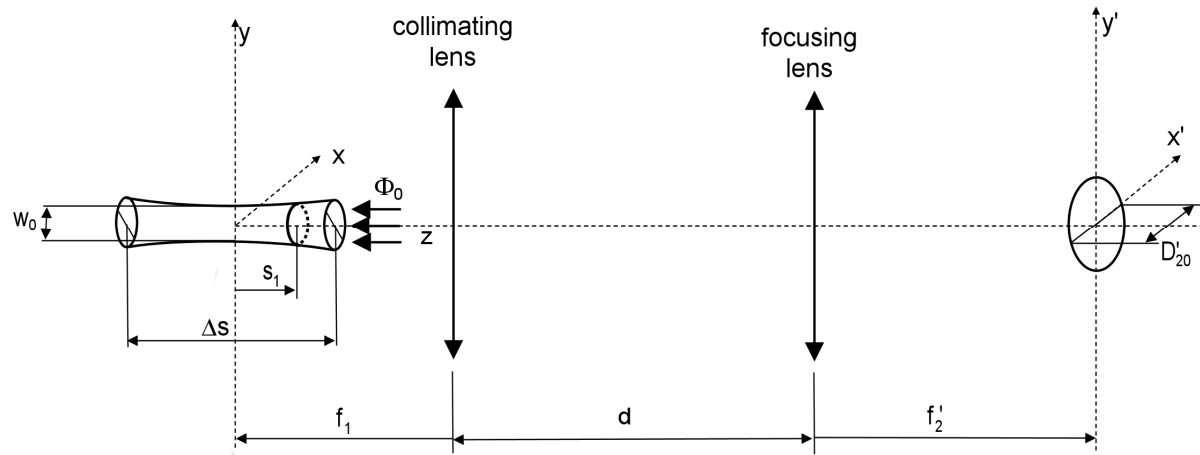
$$\Phi = D \beta \Phi_0 \int \Omega(s) T(s) ds$$



Scattering geometry:

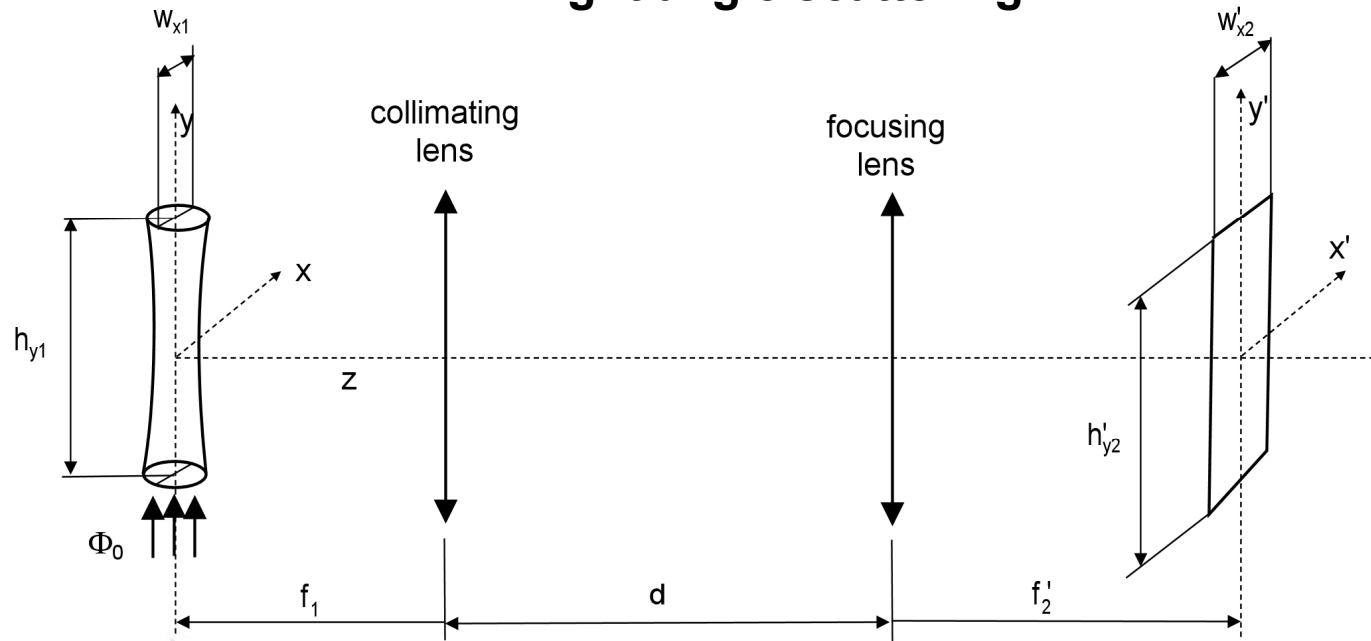


Right-angle

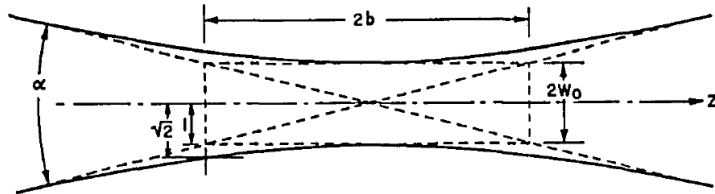


Collinear (back / forward)

Right angle scattering



$$\Phi_{90} = D \beta T \Phi_0 h_{y1} \Omega_1 \cong D \beta \Phi_0 h_{y1} \pi NA_{10}^2 = D \beta \Phi_0 h'_{y2} \frac{f'_2}{f'_1} \pi NA_{20}^2$$

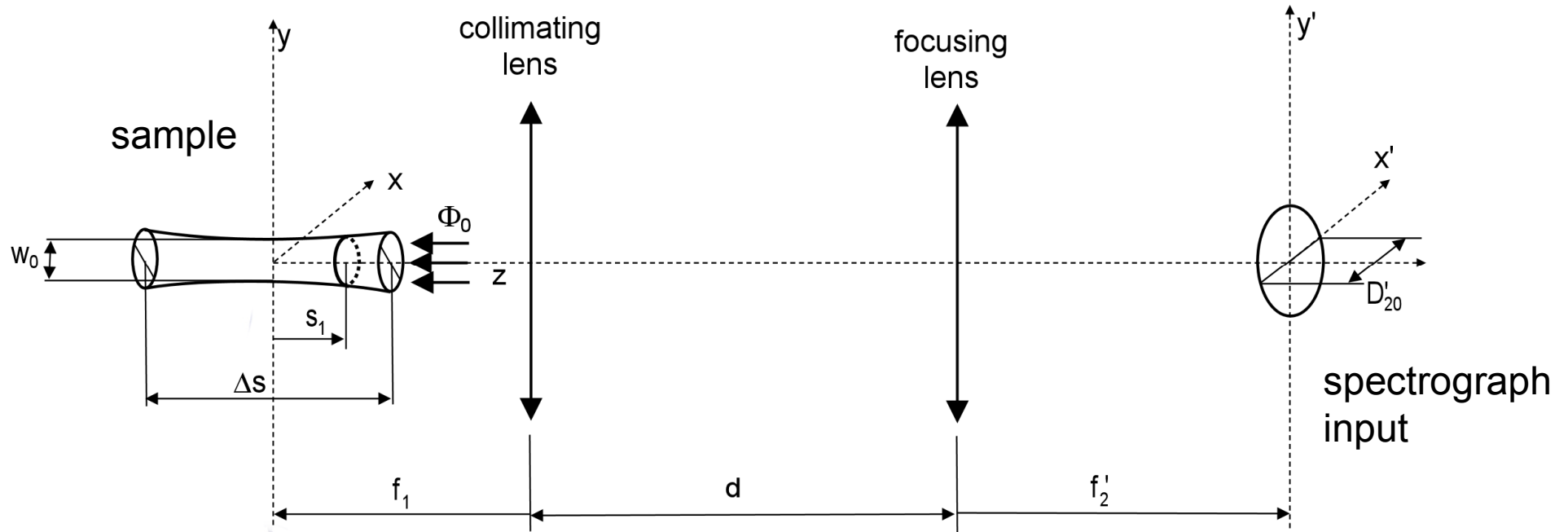


Gaussian beam

$$\omega_0 = \frac{2\lambda}{\pi\alpha}$$

$$b = \frac{2\pi\omega_0^2}{\lambda} = \frac{8\lambda}{\pi\alpha^2}$$

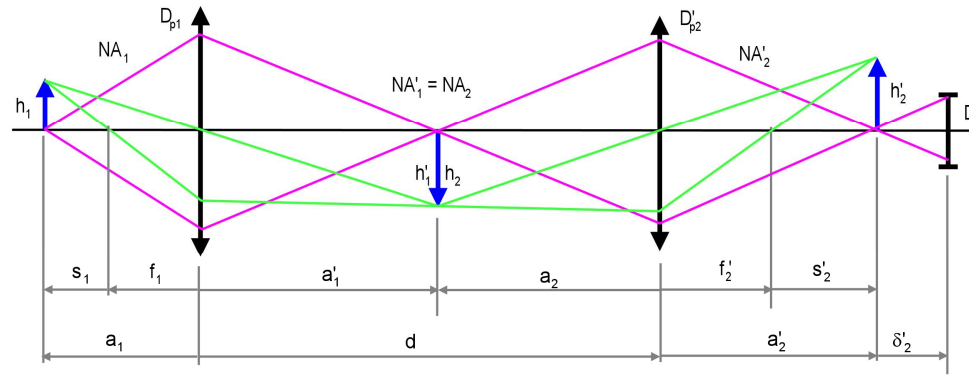
Collinear (back / forward) scattering



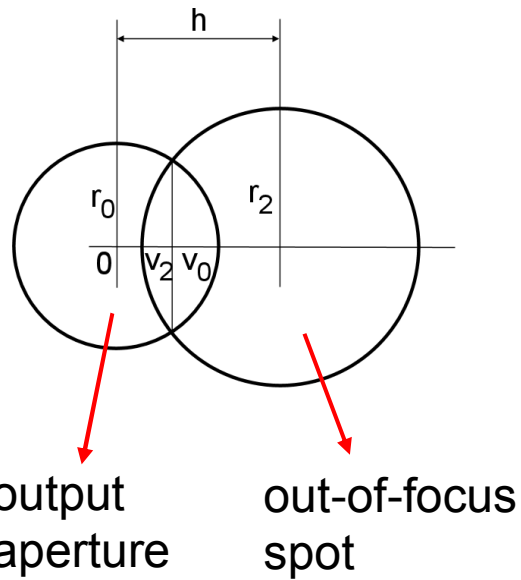
$$d^3\Phi = JT dA dz d\Omega = D \beta T d\Phi_0 dz d\Omega$$

$$\Phi_{2a} = D \beta \Phi_0 \int_{s_{1\min}}^{s_{1\max}} \pi \frac{D_{pl}^2}{4(f_1 - s_1)^2} ds_1 = \boxed{D \beta \Phi_0 \pi D'_{20} NA'_{20}}$$

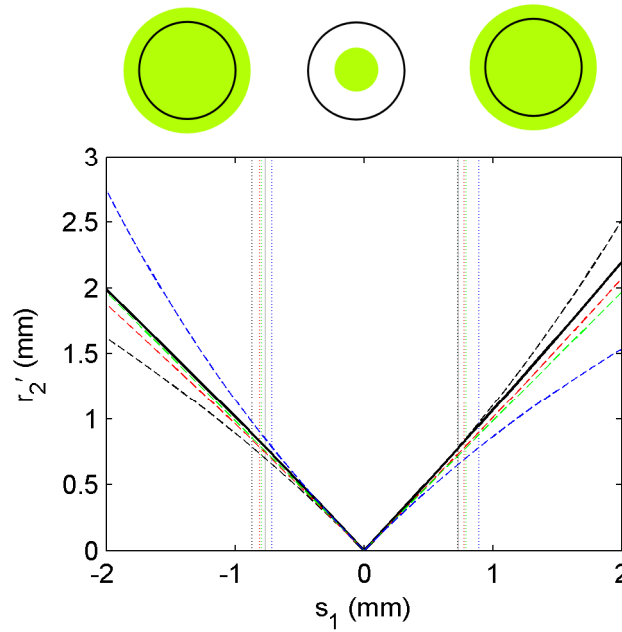
sample



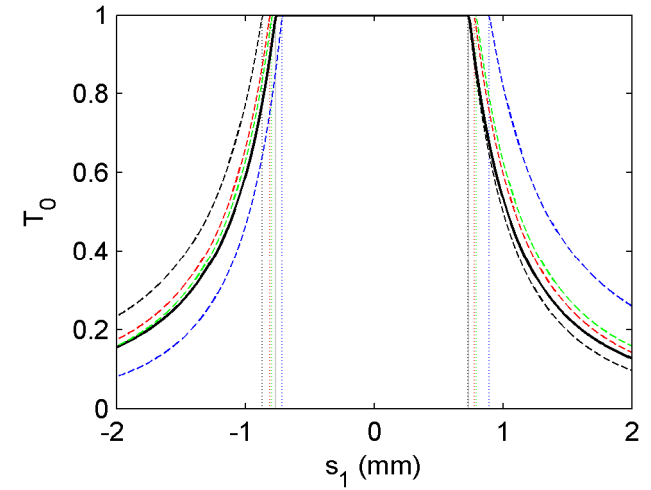
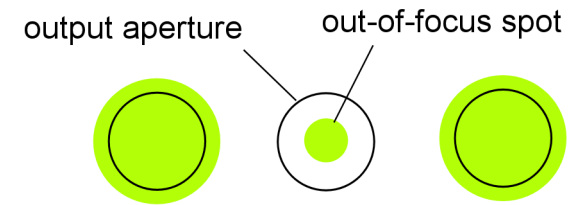
spectrograph
input



radius of out-of focus point

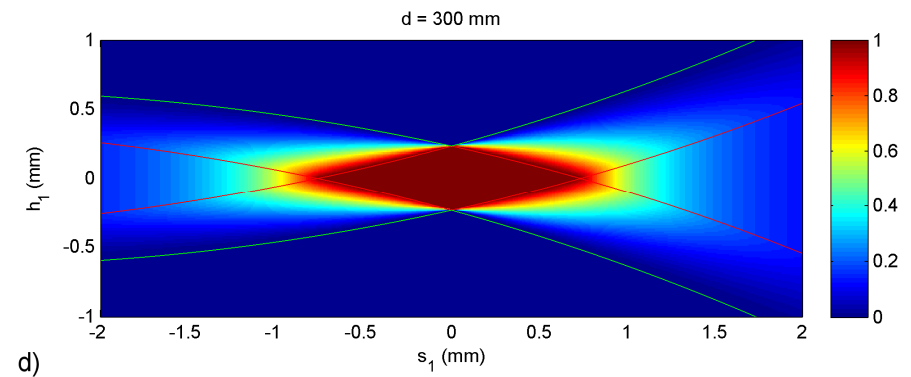
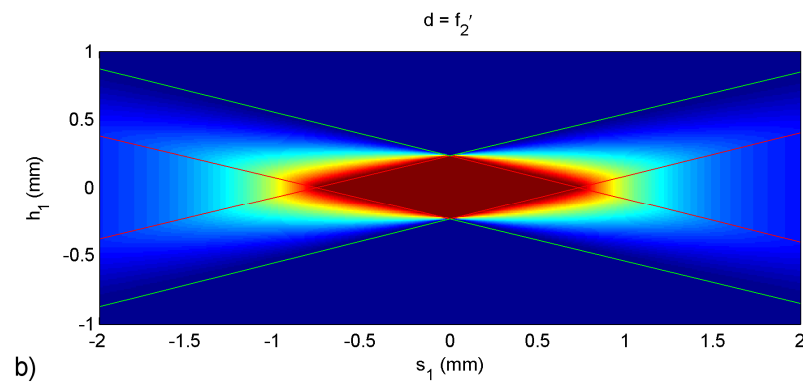
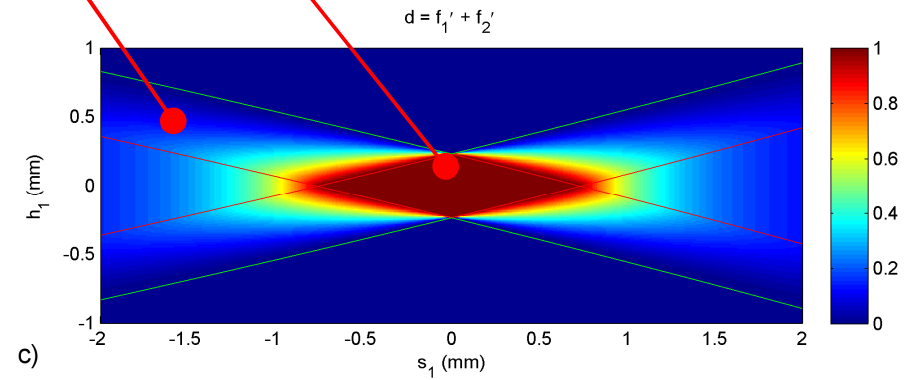
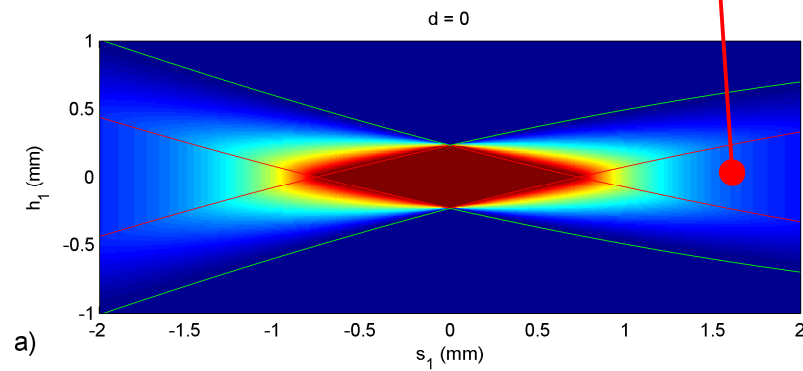
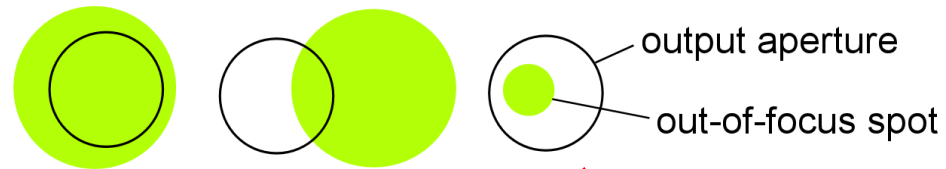


transmittance factor

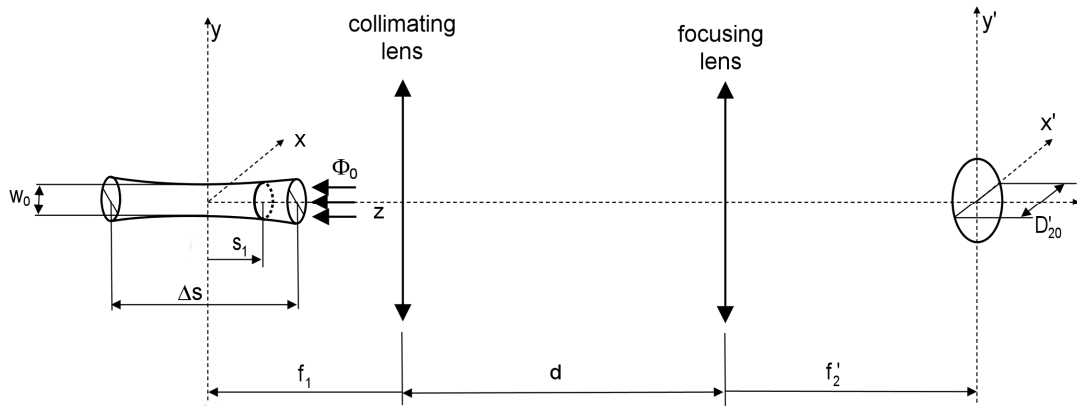


Calculation of transmittance factor in dependence of position in object space

Dependence on distance between lenses 1 and 2



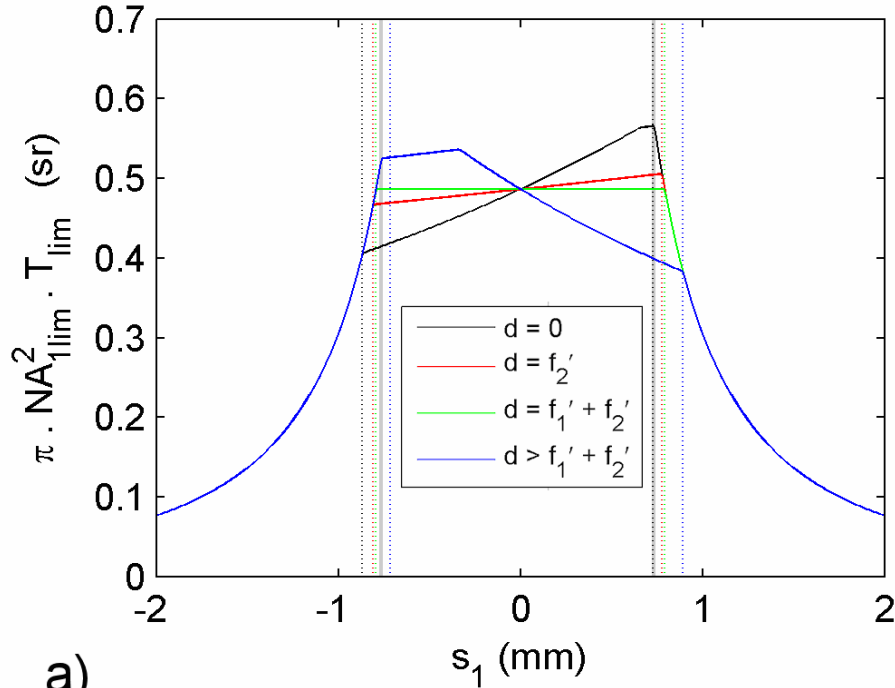
Collinear (back / forward) scattering



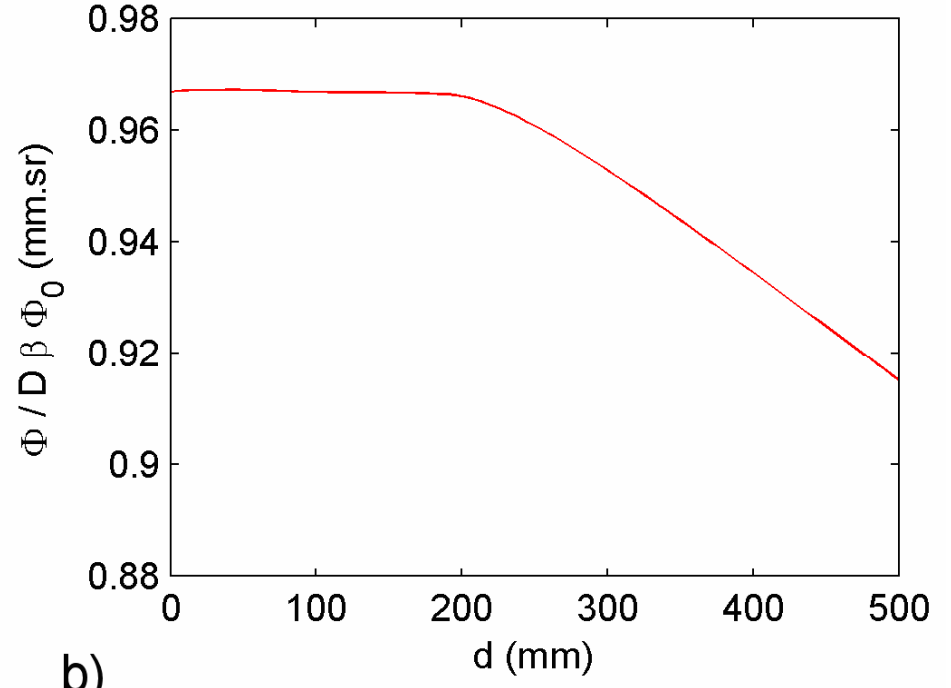
$$\Phi_{collinear} = D \beta \Phi_0 \pi D'_{20} NA'_{20}$$

flux from sample (axial points)

integrated flux – dependence on distance between collimating and focusing lens

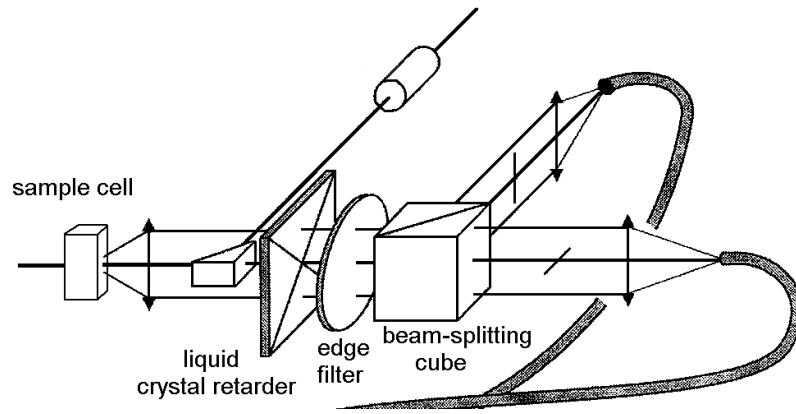


a)



b)

Collinear (back / forward) scattering



$$\Phi_{collinear} = D \beta \Phi_0 \pi D'_{20} NA'_{20}$$

Sample volume:

$$V = \pi \frac{D_{20}^3}{NA_{20}} \left(\frac{f'_1}{f'_2} \right)^4$$

Numerical example:

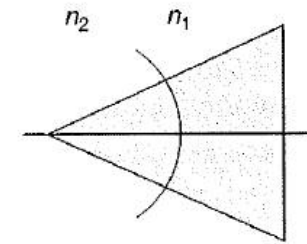
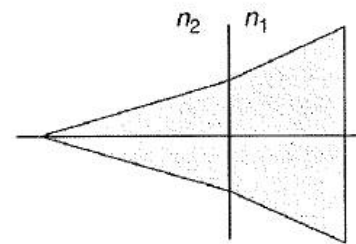
$$f'_1 = 26 \text{ mm}$$

$$f'_2 = 100 \text{ mm}$$

$$D_{20} = 1.6 \text{ mm}$$

$$NA_{20} = 0.12$$

$$V = 0.5 \mu\text{L}$$



Real-life volume (path-length 4 mm): 30 μL

Comparison of right angle and collinear scattering

Spectrograph input aperture area: $\frac{\pi}{4} D'_{20}{}^2 = w'_{x2} h'_{y2}$

$$\frac{\Phi_{90}}{\Phi_{180}} = \frac{D \beta \Phi_0 h'_{y2} \frac{f_2'}{f_1} \pi NA'_{20}{}^2}{D \beta \Phi_0 \pi D'_{20} NA'_{20}} = \sqrt{\frac{\pi}{4} \frac{h_{y1}}{w_{x1}}} NA_{10}$$

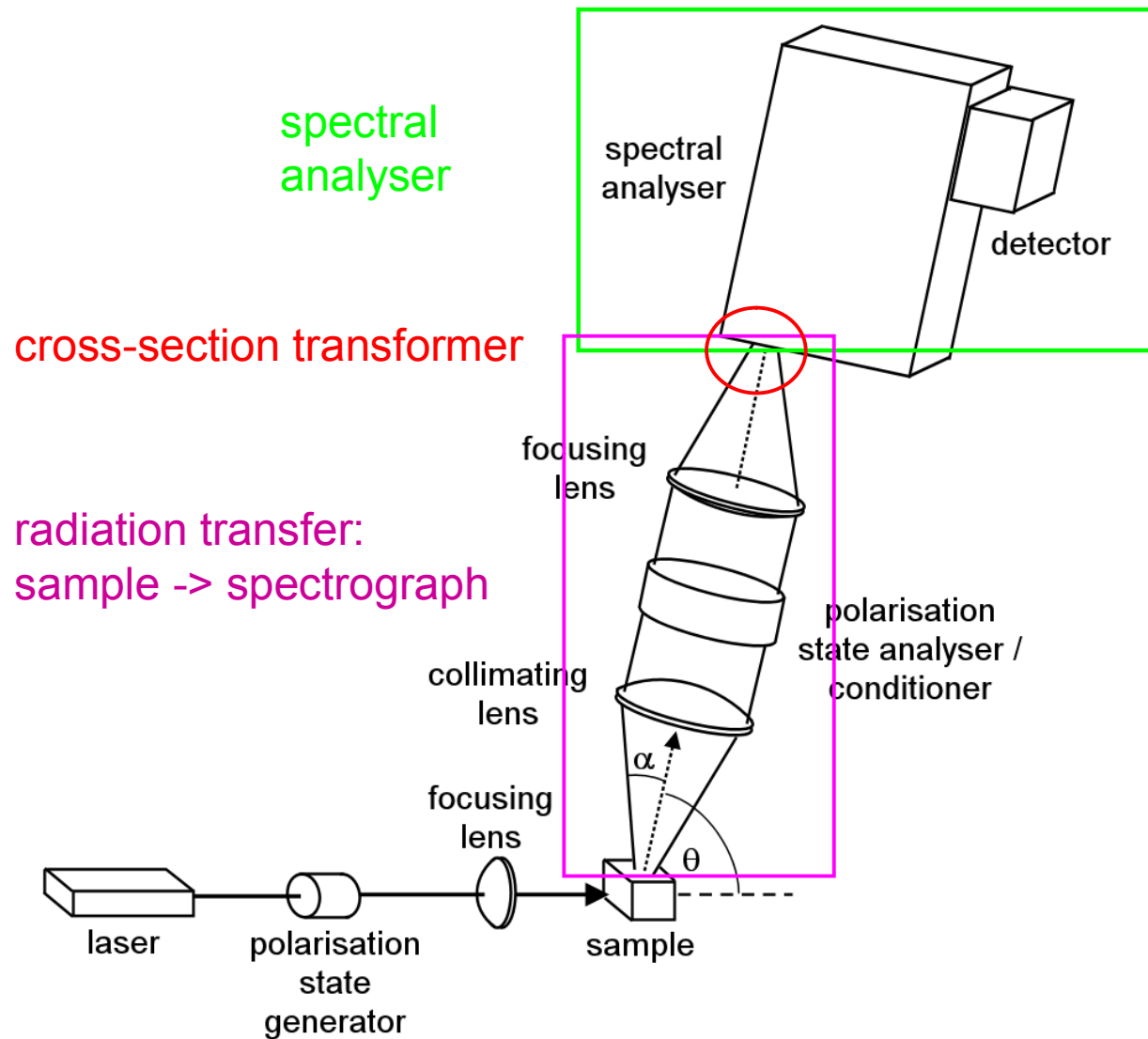
Numerical example

$$NA_1 = 0.5$$

$$h_{y1} : w_{x1} = 256:2$$

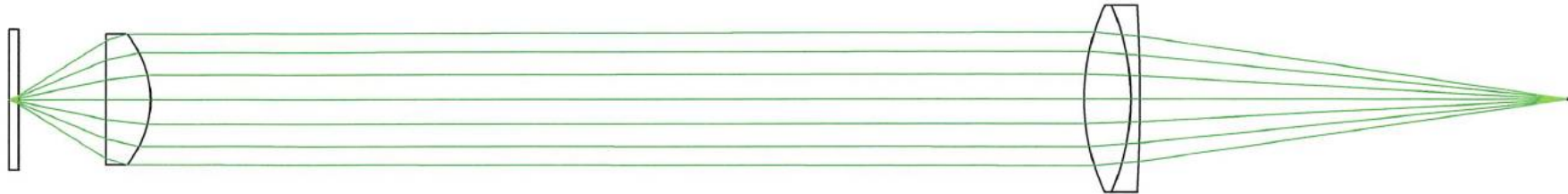
$$\frac{\Phi_{90}}{\Phi_{180}} = 5$$

Radiation transfer: from sample to spectrograph



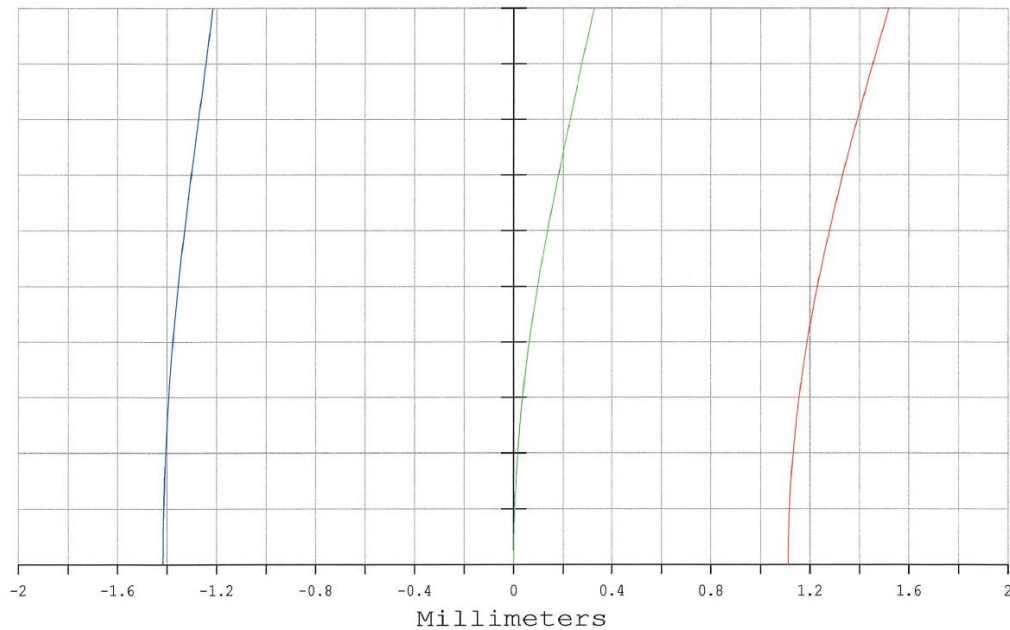
Collinear (back / forward) scattering

Radiation transfer optical system:

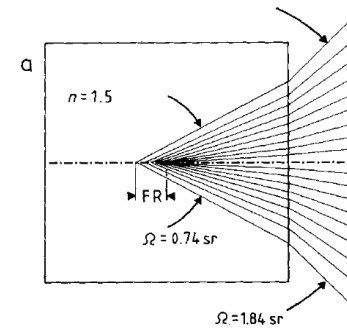


spherical and chromatic aberration:

Pupil Radius: 14.0000 Millimeters

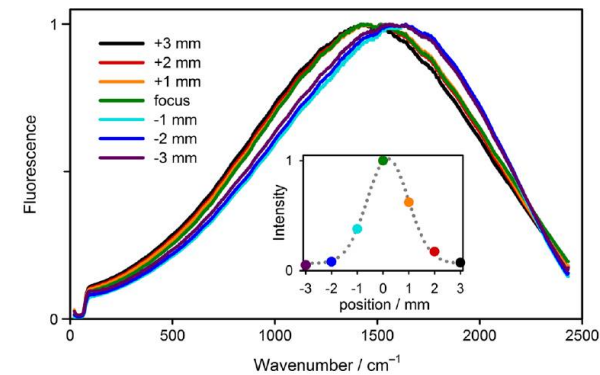


Longitudinal Aberration



B. Schrader: Infrared and Raman Spectroscopy 1995

Intensity from NIST calibration target

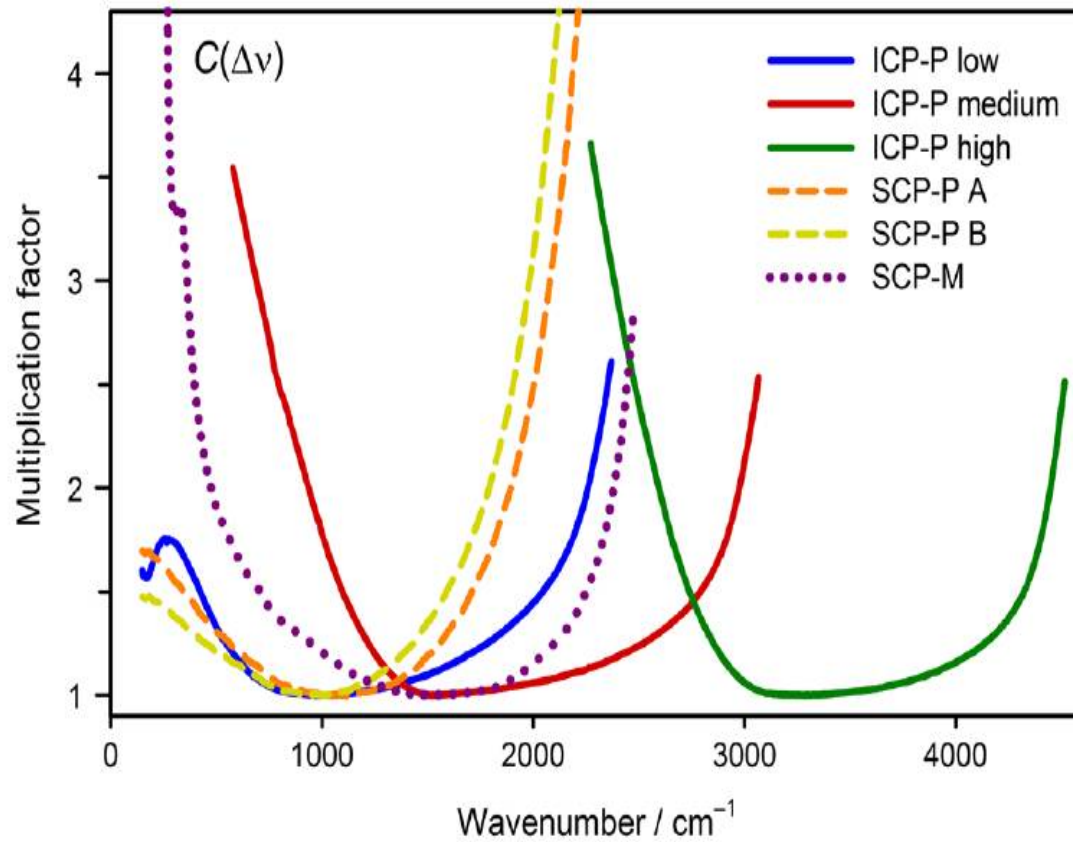


V. Profant, V. Baumruk et al., J. Raman. Spectrosc. (2014)

Raman and ROA Intensity calibration

Relative intensity correction: standard reference source needed

NIST Relative intensity correction standard reference 2242



Collinear (back / forward) scattering

Design of new optical system



Parameters for radiation transfer optics (excitation wavelength 532 nm)

Required parameter	Value
Collimating objective	Aspheric singlet lens
Diameter	30 mm
Focal length	26,0 mm (for 780 nm)
Material	S-LAH64
Sample	
Water	0 – 4 mm, center at 2,0 mm
Max. distance from optical axis	0,05 mm
Distance between focusing and collimating lens	200 – 400 mm
Numerical aperture of focusing lens	0,118
Wavelength range	530 – 600 nm

Collinear (back / forward) scattering

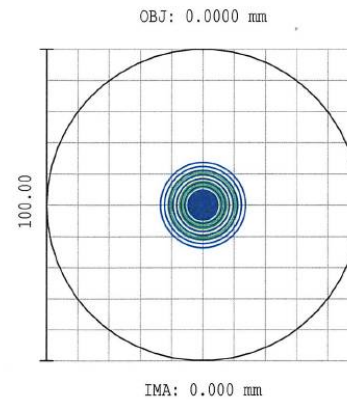
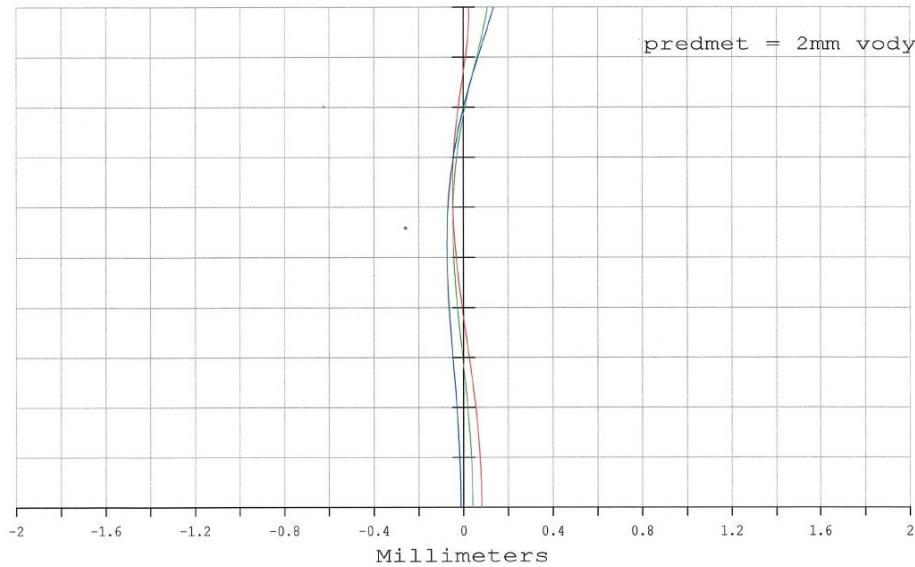
Design of new optical system



spherical and chromatic aberration

spot diagram

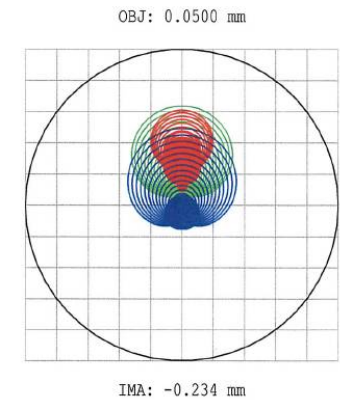
Pupil Radius: 2.0513 Millimeters



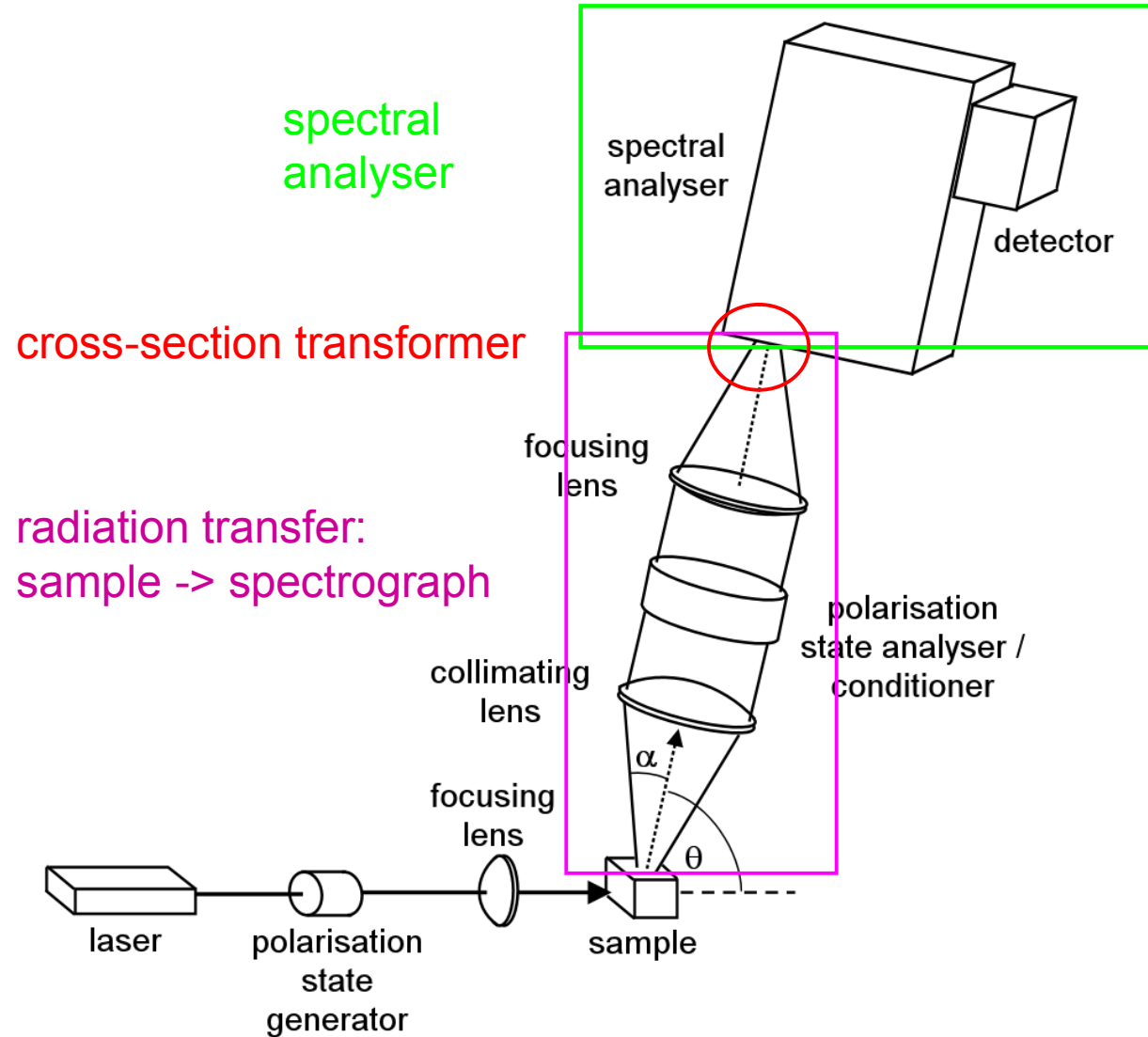
532nm

562 nm

590 nm

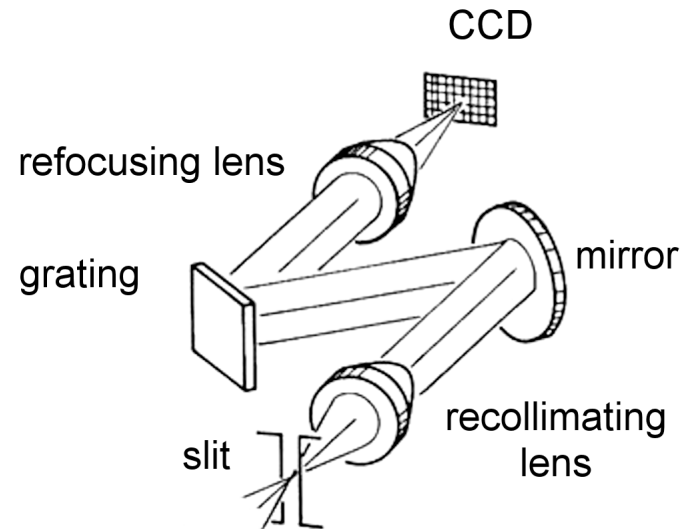
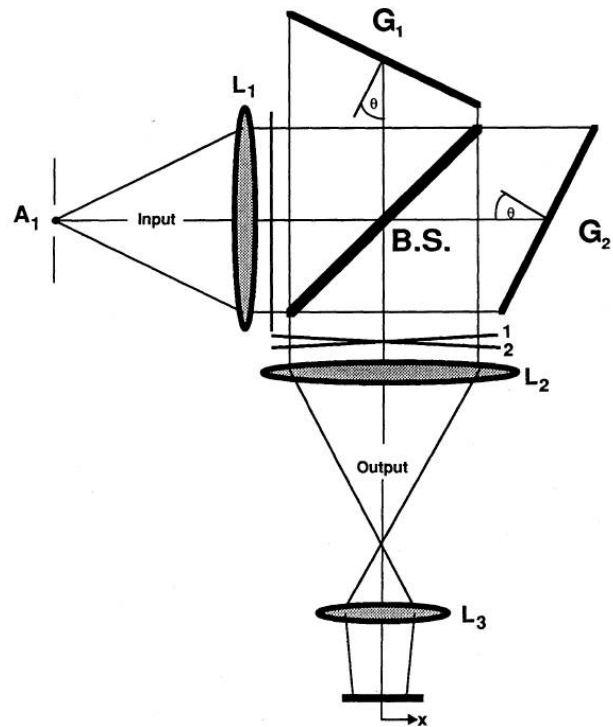


3. Spectral Analyzers



3. Properties of spectral analyzers

- How to compare and evaluate various spectral analysers?



- spectral resolution (resolving power)
- spectral range

- geometrical throughput
- source size (confocal/bulk)

$$R = \frac{\lambda}{d\lambda} = \frac{\tilde{\nu}}{d\tilde{\nu}}$$

$$d^2G \equiv n^2 dA \cos \theta d\Omega$$

3. Properties of spectral analyzers

Required resolving power for various excitation wavelengths:

λ_0 (nm)	$\tilde{\nu}_{vib} = 600 \text{ cm}^{-1}$	$\tilde{\nu}_{vib} = 1800 \text{ cm}^{-1}$	$d\tilde{\nu} = 7 \text{ cm}^{-1}$	$R = \lambda / d\lambda$
1064	1137 nm	1316 nm	1,0 nm	1200
532	550	588	0,22 nm	2500
356	364	380	0,095 nm	3900
229	232	239	0,038 nm	6100

3. Properties of spectral analyzers

Étendue, geometrical throughput: $d^2G \equiv n^2 dA \cos \theta d\Omega$

$$G = \iint_{\Omega_A} d^2G \cong n^2 A_D \Omega_D \cong \pi A n^2 \sin^2 \theta$$

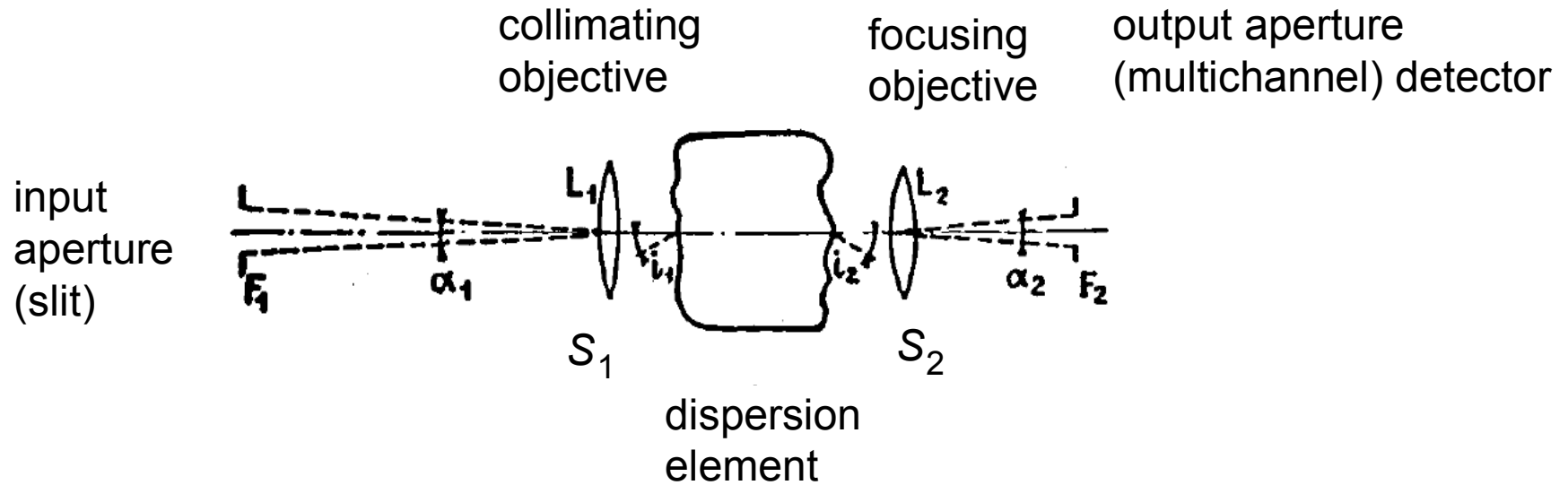
Basic radiance

$$B' \equiv \frac{B}{n^2} = \frac{d^2\Phi}{n^2 d\Omega dA \cos \theta}$$

Radiance from thin sample:

$$B_s \equiv \frac{d^2\Phi_s}{d\Omega dA \cos \theta} = \frac{J dz}{\cos \theta}$$

Evaluation of „throughput“ of spectral analyzer (spectrograph)



Signal (radiant/photon flux) for multichannel detectors:

$$\Phi = \tau B S_i \Omega_i N_R = \tau B_\lambda d\lambda \boxed{S_2} (\alpha_2 N_R) \beta = B_\lambda d\lambda \tau \frac{\pi d_2^2}{4} \frac{x_2 y_2}{f_2^2} = \frac{\pi}{4} B_\lambda d\lambda \tau \frac{S_{\text{det}}}{(f/\#)^2}$$

$i = 1, 2$

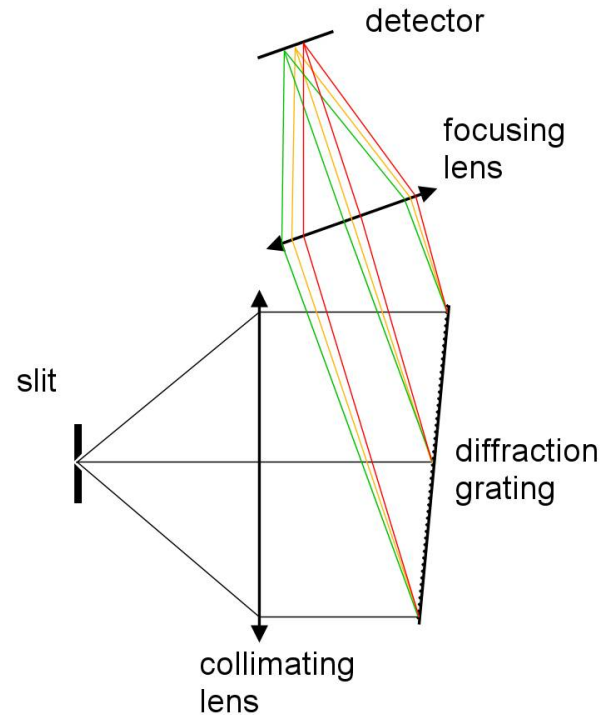
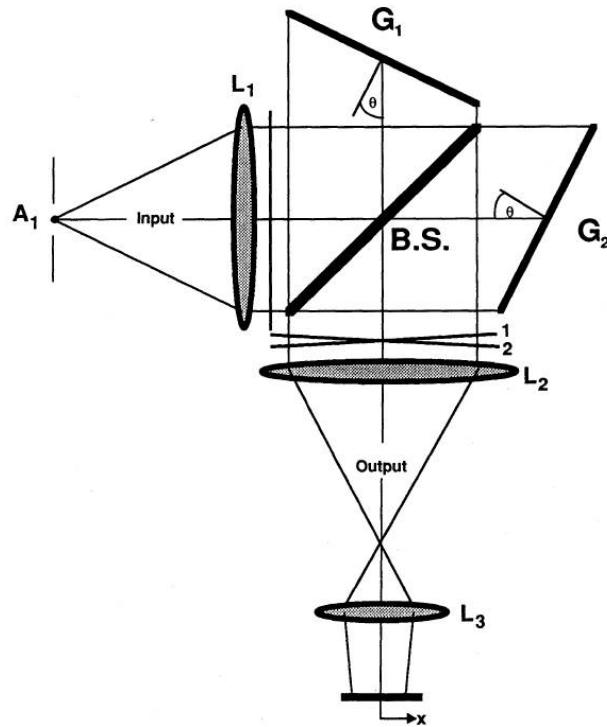
Pupil diameter

effective area of the detector

F-number

transmittance of spectrograph

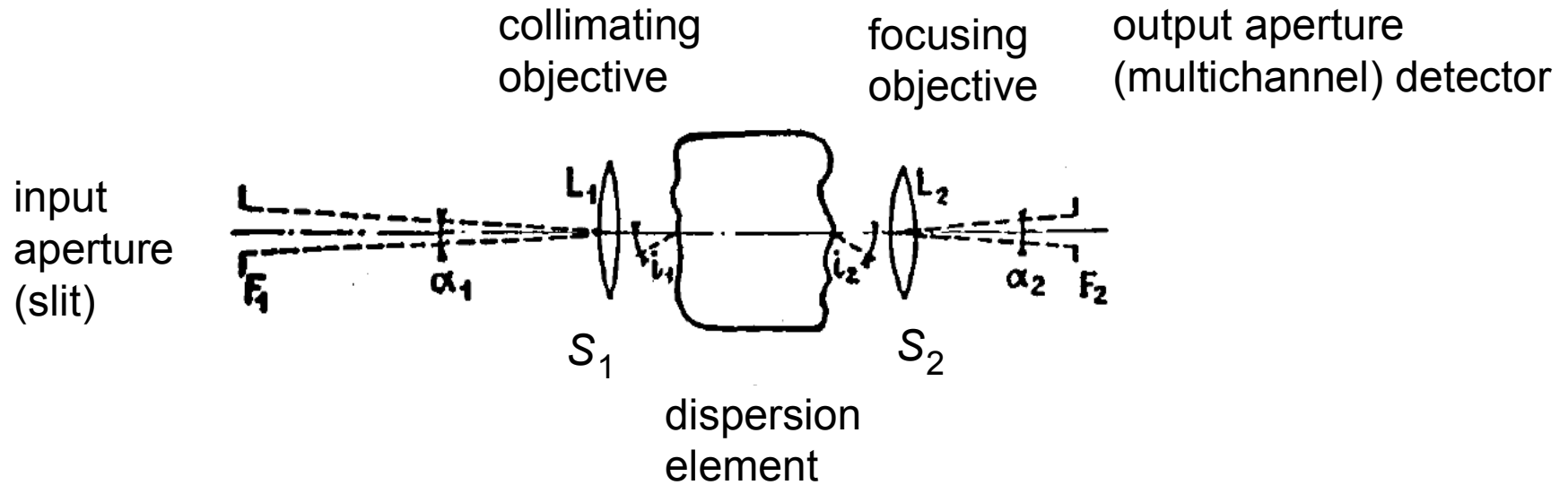
3. Properties of spectral analyzers



Signal/Noise considerations:

- shot noise limit (UV, VIS): dispersive multichannel spectrographs
- readout noise limit (IR): interferometers – Jacquinot advantage (high throughput)
- background noise limit (fluorescence): go to NIR or UV spectral region

Evaluation of „throughput“ of spectral analyzer (spectrograph)



- radiant flux $\Phi = \tau B S \Omega = \tau B_\lambda d\lambda S_i \alpha_i \beta = \tau B_\lambda (d\lambda)^2 S_i D_i \beta \quad i = 1, 2$

- diffraction grating:

$$S_i D_i \beta = A \frac{\sin i_1 + \sin i_2}{\lambda} \beta = S_i \frac{\sin i_1 + \sin i_2}{\lambda \cos i_i} \beta$$

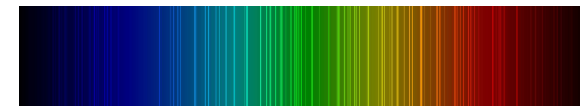
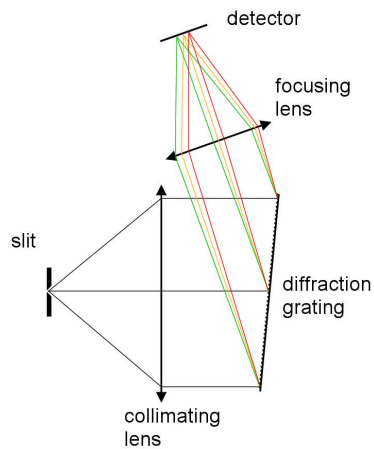
Evaluation of „throughput“ of spectral analyzer (spectrograph)

- Throughput

$$\Phi = \frac{\pi}{4} B_{\lambda} d\lambda \tau \frac{S_{\text{det}}}{(f/\#)^2}$$

- Diffraction grating:

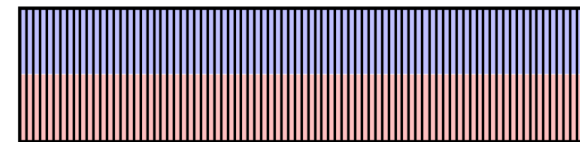
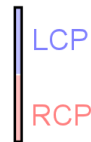
$$S_i D_i \beta = A \frac{\sin i_1 + \sin i_2}{\lambda} \beta = S_i \frac{\sin i_1 + \sin i_2}{\lambda \cos i_i} \beta$$



detection element

multichannel detector

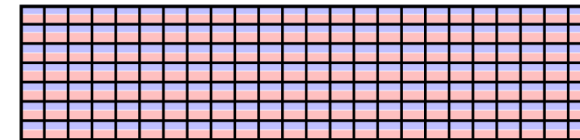
conventional spectrograph



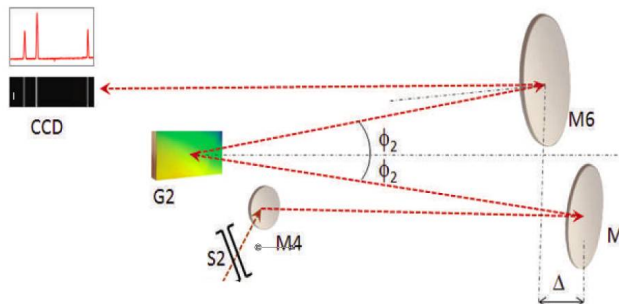
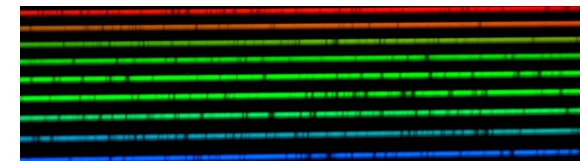
dispersion



Echelle spectrograph

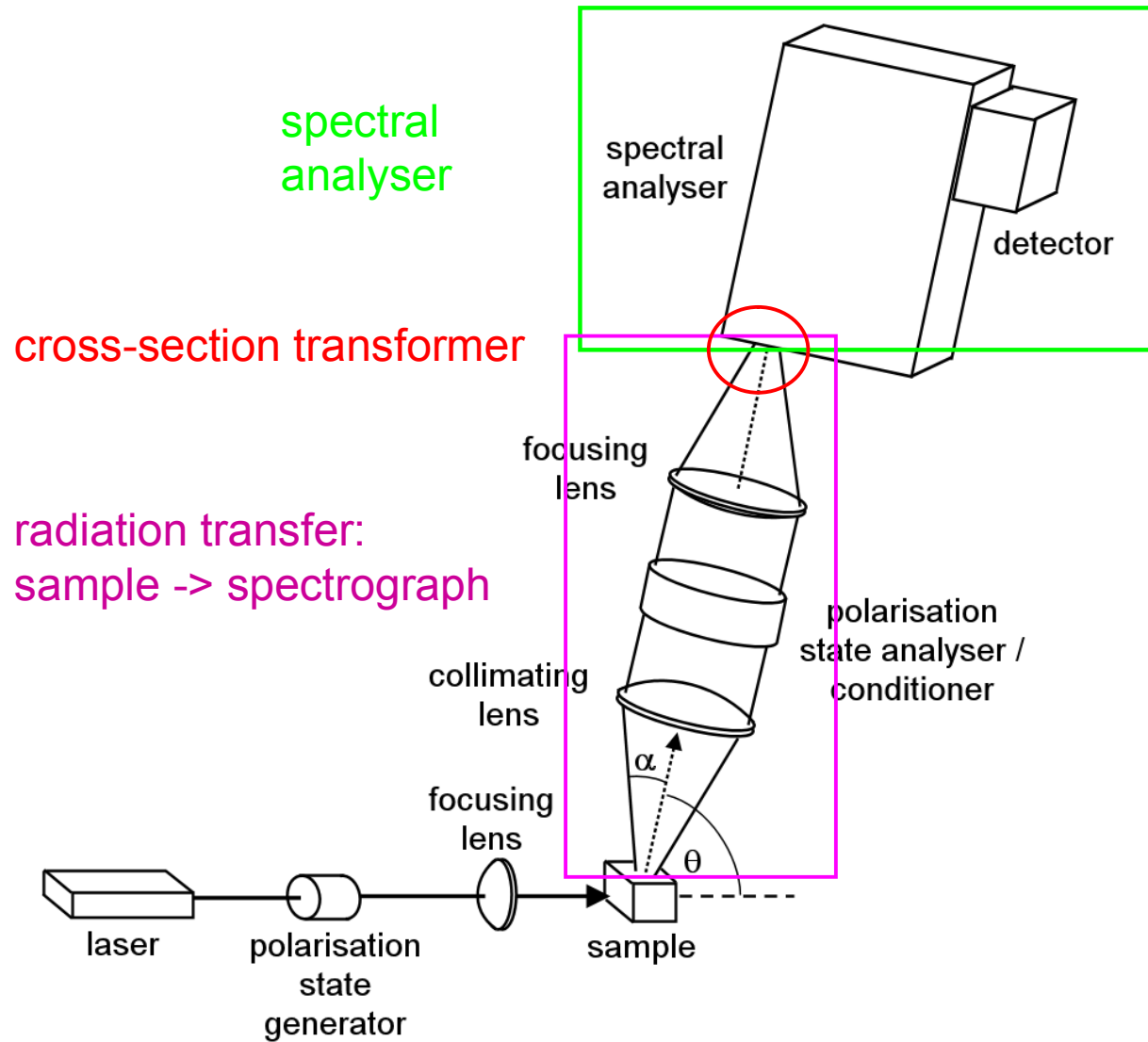


dispersion

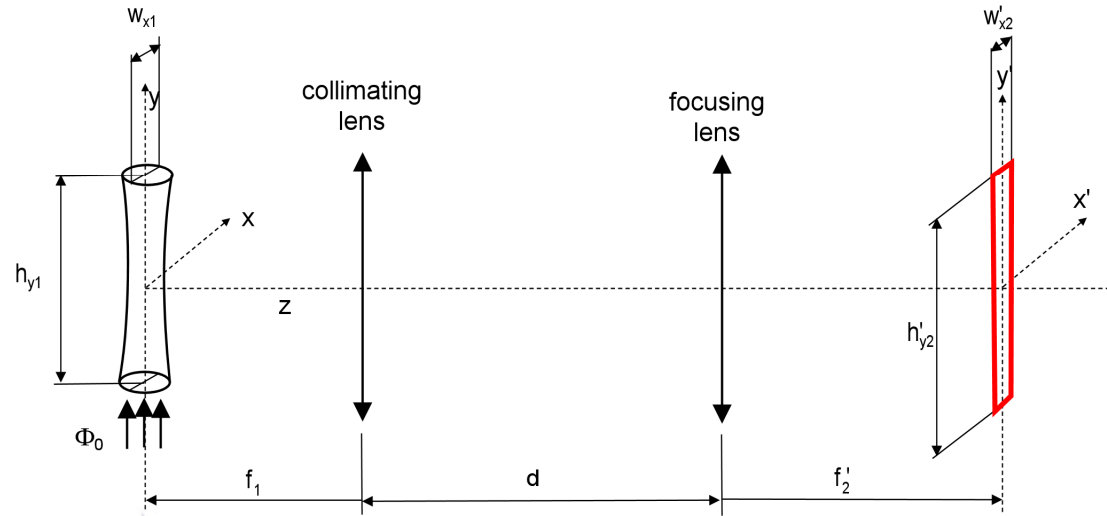


- cross dispersion needed

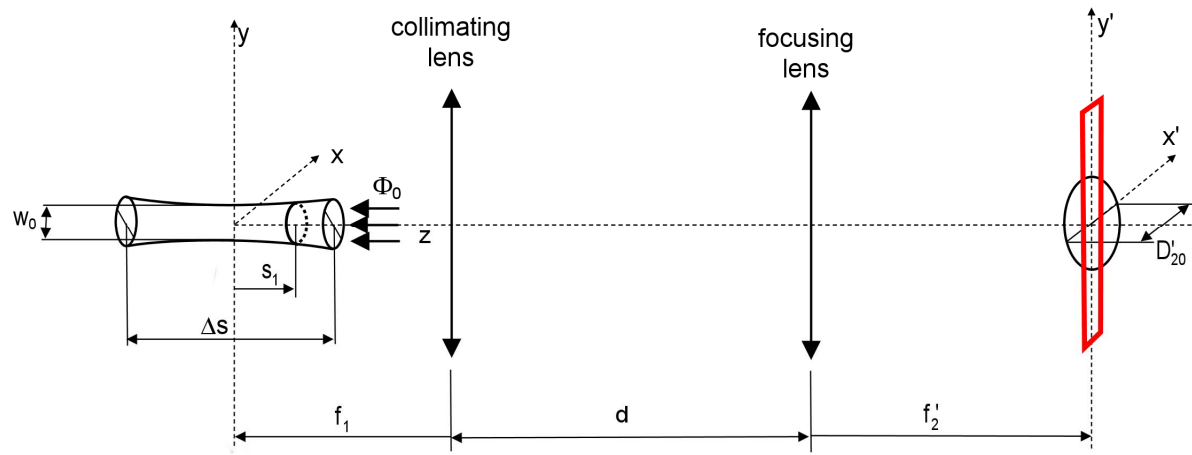
Cross-section transformer



Utilization of geometrical throughput – cross-section transformer



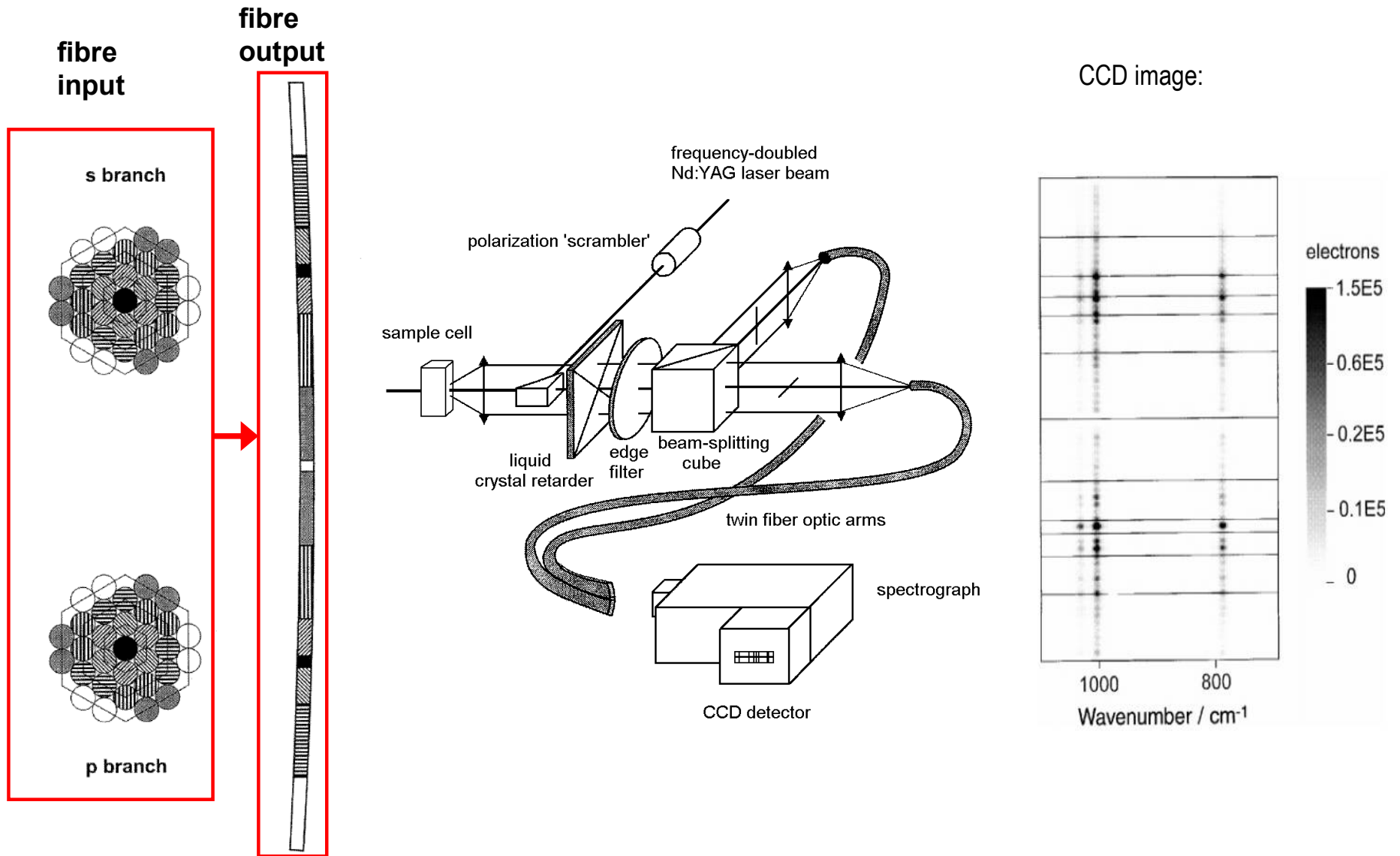
Right angle scattering geometry



Backscattering geometry

Cross section transformer

Solution 1: fibre optics



Cross section transformer

Solution 2a: slit slicing

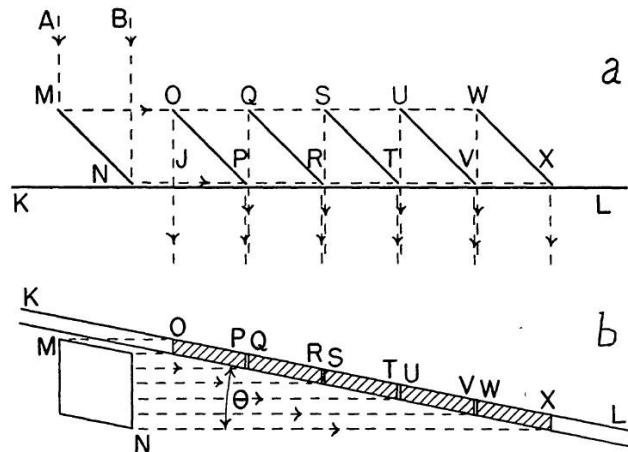
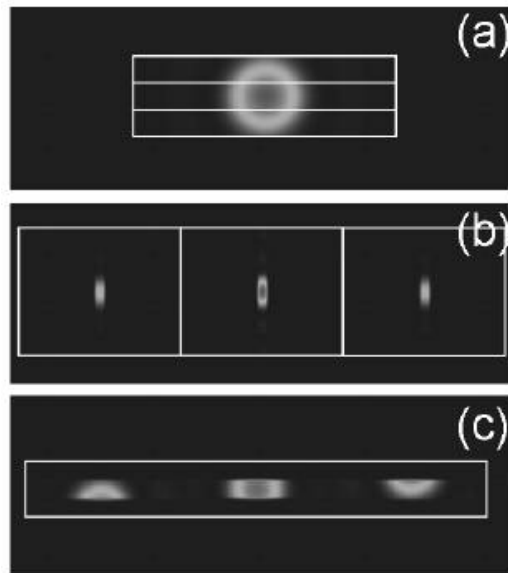
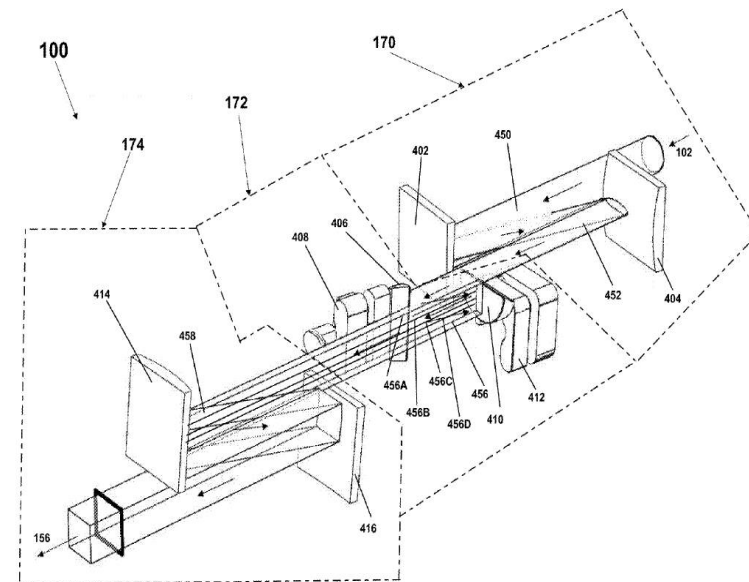


FIG. 1



Solution 2b: pupil slicing



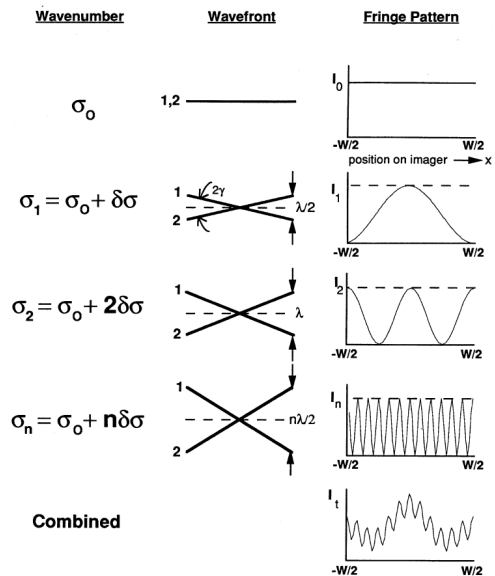
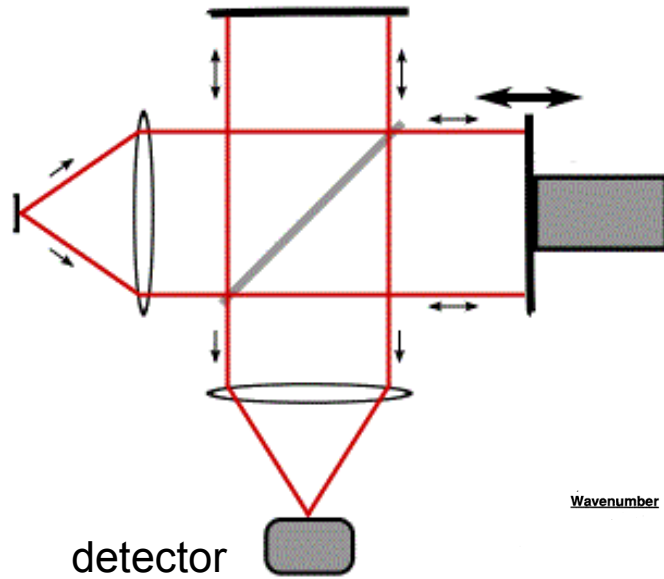
Patent Application Publication Dec. 8, 2011

US 2011/0299075 A1

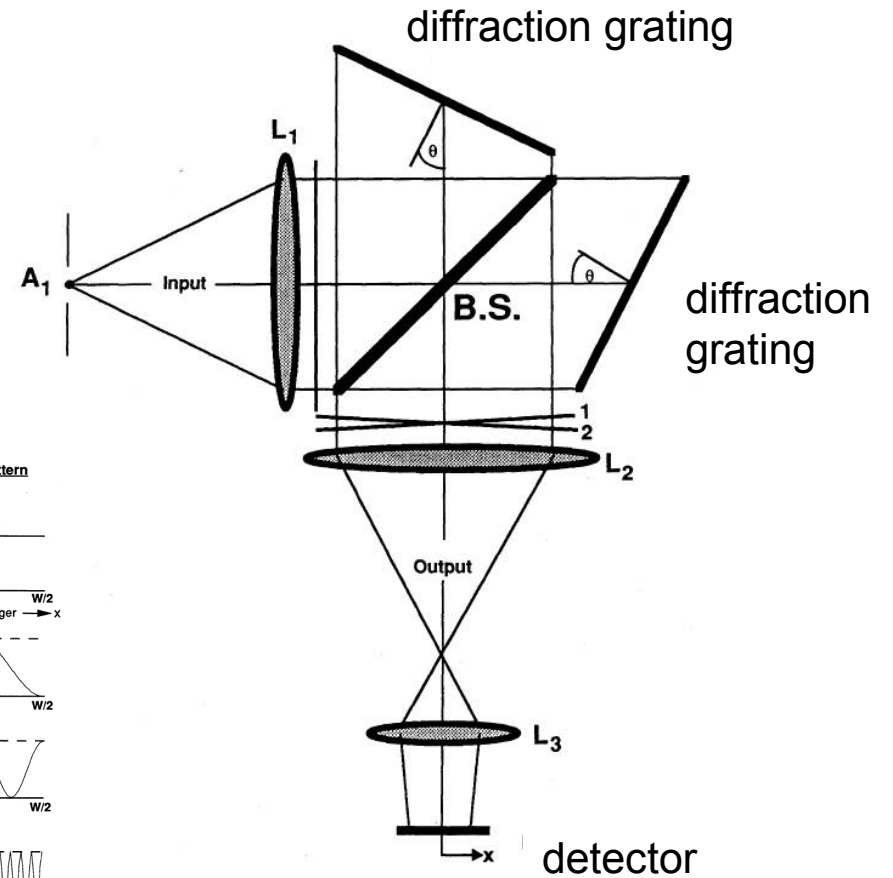


Solution 3: interferometers

Michelson interferometer

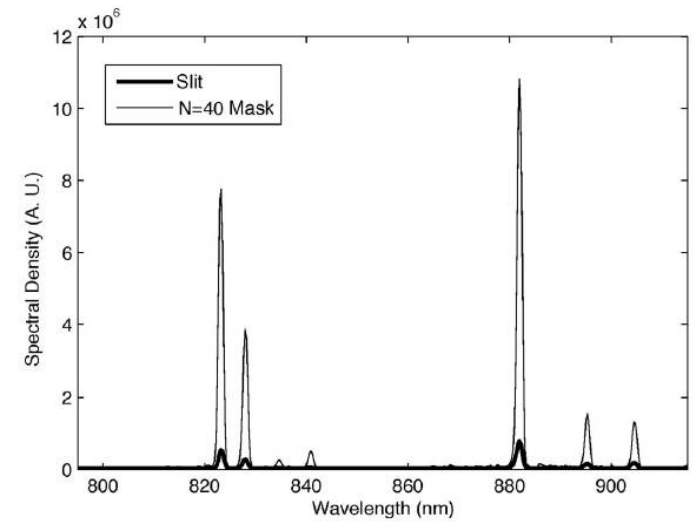
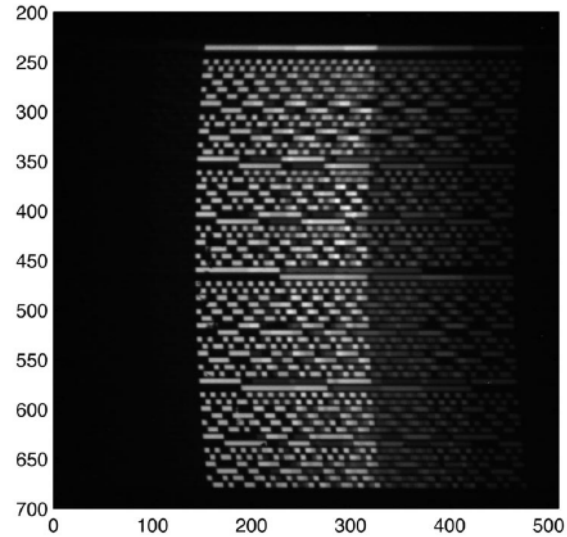
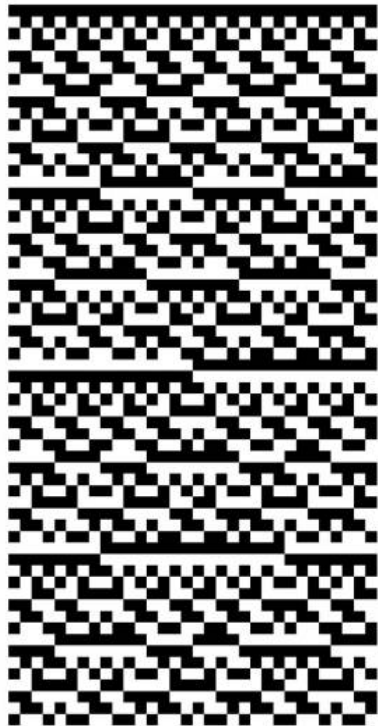


Harlander interferometer



Cross section transformer

Solution 4: use of coded apertures



Hadamard mask

M. E. Gehm, Appl. Optics, 2006, 45, 2965

Raman Optical Activity

Raman scattering: two-photon process

1. Excitation wavelength

- 488 – 532 nm
- 785 nm

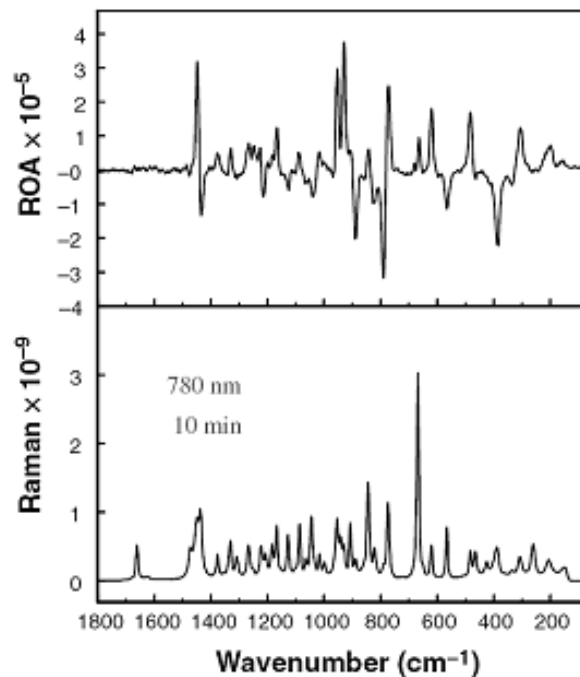
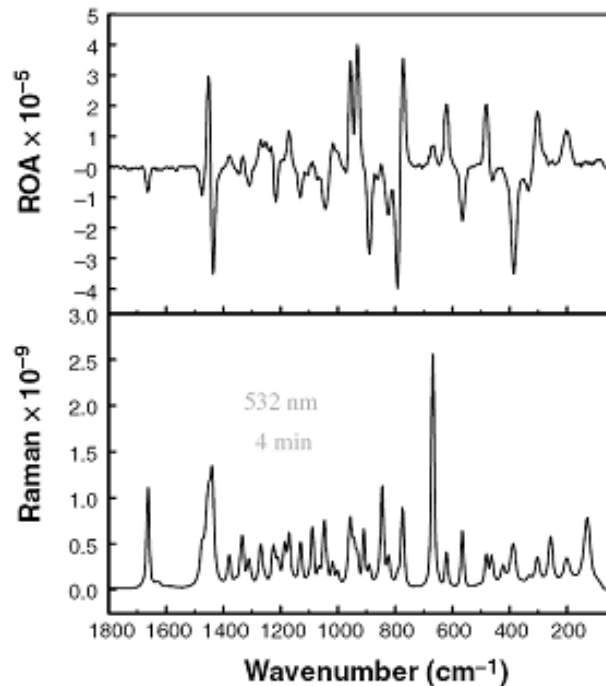
L. A. Nafie, Appl. Spectrosc. 2007, 61, 1103

Raman scattering cross-section

$$\beta' \equiv \frac{d\sigma'}{d\Omega} = \frac{k_{\tilde{\nu}} \tilde{\nu}_s^3}{h c} F(\theta, p_i, p_s, T_{fi})$$

$$\text{ROA} \approx \tilde{\nu}_s^4$$

S-(-)- α -pinene



Raman Optical Activity

Raman scattering: two-photon process

1. Excitation wavelength

- 488 – 532 nm
- 785 nm

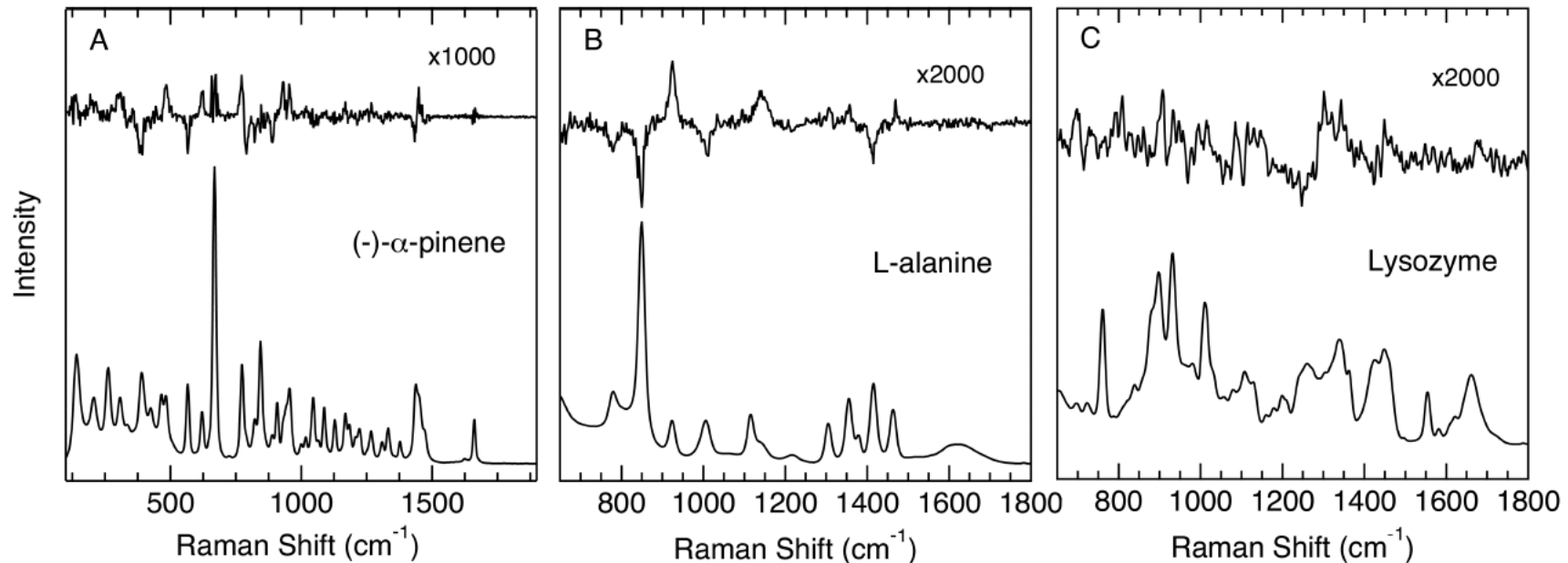
L. A. Nafie, Appl. Spectrosc. 2007, 61, 1103

M. Unno, et. al, J. Phys. Chem. B 2013, 117, 1321

Raman scattering cross-section

$$\beta' \equiv \frac{d\sigma'}{d\Omega} = \frac{k_{\tilde{\nu}} \tilde{\nu}_s^3}{h c} F(\theta, p_i, p_s, T_{fi})$$

$$\text{ROA} \approx \tilde{\nu}_s^4$$



Raman Optical Activity

Raman scattering: two-photon process

1. Excitation wavelength

- 488 – 532 nm
- 785 nm
- 244 nm (this work)

+ higher intensity of Raman/ROA scattering

- but lower laser power (photo-damage)

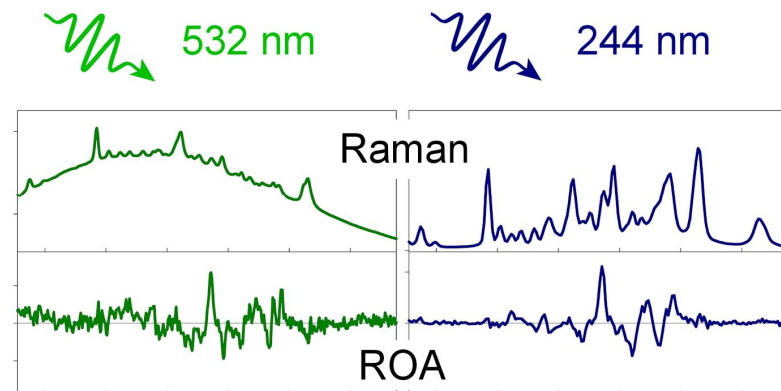
+ absence of fluorescence background

+ pre/resonance enhancement

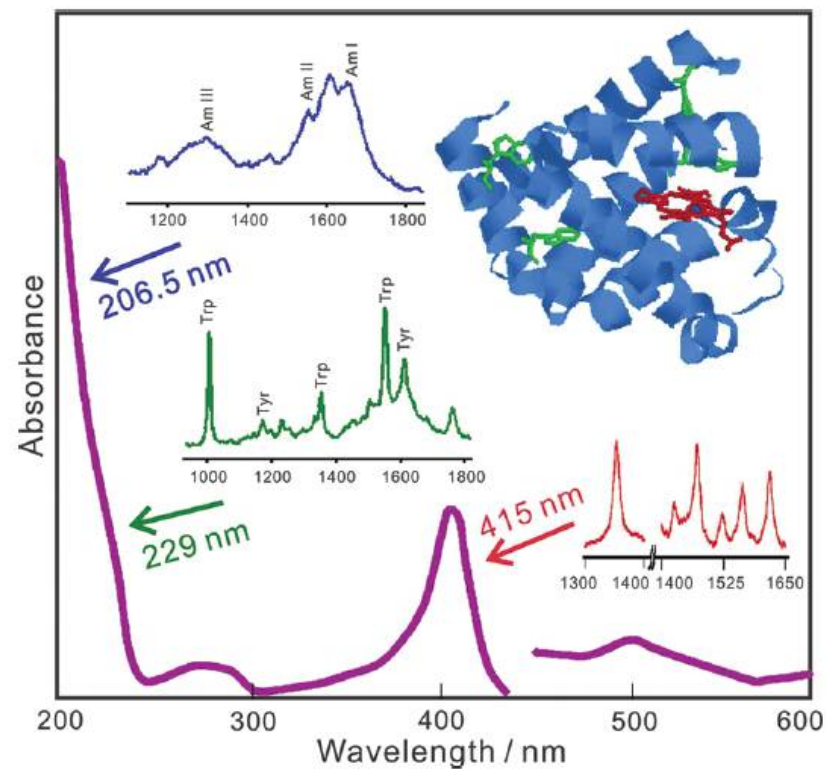
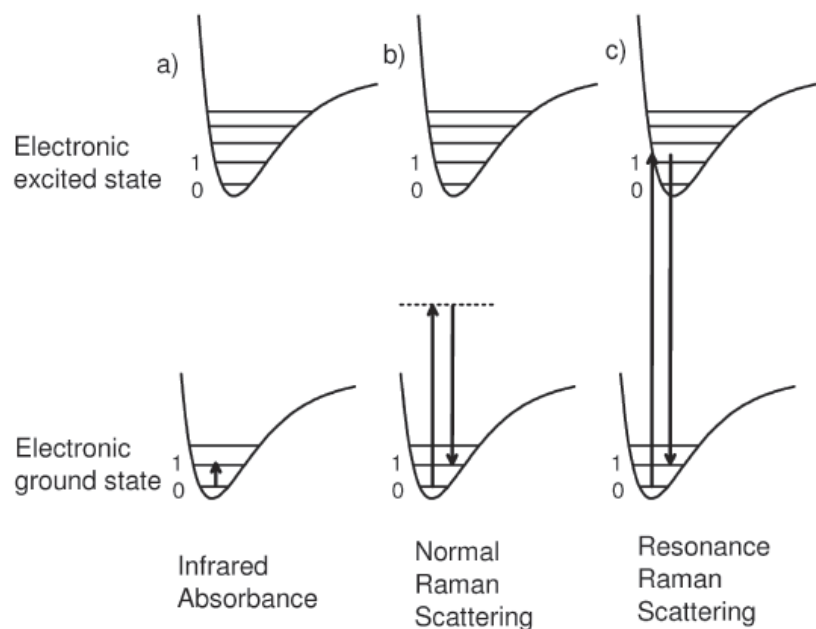
Raman scattering cross-section

$$\beta' \equiv \frac{d\sigma'}{d\Omega} = \frac{k_{\tilde{\nu}} \tilde{\nu}_s^3}{h c} F(\theta, p_i, p_s, T_{fi})$$

$$\text{ROA} \approx \tilde{\nu}_s^4$$



Resonance Raman scattering



Raman spectra of myoglobin

Raman Optical Activity

Raman scattering: two-photon process

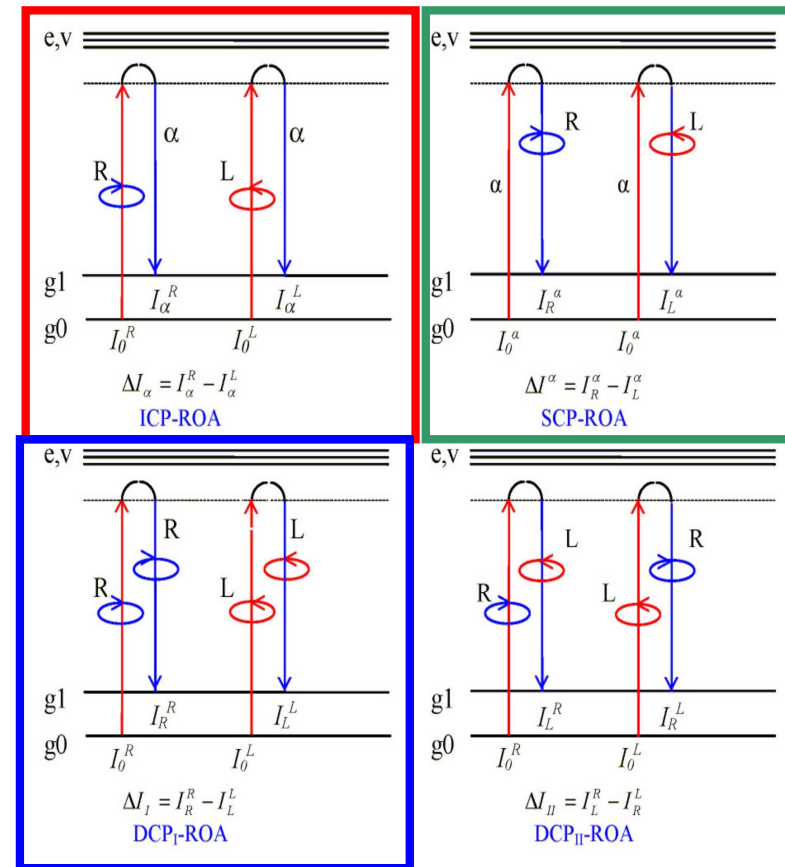
1. Excitation wavelength

- 488 – 532 nm
- 785 nm
- 244 nm

2. Scattering geometry (scattering angle)

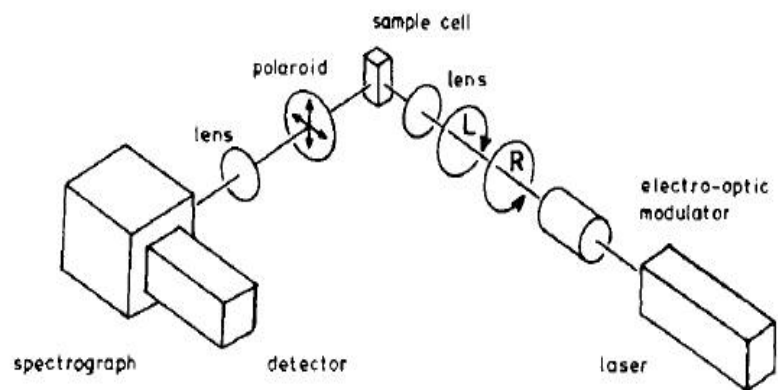
- backscattering geometry
- right-angle scattering geometry
- forward scattering geometry

3. Modulation scheme

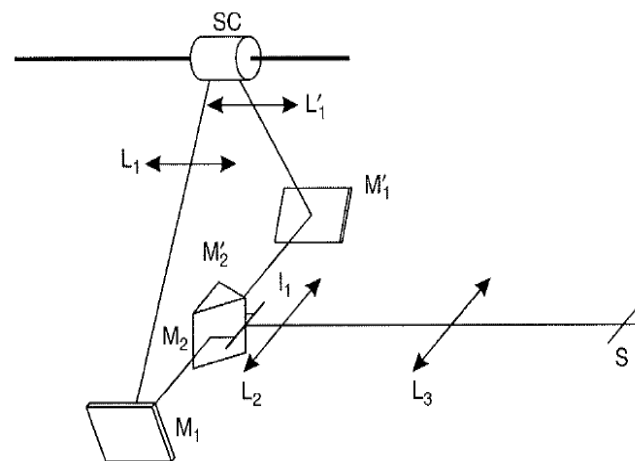


ROA first observed (as ICP) in 1973 by L.D. Barron, M.P. Bogaard and A.D. Buckingham, JACS 95, 603 (1973).

Right angle scattering ICP ROA Instrument



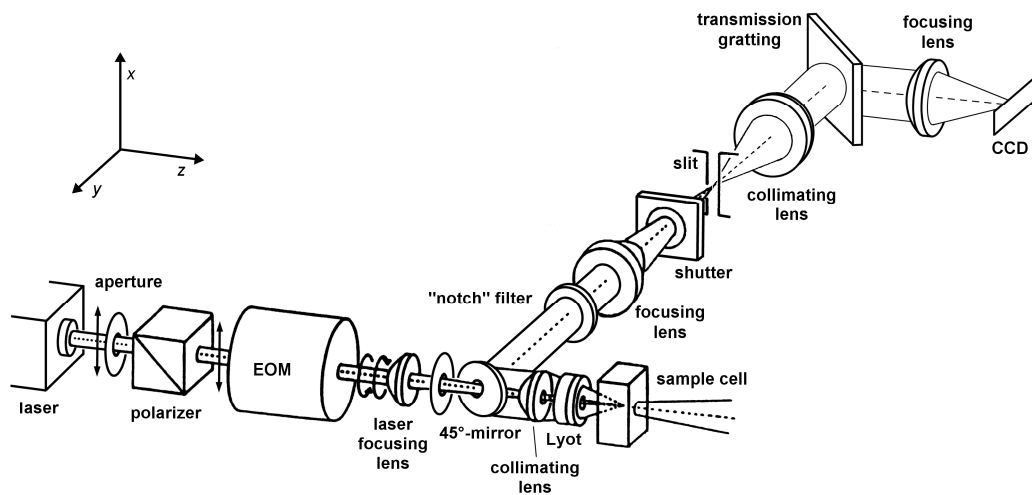
L. D. Barron, J. Raman Spectrosc. 18, 281 (1987).



W. Hug, Appl. Spectrosc. 35, 115 (1981)

Backscattering

ICP ROA Instrument



W. Hug, Raman Spectroscopy (1982)

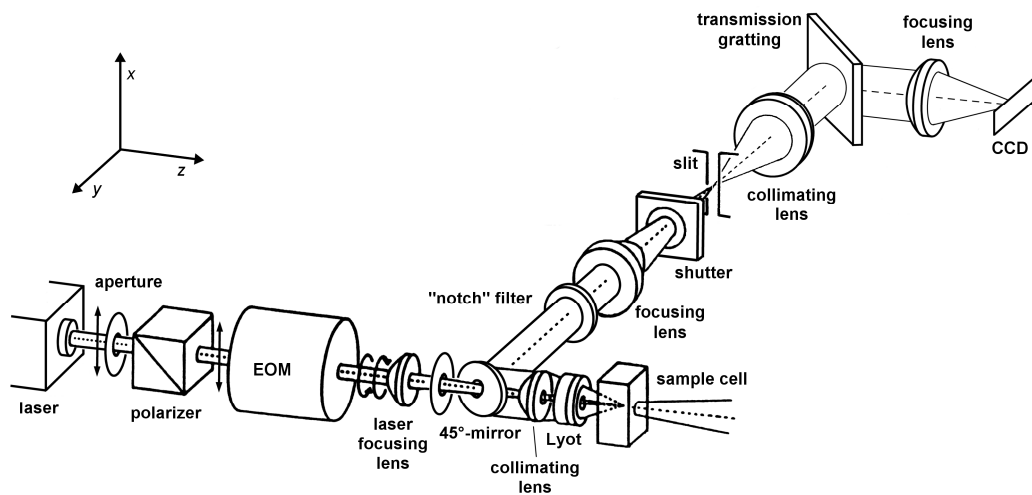
L. D. Barron, JACS 111, 8731 (1989),

L. Hecht, L. D. Barron, J. Raman Spectrosc. 23, 401 (1992),

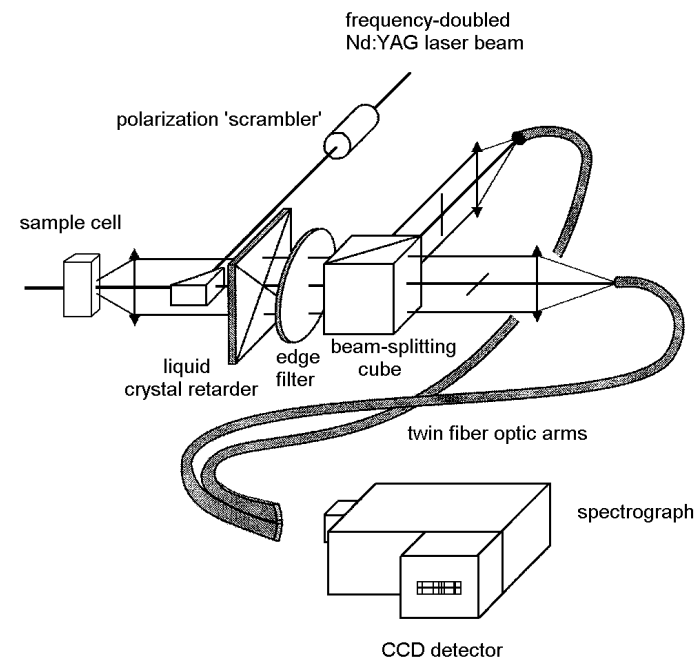
L. Hecht, L. D. Barron, J. Raman Spectrosc. 30, 815 (1999).

Backscattering

ICP ROA Instrument



SCP ROA Instrument



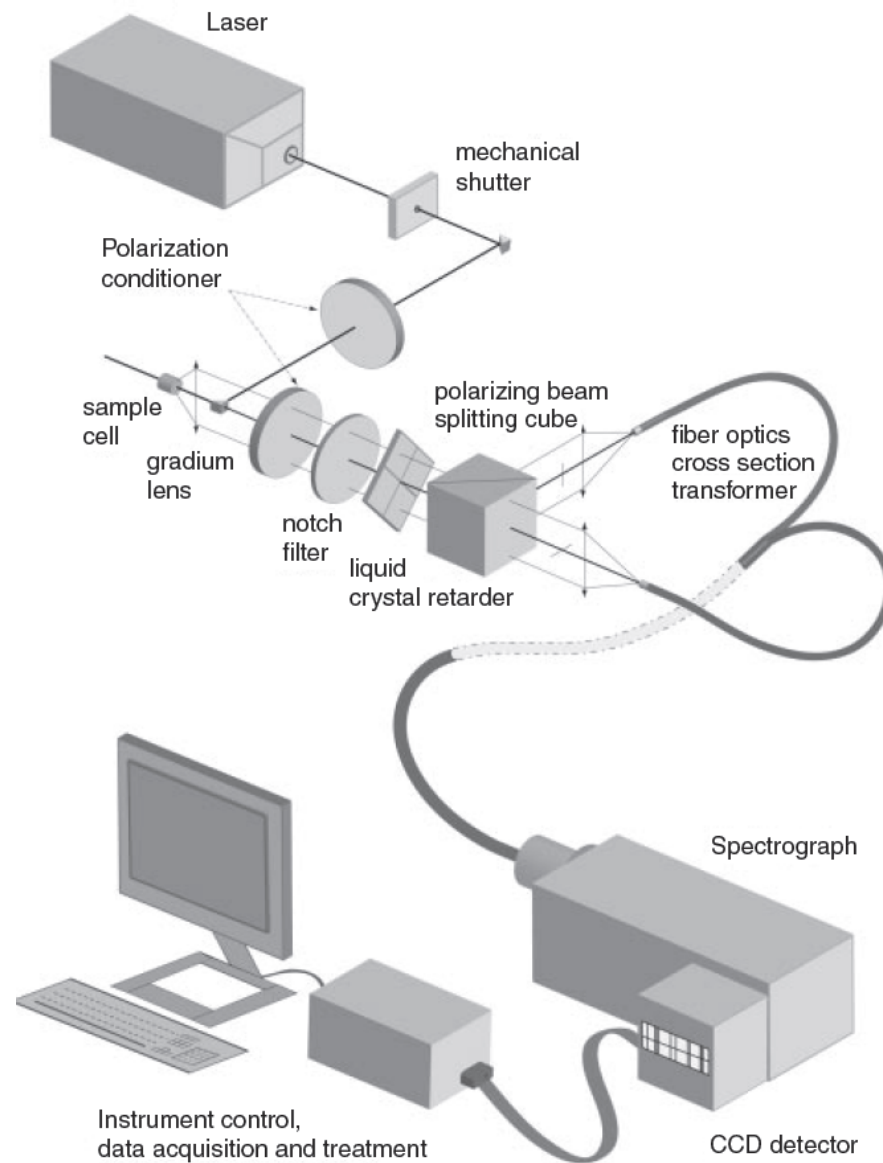
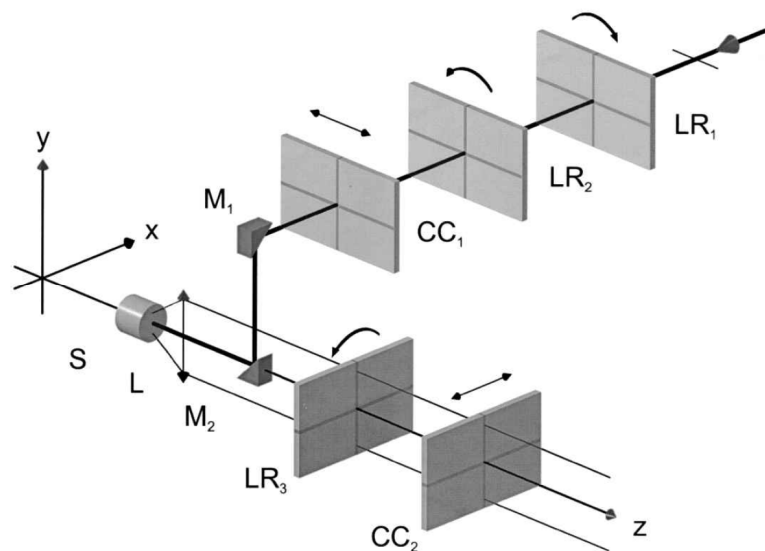
W. Hug, Raman Spectroscopy (1982)
L. D. Barron, JACS 111, 8731 (1989),
L. Hecht, L. D. Barron, J. Raman Spectrosc. 23, 401 (1992),
L. Hecht, L. D. Barron, J. Raman Spectrosc. 30, 815 (1999).

W. Hug, J. Raman Spectrosc. 30, 841 (1999).
W. Hug, Comprehensive Chiroptical Spectroscopy, Vol. I (2012)

State-of-the-art ROA spectrometer

W. Hug, J. Raman Spectrosc. 30, 841 (1999).

W. Hug, Appl. Spectrosc. 57, 1 (2003)



Building blocks of an SCP ROA spectrometer.

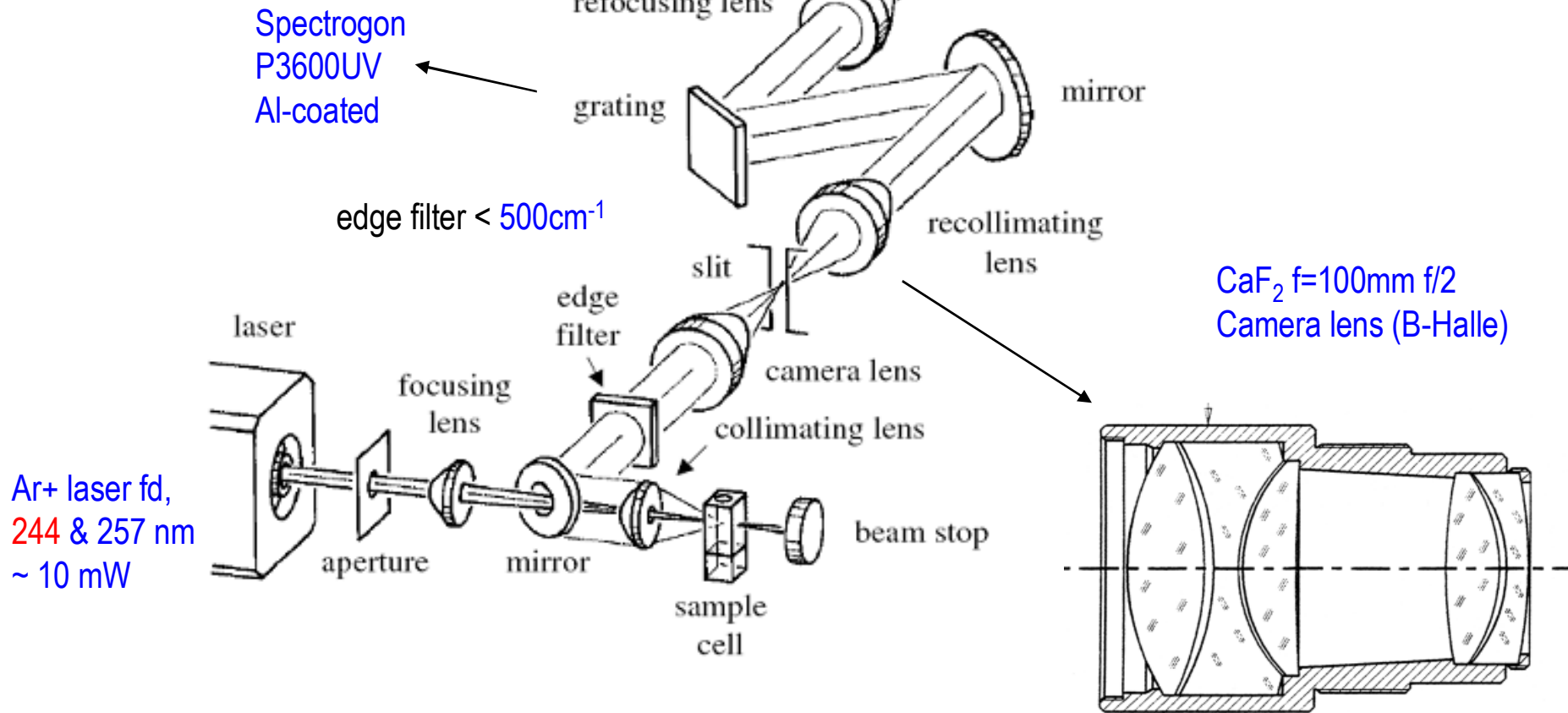


W. Hug, Comprehensive Chiroptical Spectroscopy, Vol. I, 147 (2012)

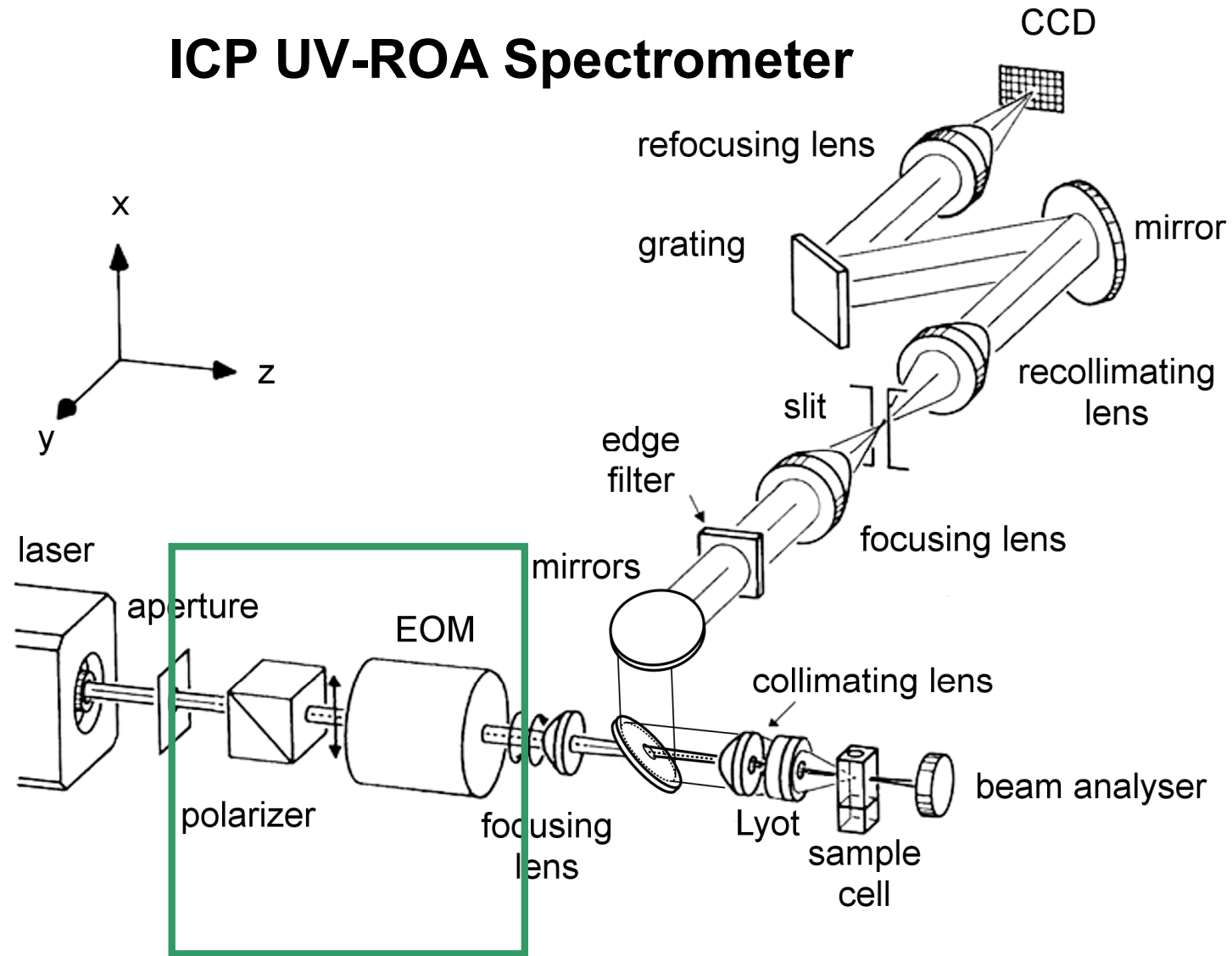
UV Raman spectrometer

Excitation wavelength 244 & 257 nm

UV enhanced CCD
576 x 256 pixels
26 μm pixels
Q.E. ~10%

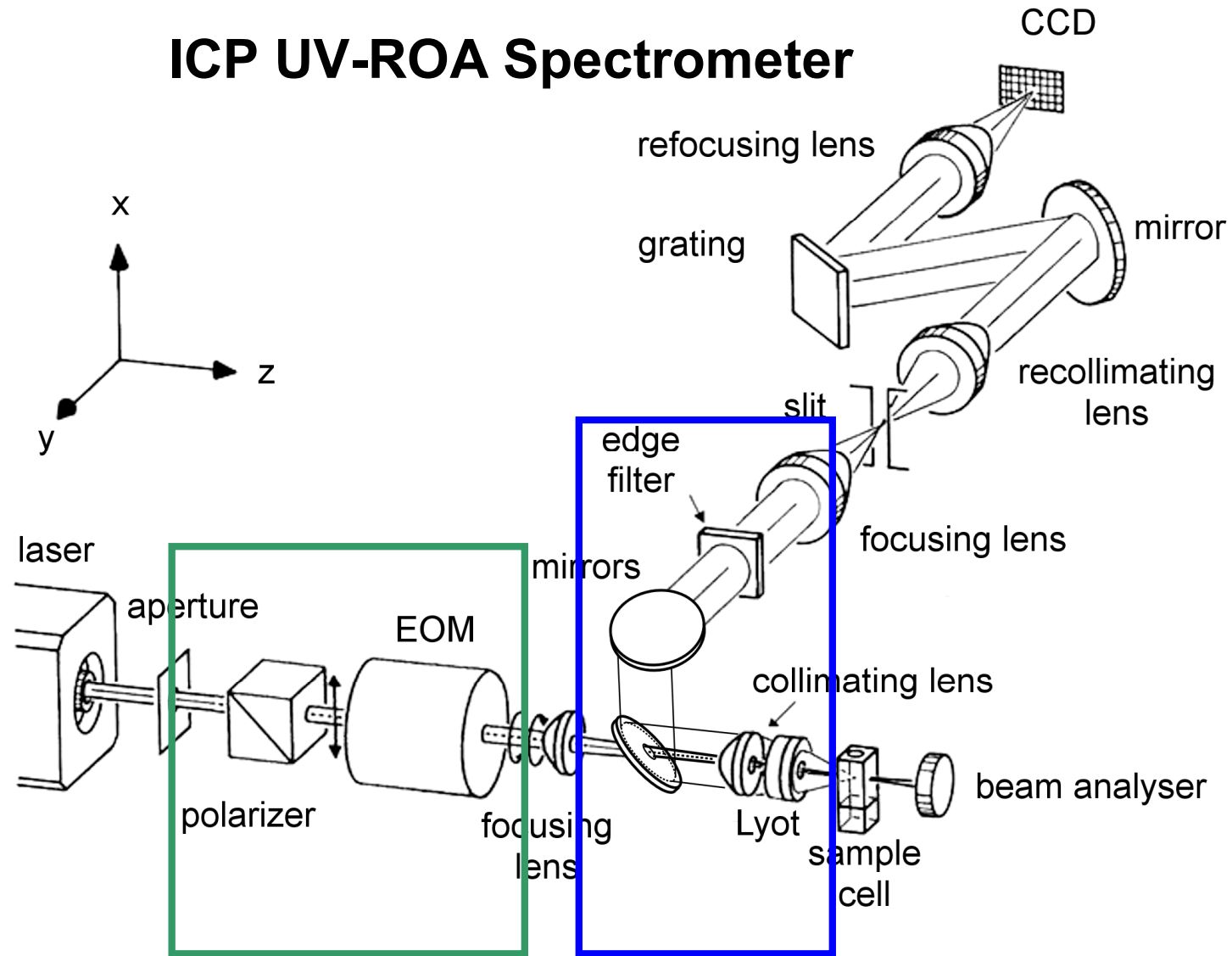


ICP UV-ROA Spectrometer



Polarization optics
for incident radiation

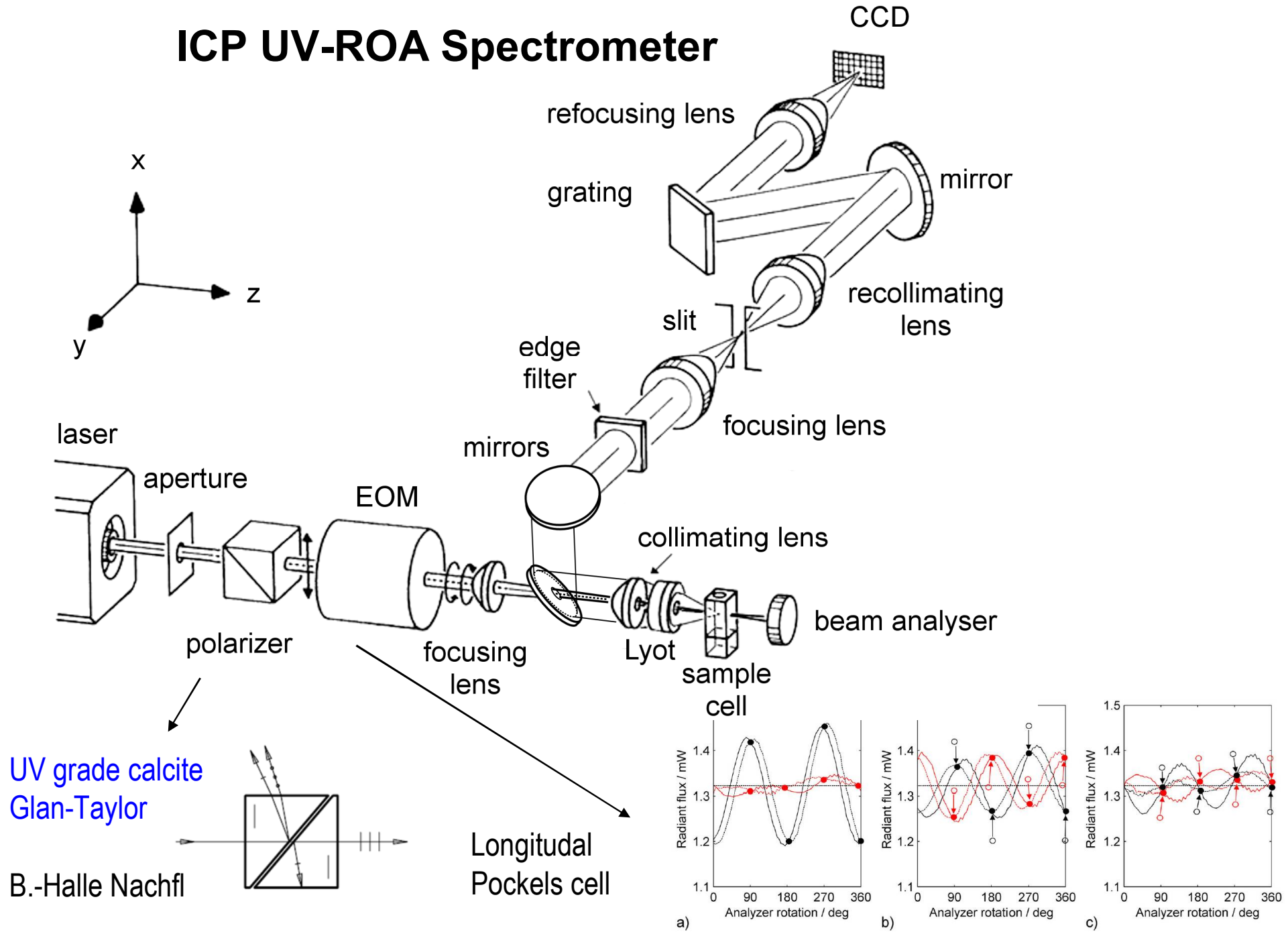
ICP UV-ROA Spectrometer



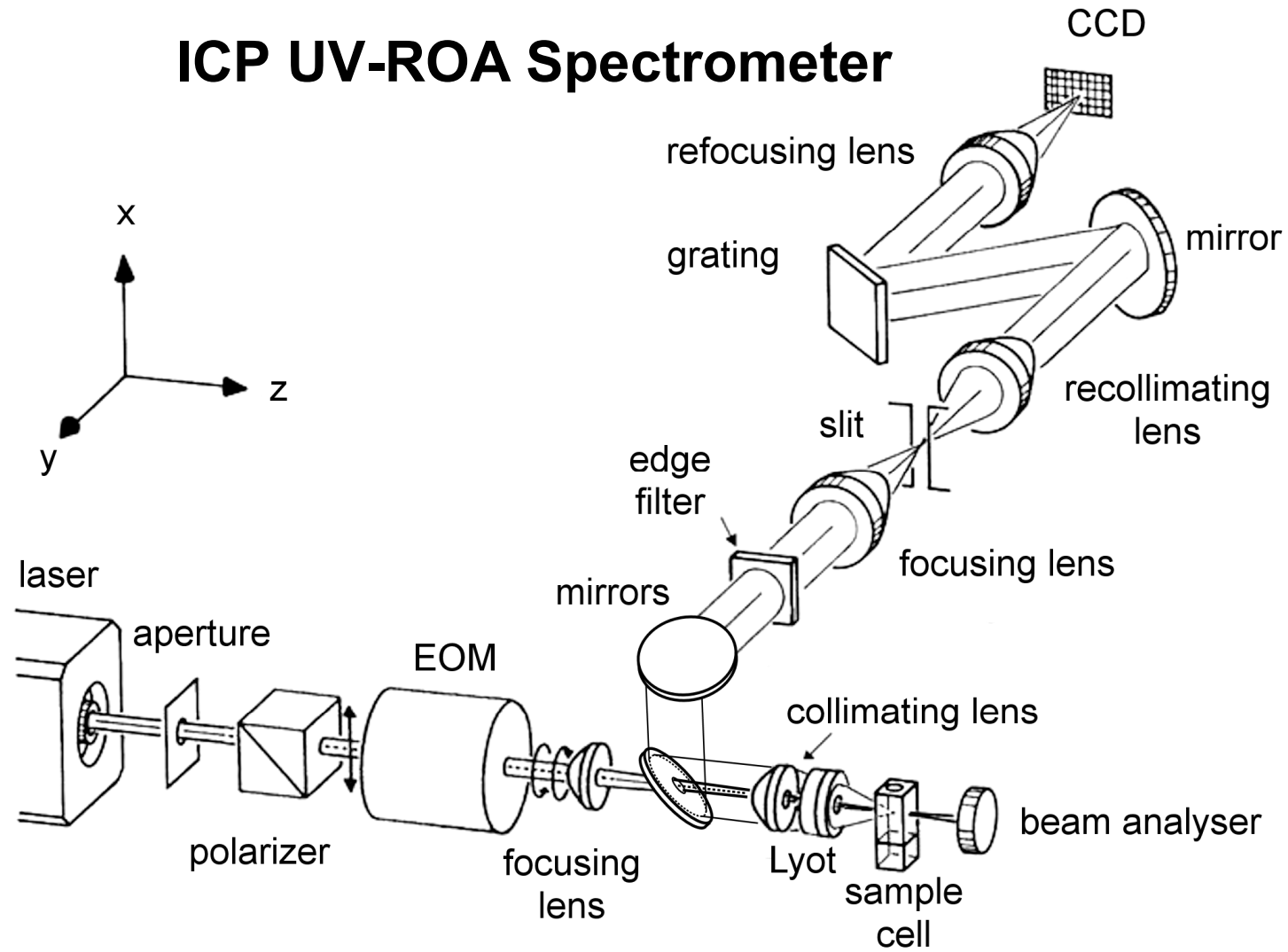
Polarization optics
for incident radiation

Optics for scattered
radiation

ICP UV-ROA Spectrometer

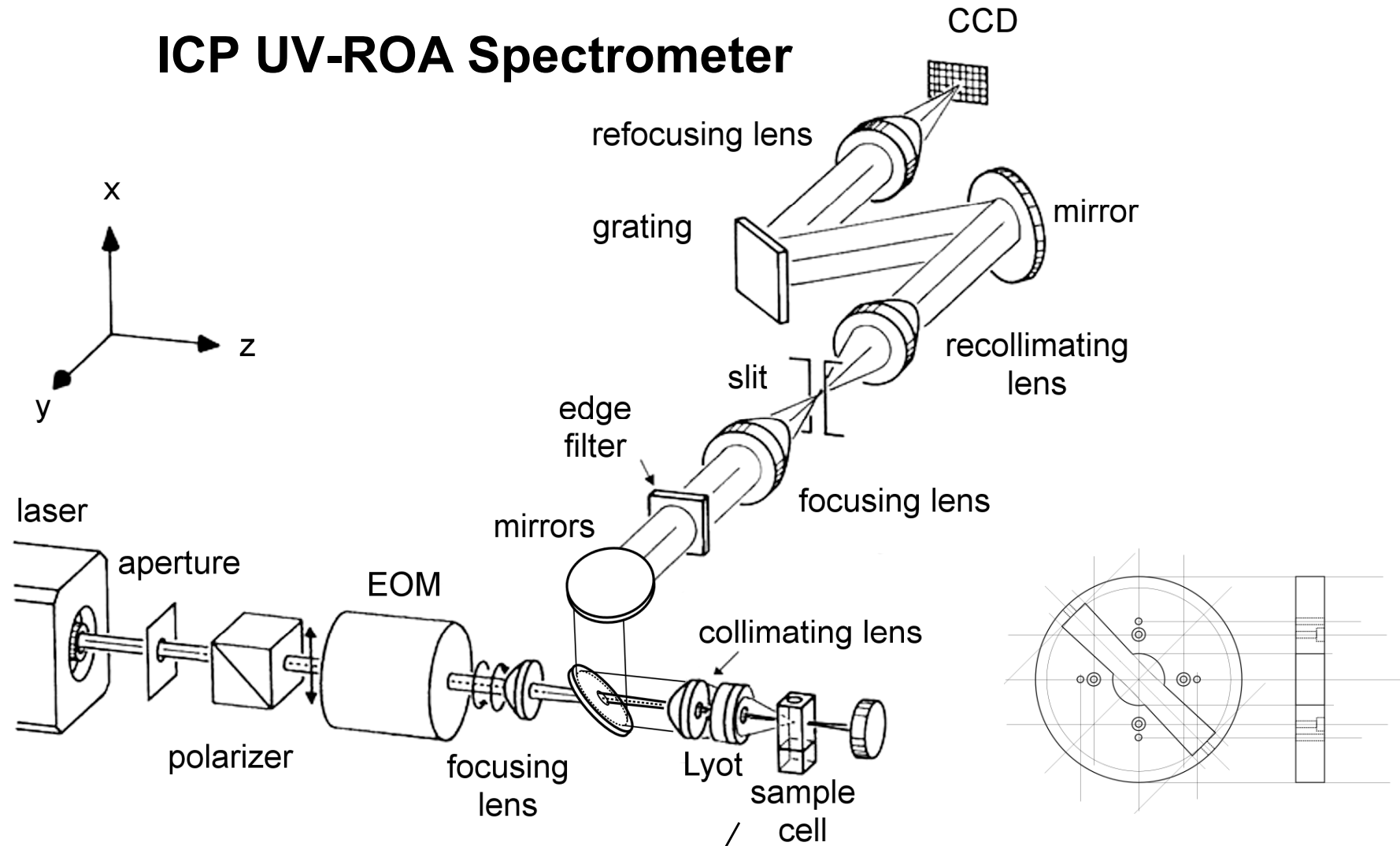


ICP UV-ROA Spectrometer



- Beam focusing
- Spatial filter

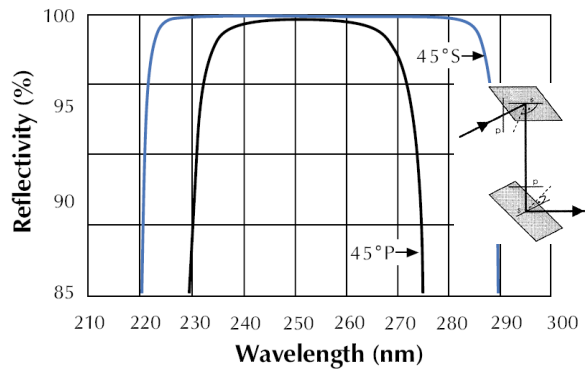
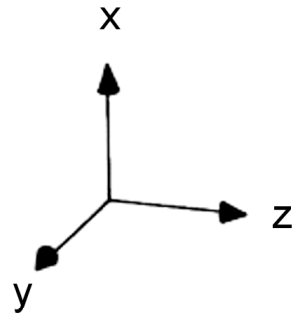
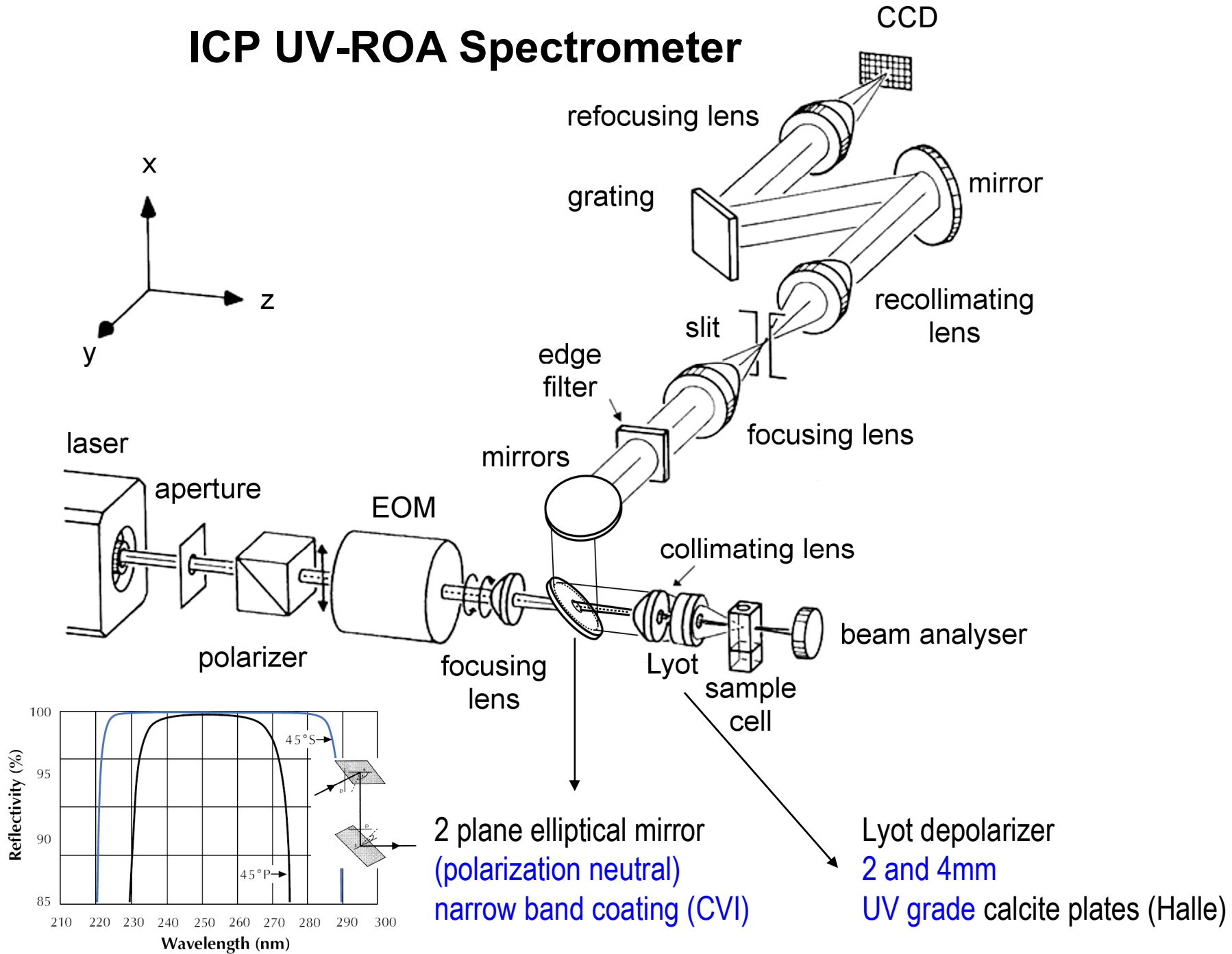
ICP UV-ROA Spectrometer



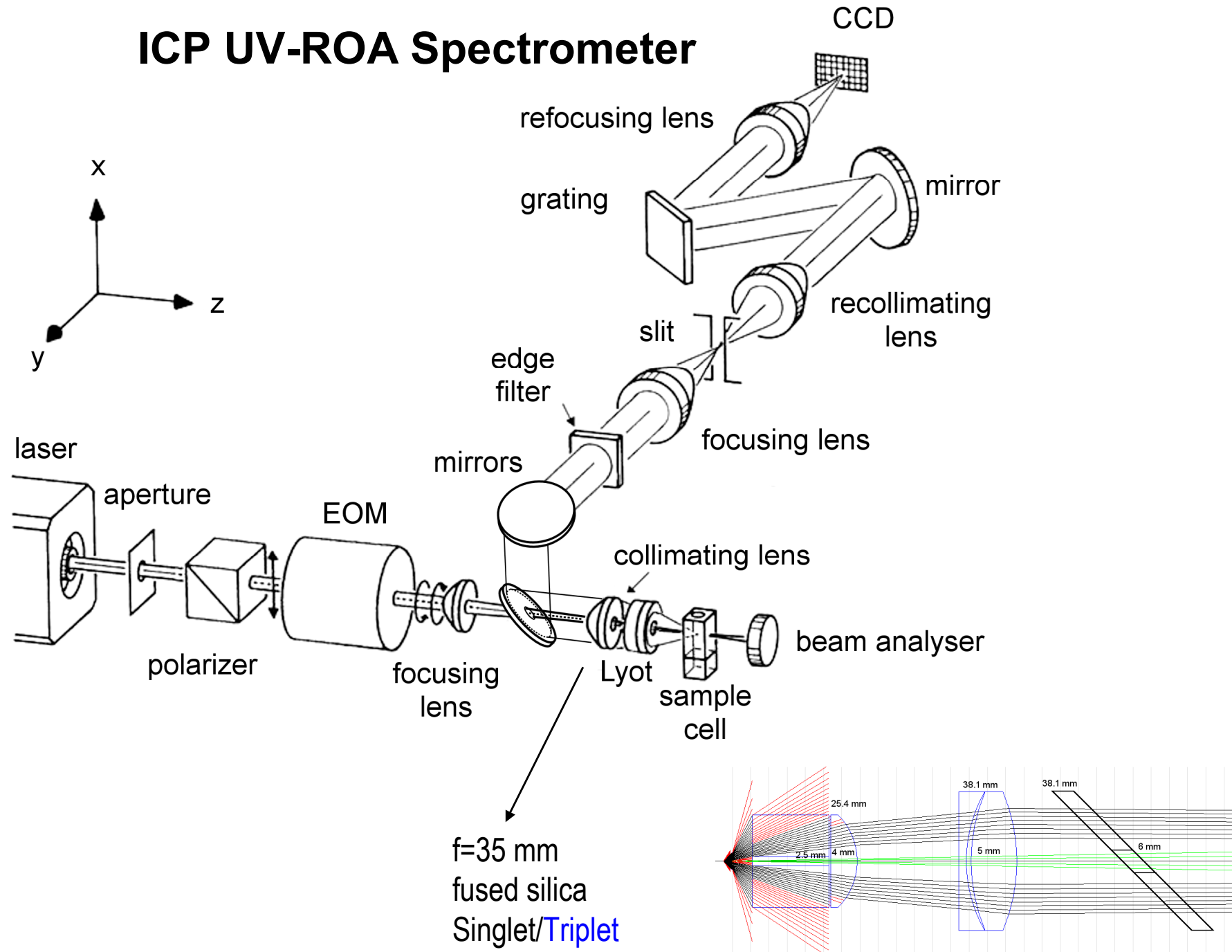
- 4x4 mm rectangular quartz cell
- Rotating cylindrical cell
10mm path, 19mm diam (~20 Hz)



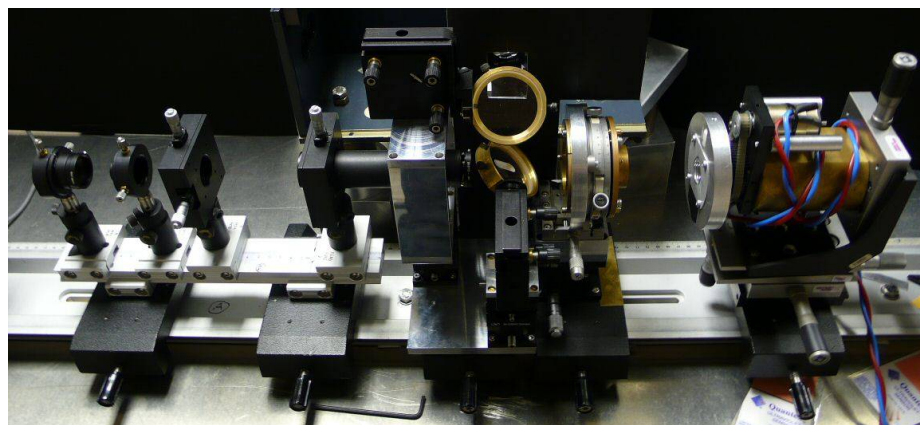
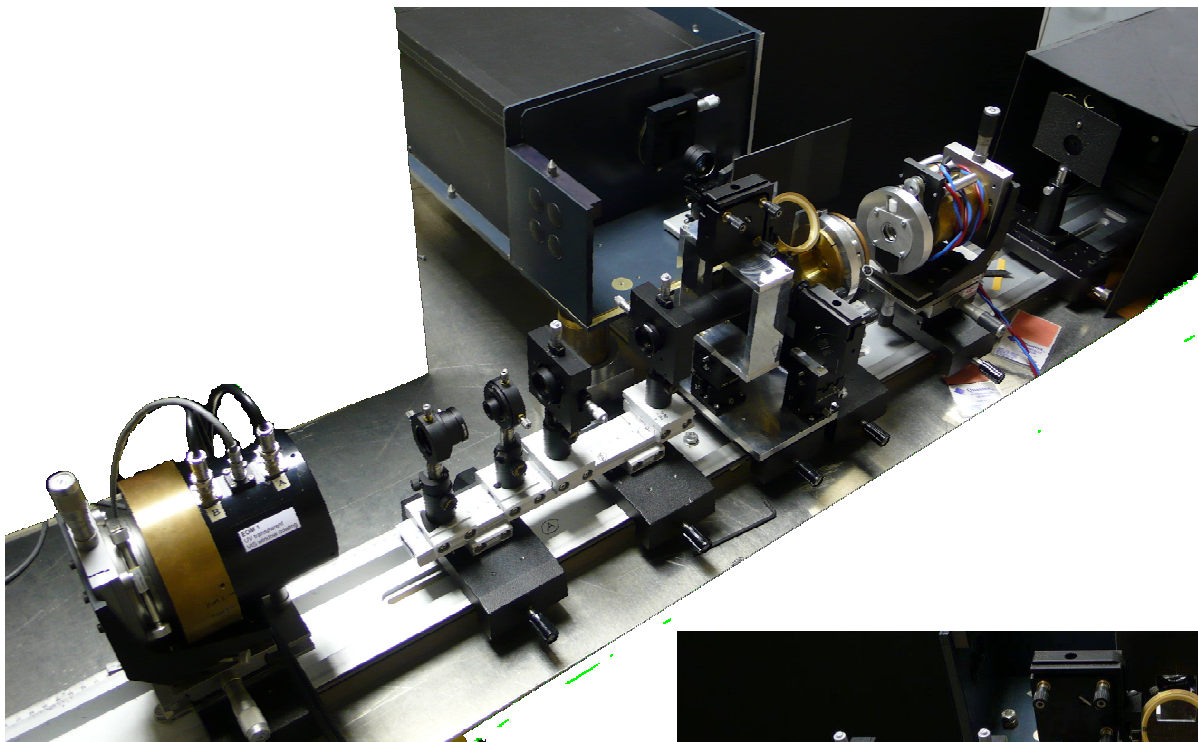
ICP UV-ROA Spectrometer



ICP UV-ROA Spectrometer

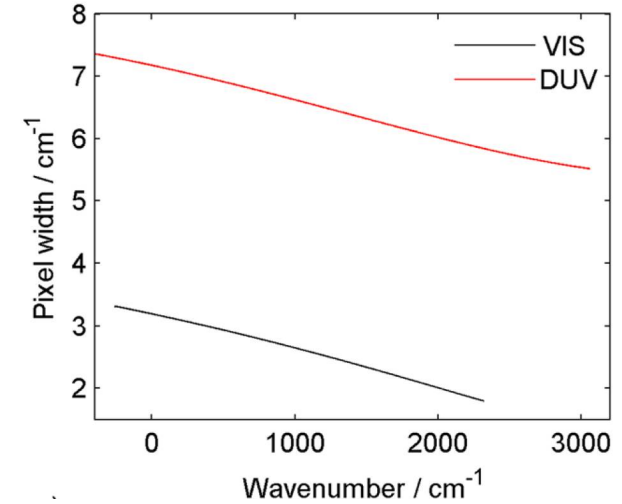


Glasgow ICP UV-ROA Spectrometer

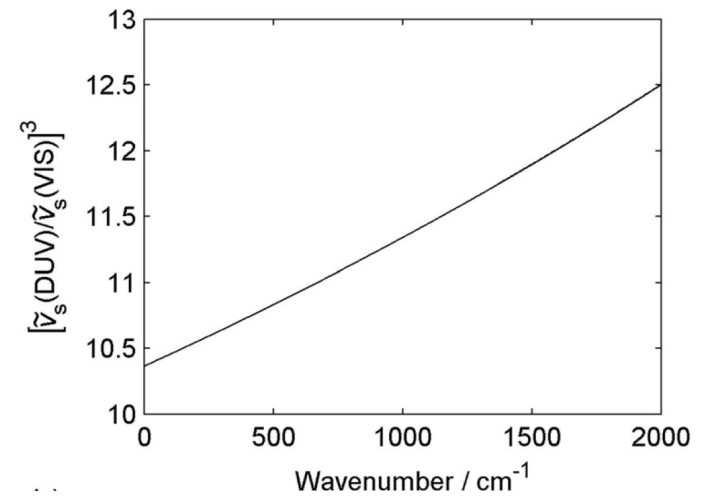


Comparison of DUV and VIS Raman Intensities

Spectral resolution / pixel width

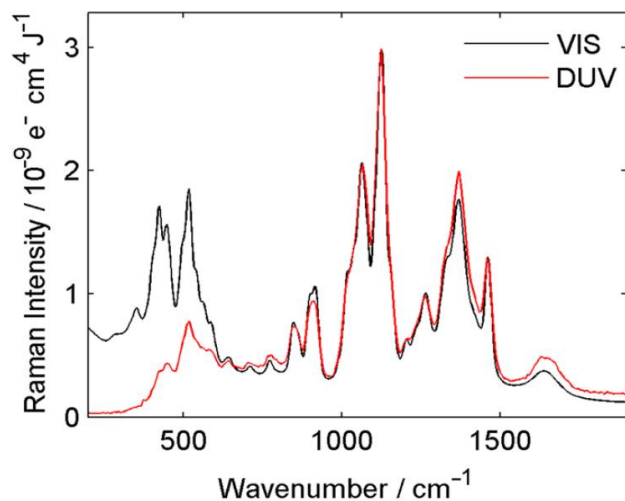


Ratio of wavenumber dependence of Raman scattering for DUV (244 nm excitation) and VIS (532 nm excitation)



Comparison of DUV and VIS Raman Intensities

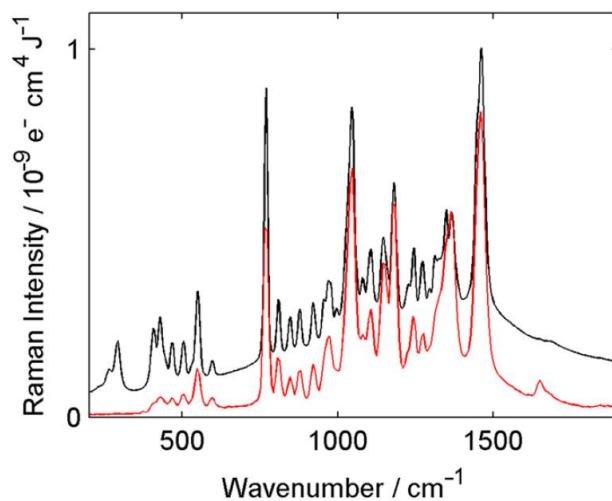
Glucose



For same laser power and accumulation time and wavenumber of scattered radiation:

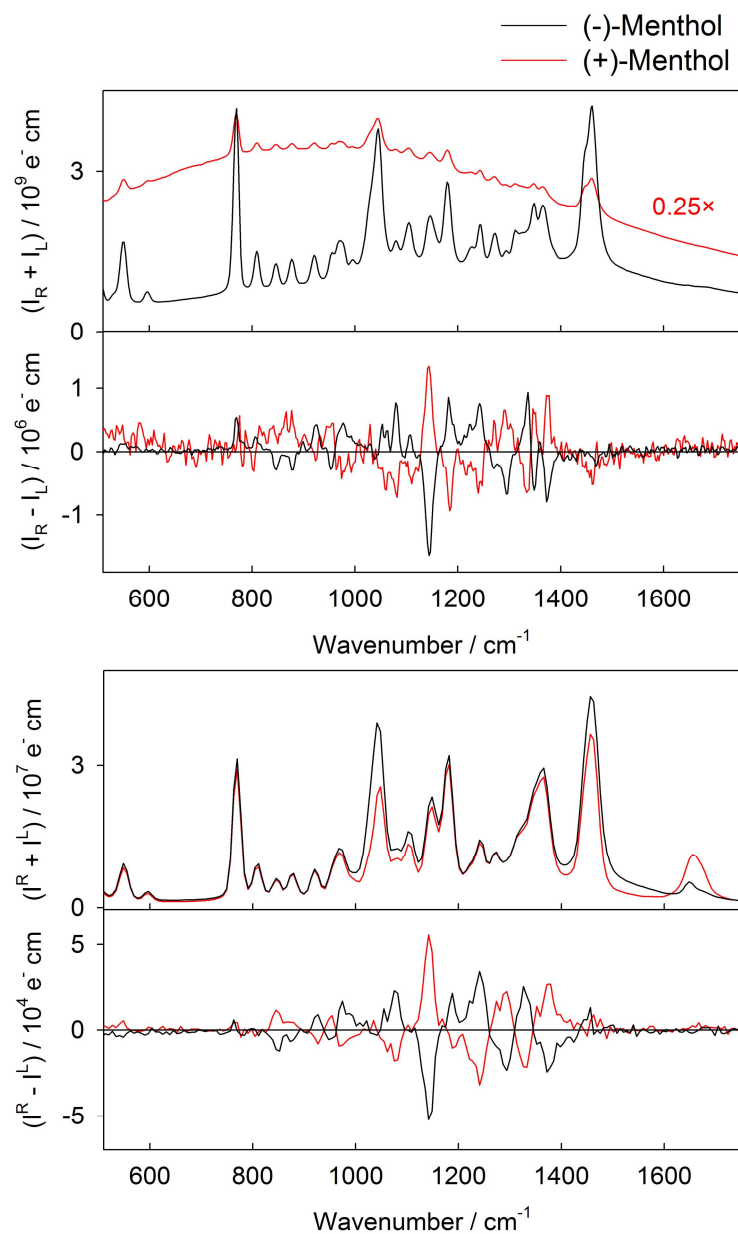
VIS/DUV ~1400

Menthol



Spectrometer element efficiency	DUV (%)	VIS (%)	Factor VIS/DUV
CCD	10	80	8
Diffraction grating	40	80	2
Lenses	50	90	1.8
Mirror, vignetting	70	95	1.4
Edge/notch filter	60	90	1.5
Polarization optics	50	70	1.4
Total:			90

ROA Spectra

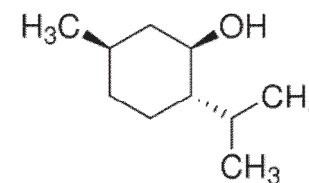


Exc. 532 nm

Exc. 244 nm

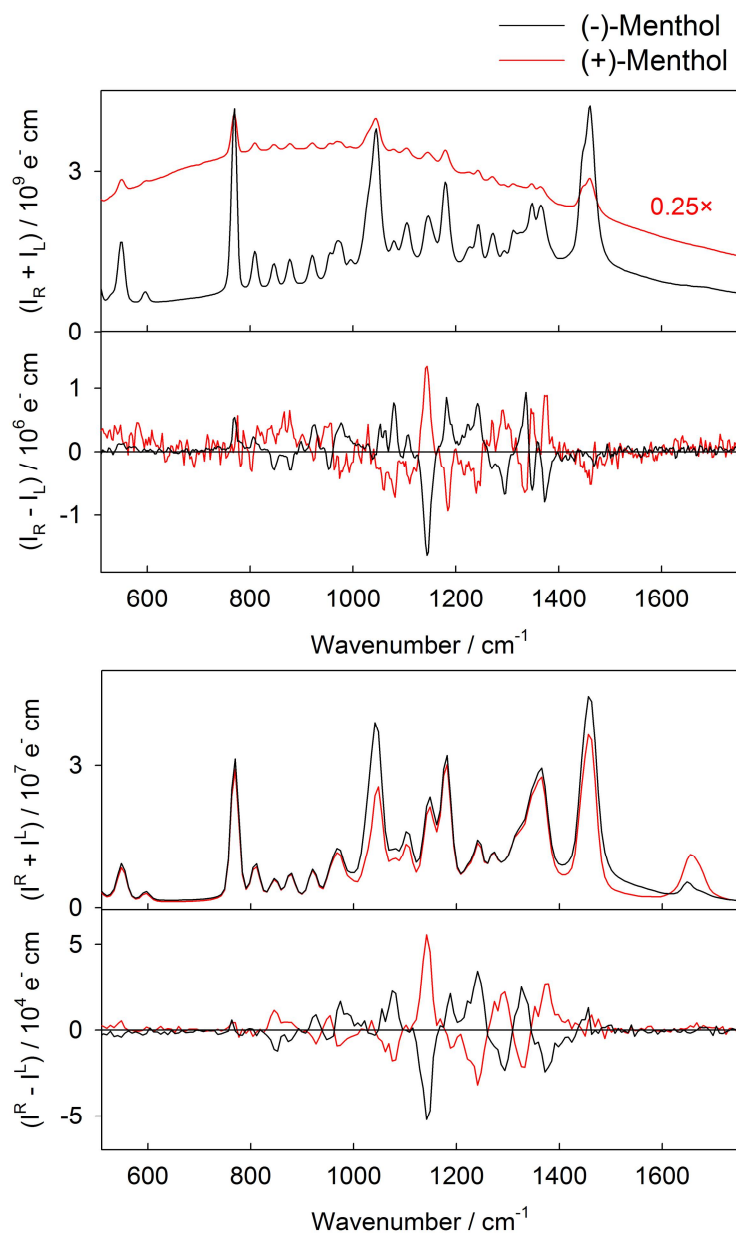
Non-absorbing samples

Menthol in methanol



Concentration	~2.3g + 1.0g Methanol
Accumulation time VIS	0.5 hours
Accumulation time UV	16 hours
Laser power VIS (532nm)	~30 mW
Laser power UV (244 nm)	~3 mW

ROA Spectra



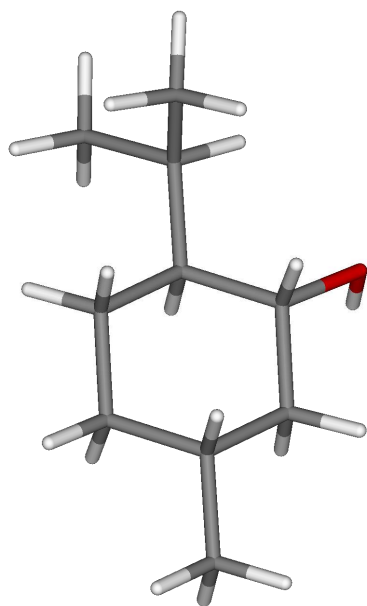
Menthol in methanol

Comparison of selected CID ratios

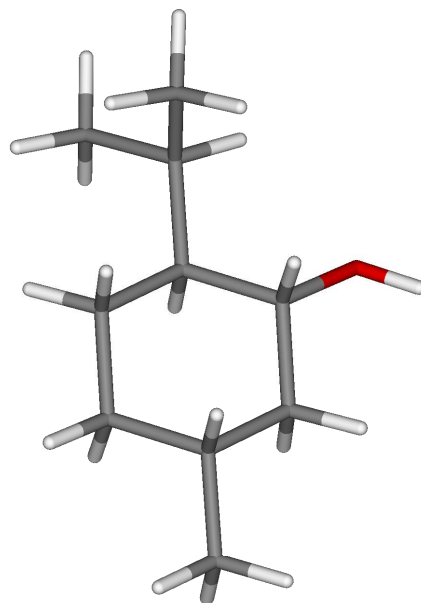
Band position/ cm^{-1}	DUV $\times 10^3$	VIS $\times 10^4$	DUV/VIS
847	-2.6	-4.2	6.2
877	-1.0	-3.6	2.8
926	2.2	8.2	2.7
954	-0.6	-3.0	2.0
972	1.7	4.5	3.8
1225	3.0	6.7	4.4
1242	3.4	6.9	4.9
1272	-1.1	-2.8	3.9
1293	-4.1	-12.2	3.4

expected values $\sim 2.2\text{--}2.5$

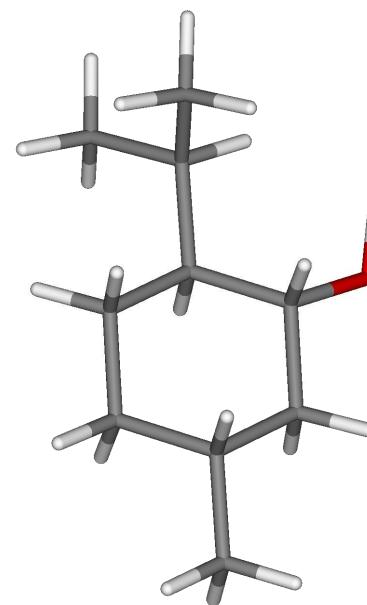
(-)-Menthol



$\Delta E = 0.0$ kcal/mol



$\Delta E = 0.0$ kcal/mol



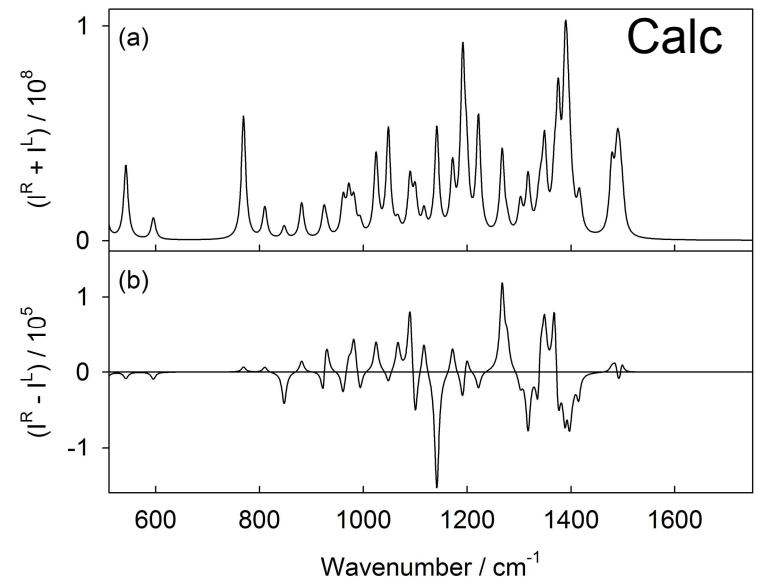
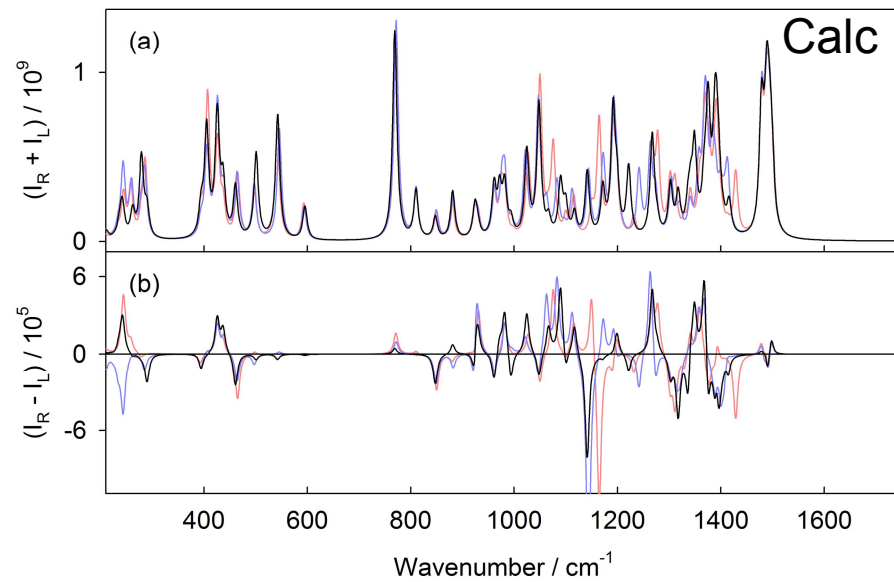
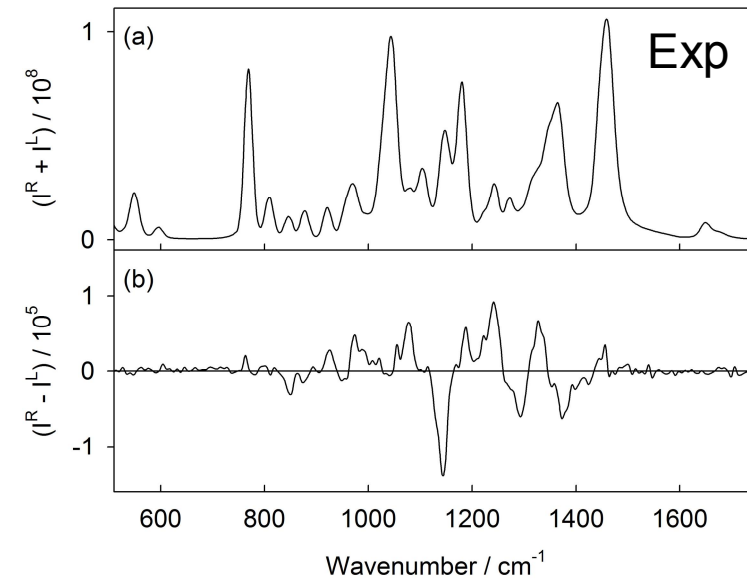
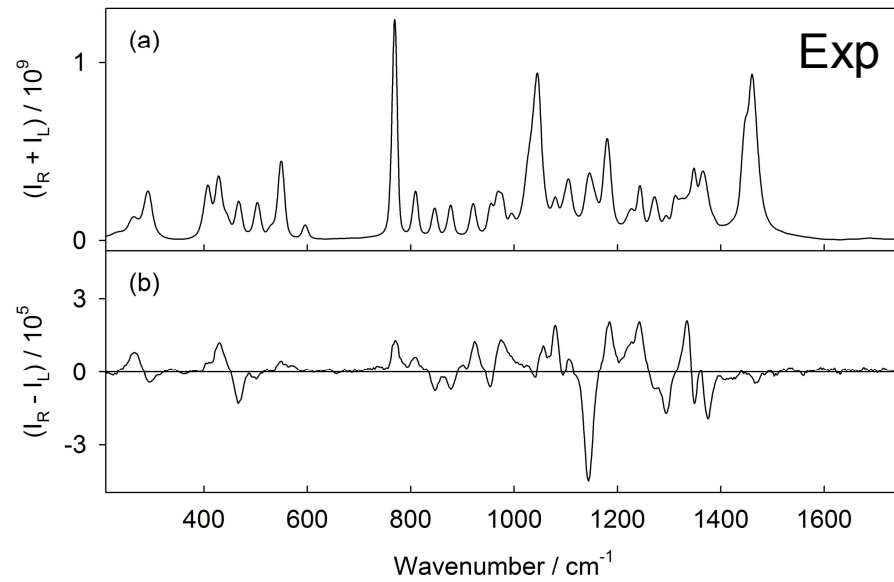
$\Delta E = 0.2$ kcal/mol

B3LYP 6-311++G** CPCM (methanol)

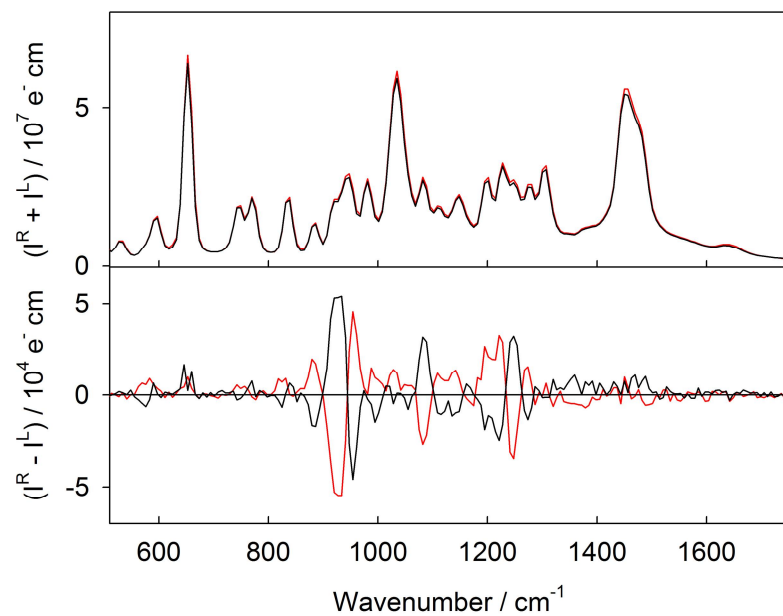
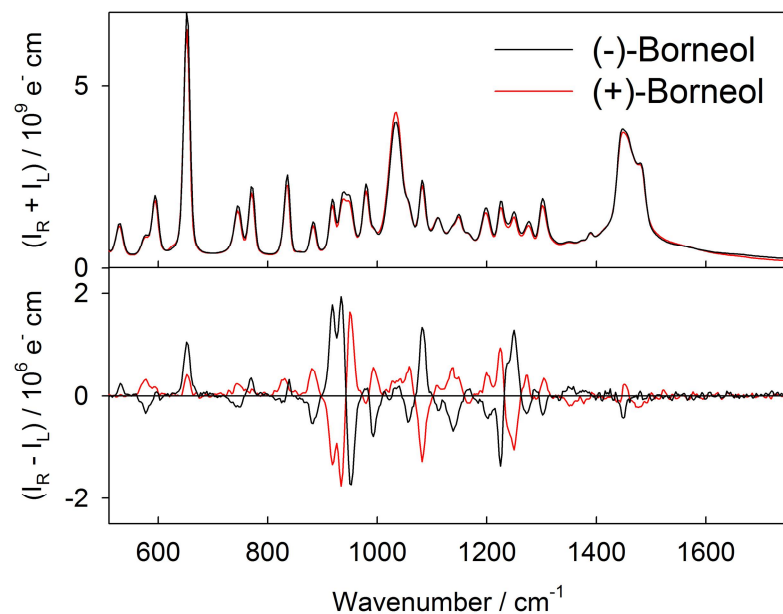
VIS

(-)-Menthol

UV



ROA Spectra



Non-absorbing samples

Borneol in methanol

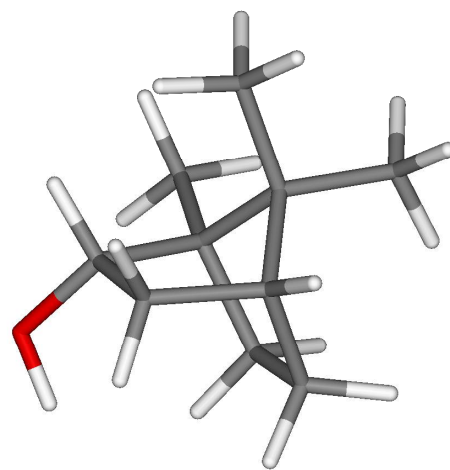


Concentration	1.0 g + 1.0 g Methanol
Accumulation time VIS	0.35 hours
Accumulation time UV	28 hours
Laser power VIS (532nm)	~80 mW
Laser power UV (244 nm)	~3 mW

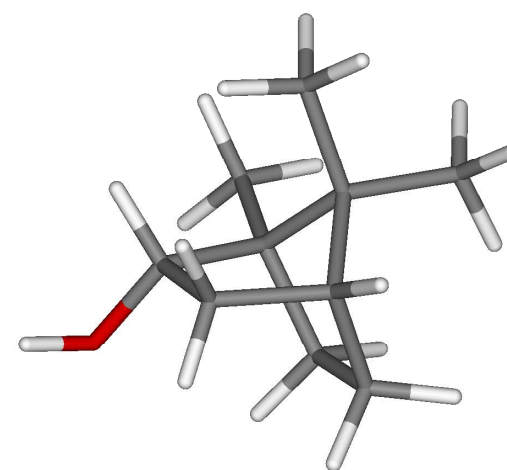
(+)-Borneol



$\Delta E = 0.0$ kcal/mol



$\Delta E = 0.4$ kcal/mol

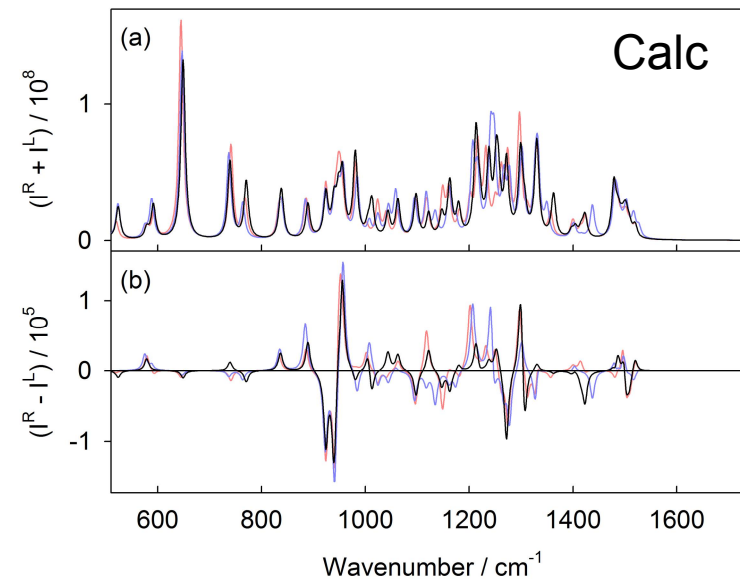
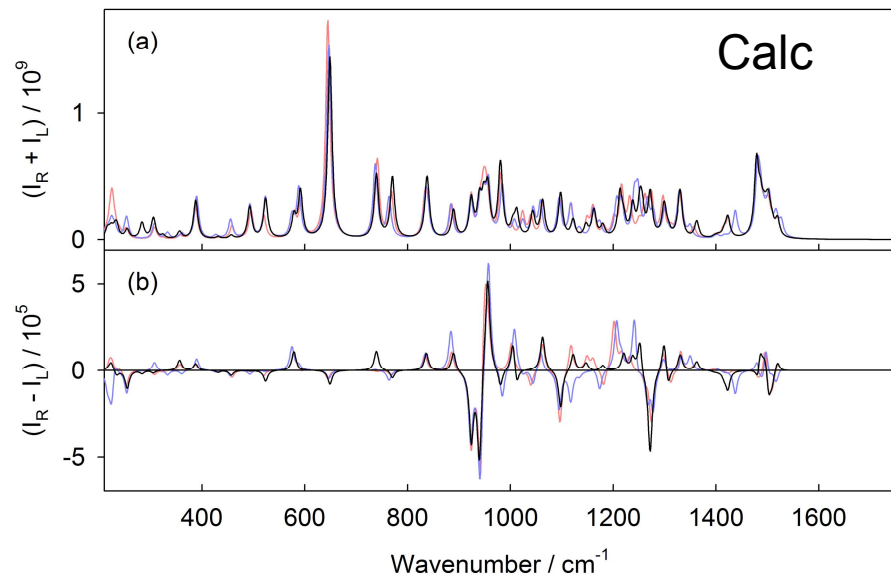
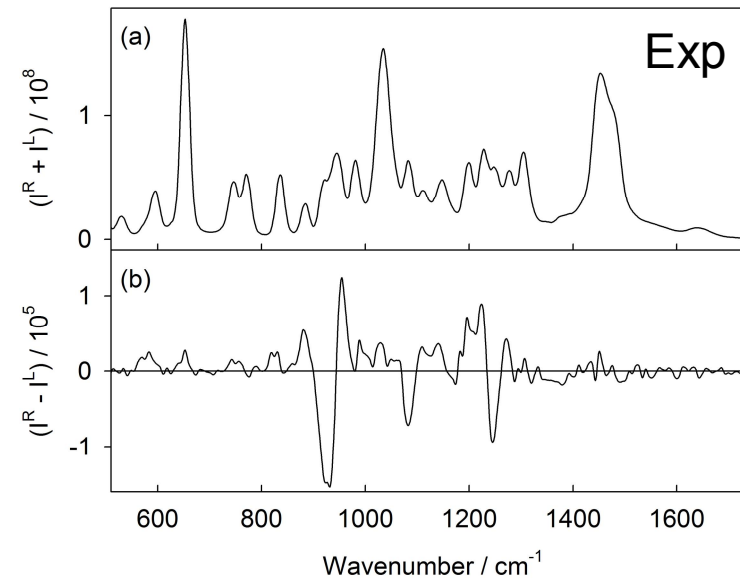
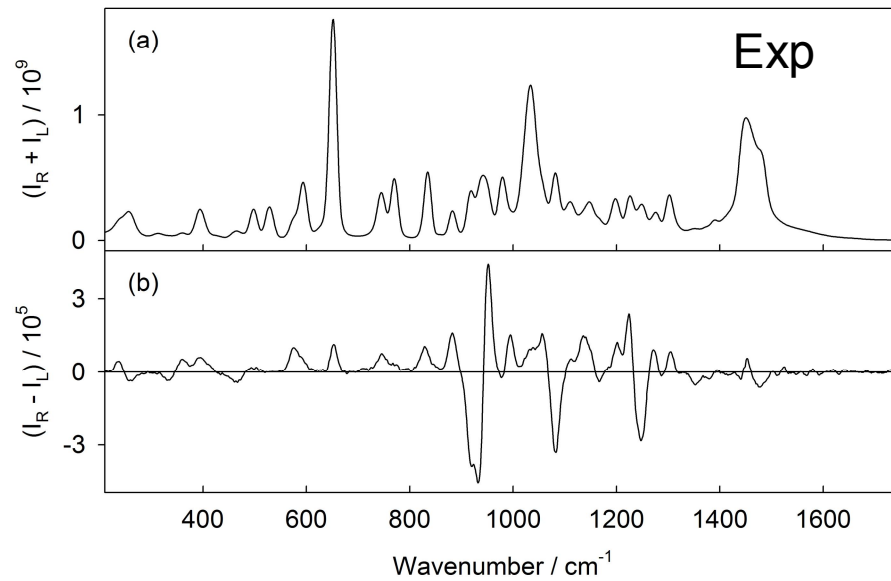


$\Delta E = 0.4$ kcal/mol

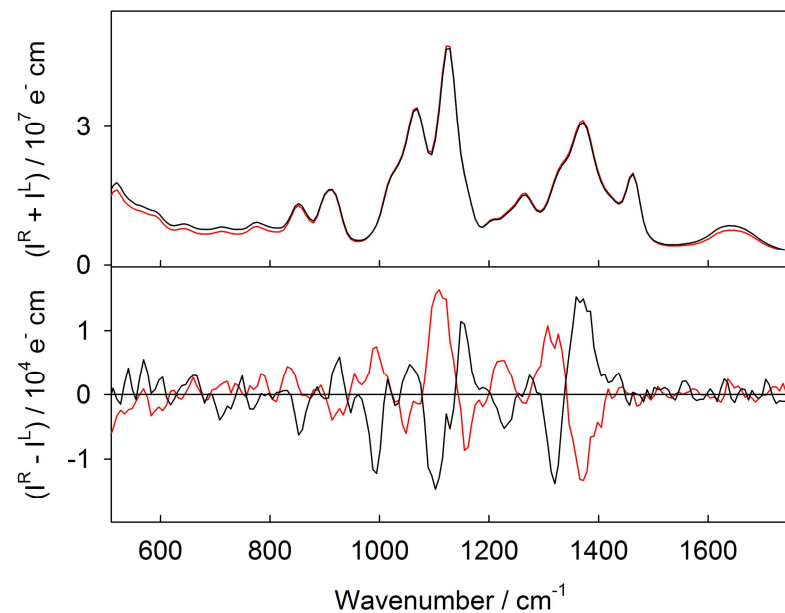
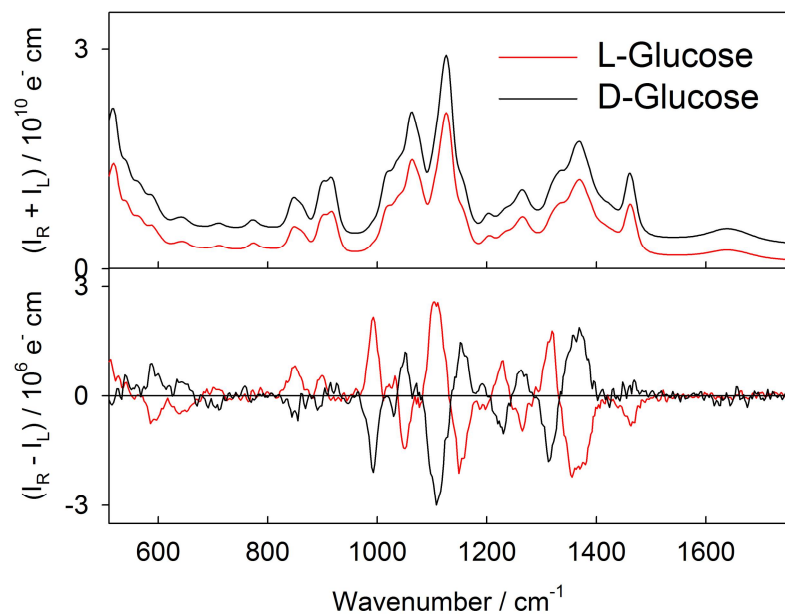
B3LYP 6-311++G** CPCM (methanol)

VIS (+)-Borneol

UV

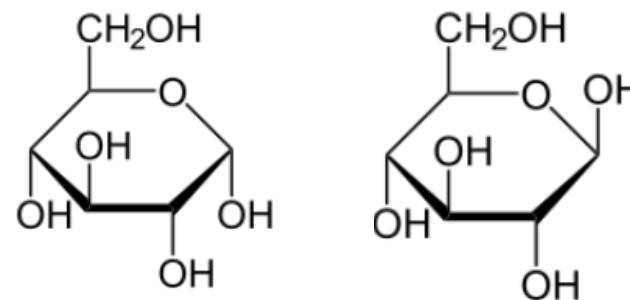


ROA Spectra



Non-absorbing samples

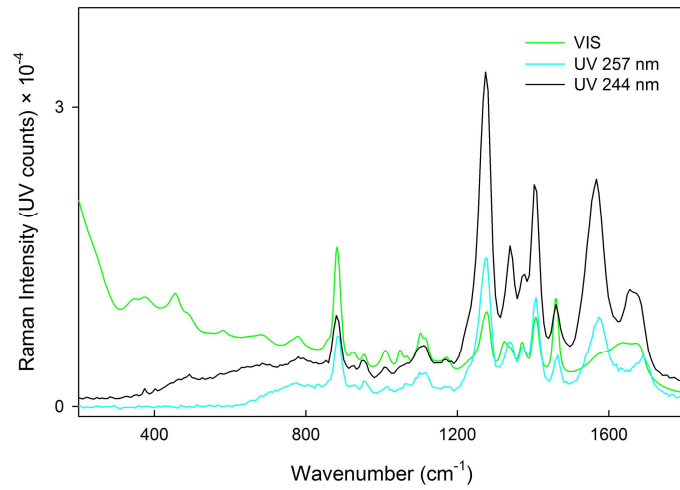
Glucose in water



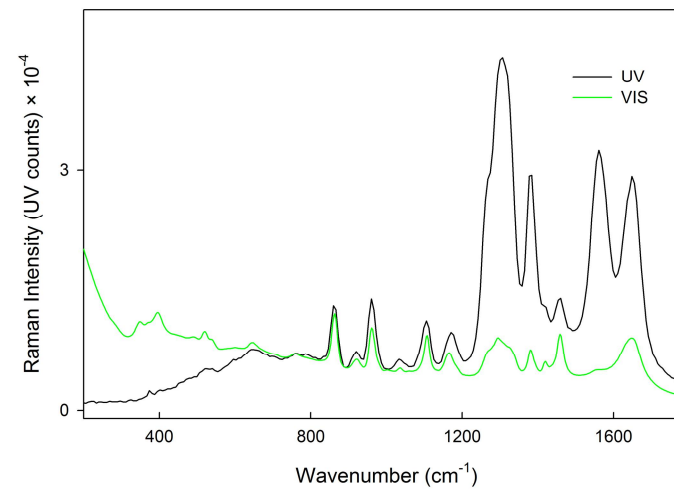
Concentration	3 mol/L
Accumulation time VIS	1 hour
Accumulation time UV	58 hours
Laser power VIS (532nm)	~240 mW
Laser power UV (244 nm)	~3 mW

Enhancement estimate of preresonance samples

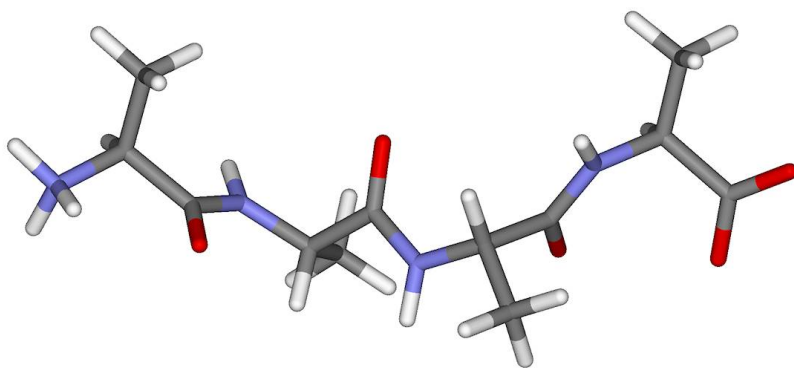
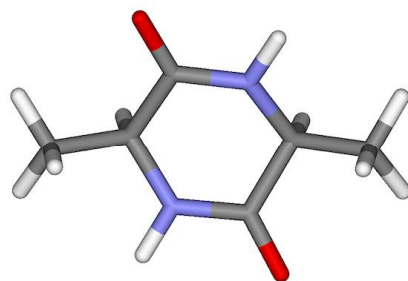
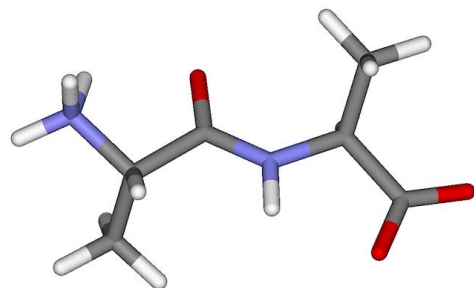
L-Ala-L-Ala (0.5 mol/L)



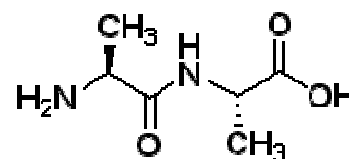
Ac-Ala-NHCH₃ (0.5 mol/L)



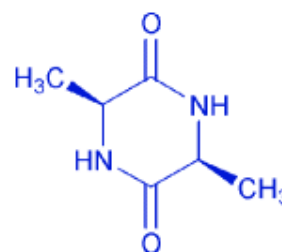
ROA Spectra



Absorbing samples



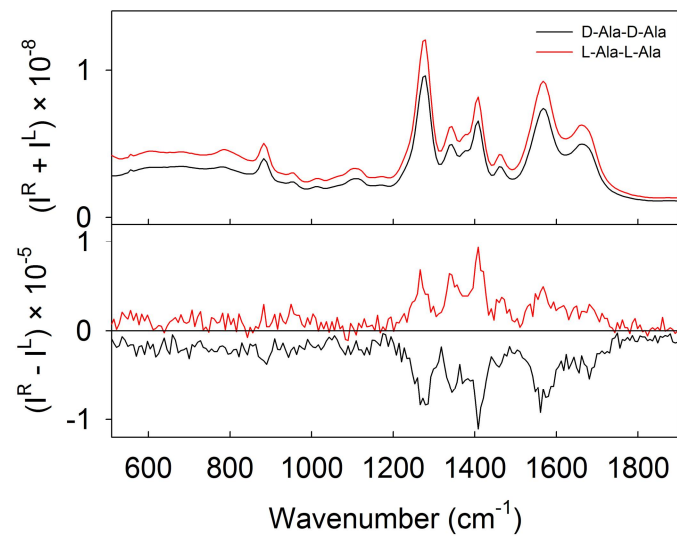
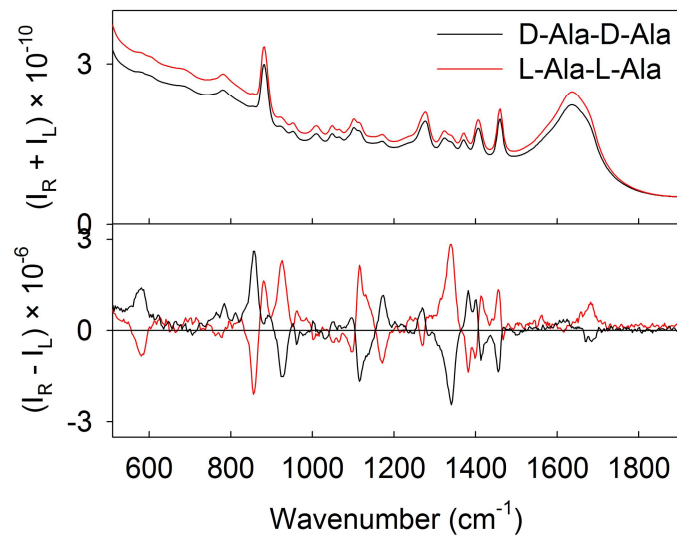
Ala-Ala



cyclo(Ala-Ala)

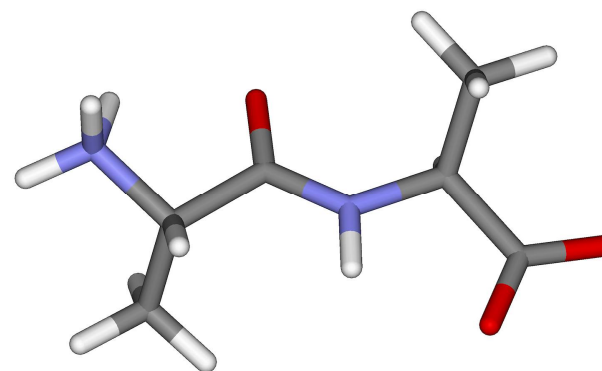
Ala-Ala-Ala-Ala

ROA Spectra



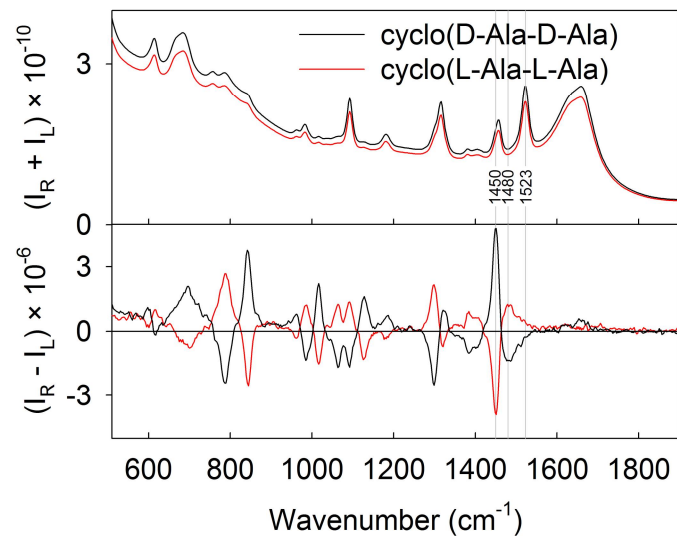
Absorbing samples

Ala-Ala

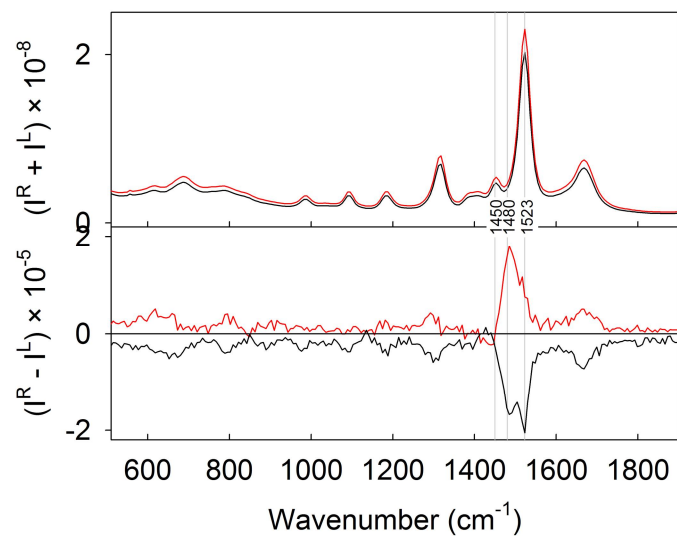


Concentration	0.125 mol/L
Accumulation time VIS	41 hours
Accumulation time UV	46 hours
Laser power VIS (532nm)	320 mW
Laser power UV (244 nm)	~4 mW

ROA Spectra



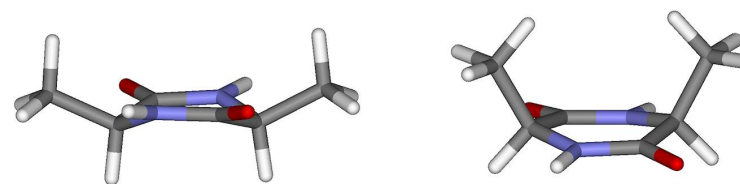
Exc. 532 nm



Exc. 244 nm

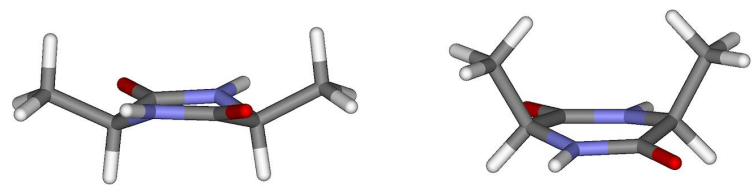
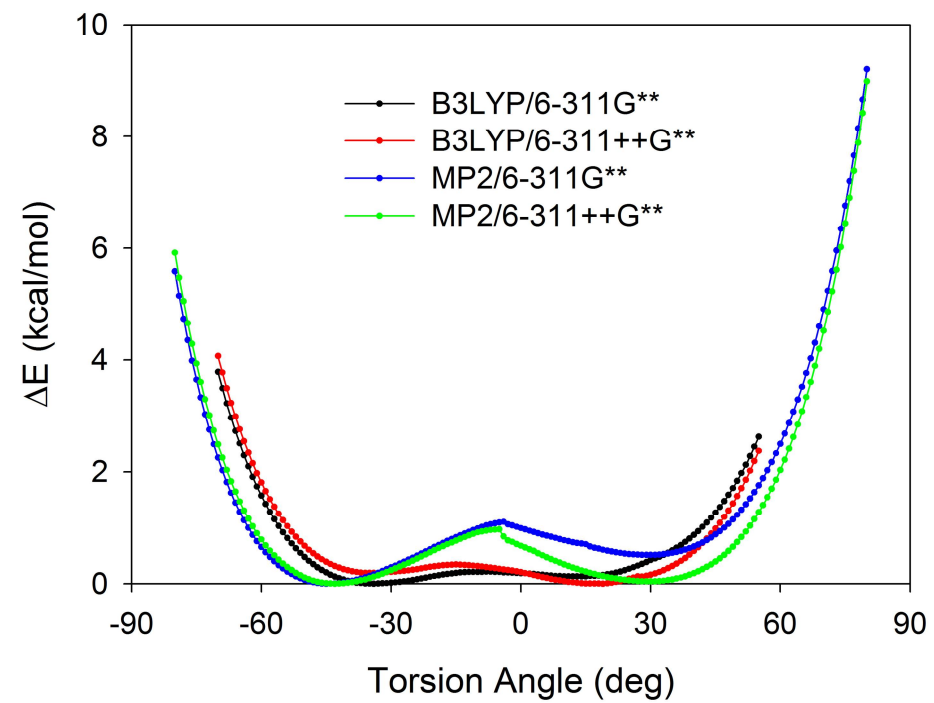
Absorbing samples

cyclo(Ala-Ala)

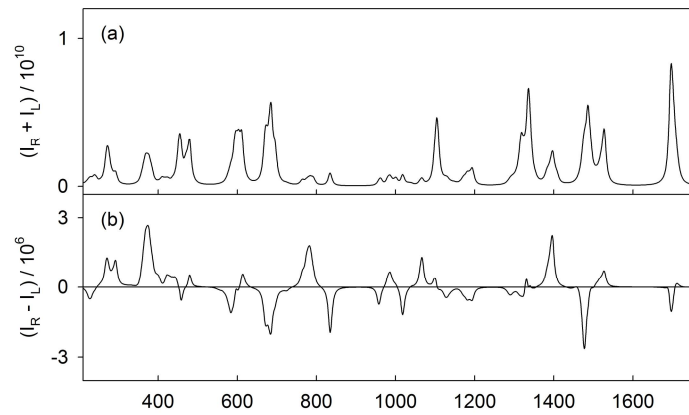
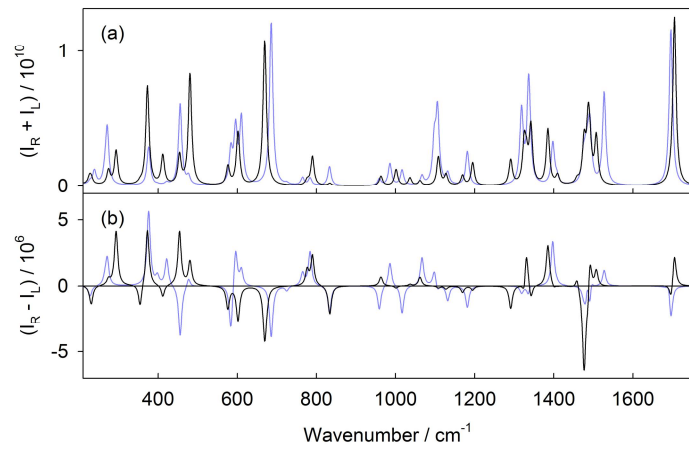
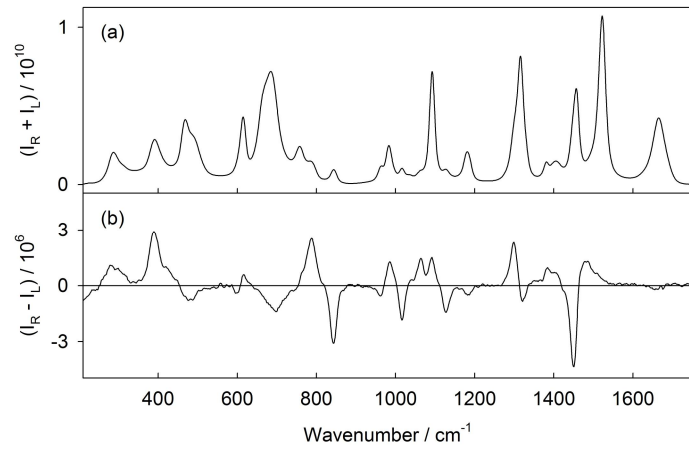


Concentration	0.1 mol/L (15 mg/mL)
Accumulation time VIS	45 hours
Accumulation time UV	40 hours
Laser power VIS (532nm)	320 mW
Laser power UV (244 nm)	3.5 mW

cyclo(Ala-Ala)



VIS



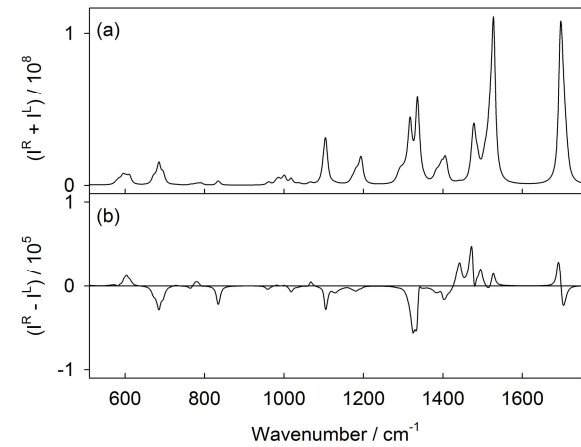
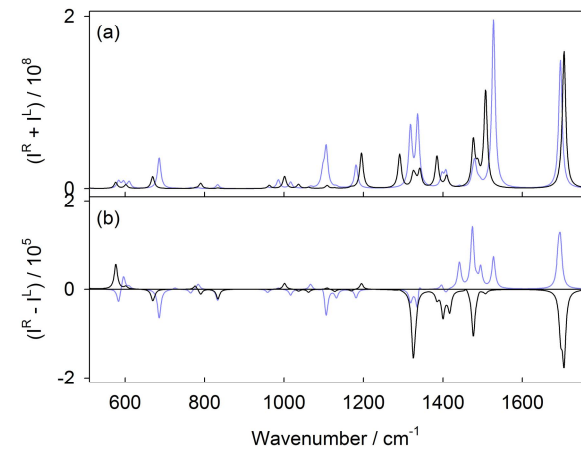
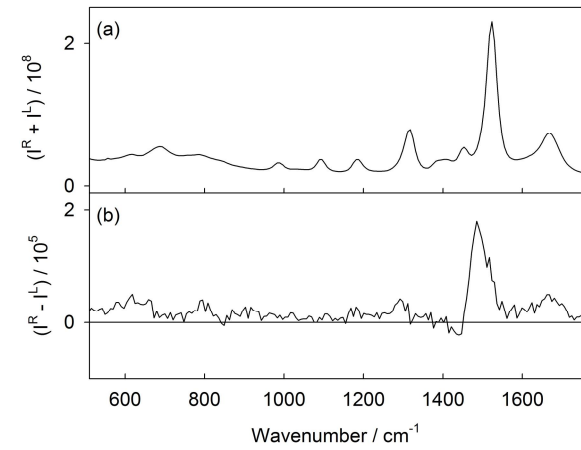
cyclo(Ala-Ala)

Experiment

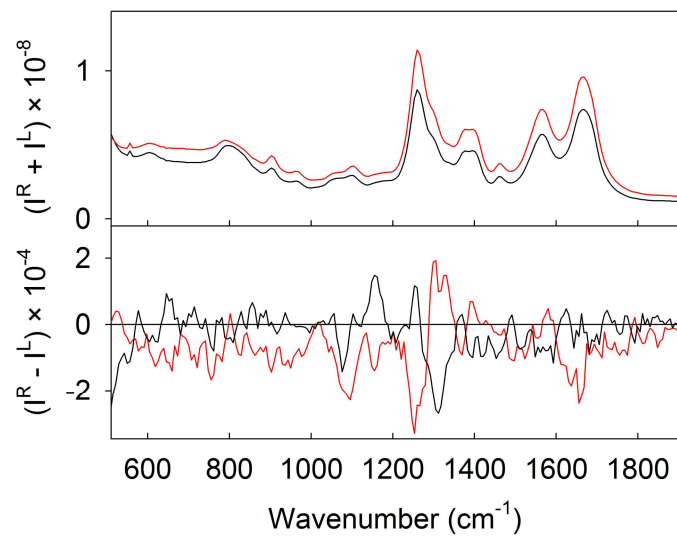
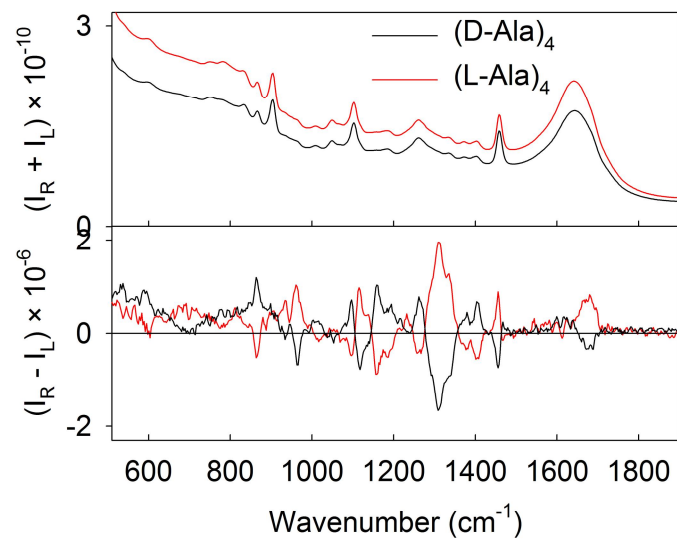
2 conformations

Boltzmann average

UV

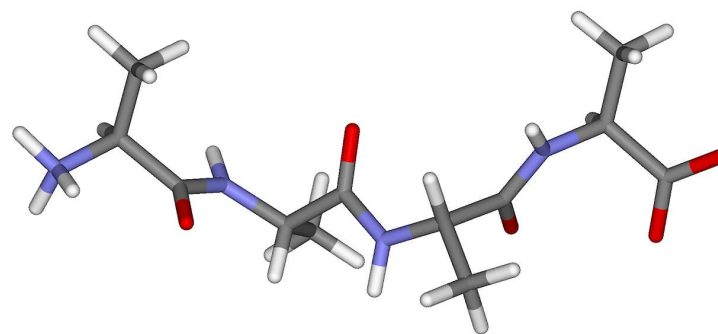


ROA Spectra



Absorbing samples

Ala-Ala-Ala-Ala



Exc. 532 nm

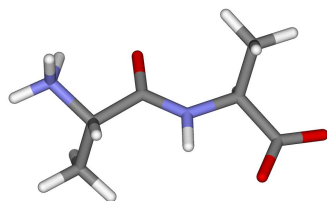
Exc. 244 nm

Concentration	15 mg/mL (0.04 mol/L)
Accumulation time VIS	39 hours
Accumulation time UV	106 hours
Laser power VIS (532nm)	320 mW
Laser power UV (244 nm)	3 mW

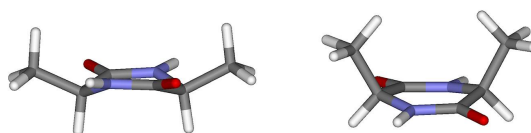
UV/VIS ROA Spectra

Absorbing samples

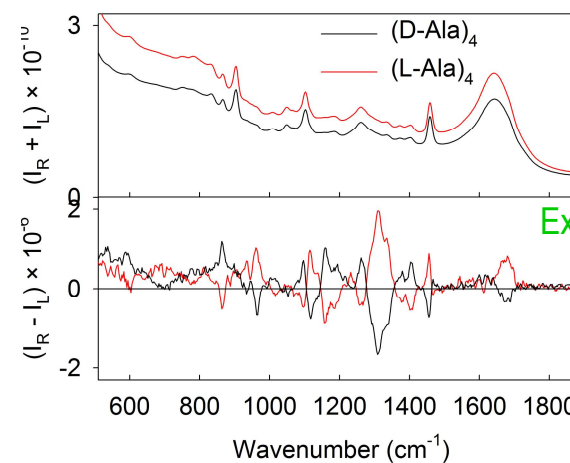
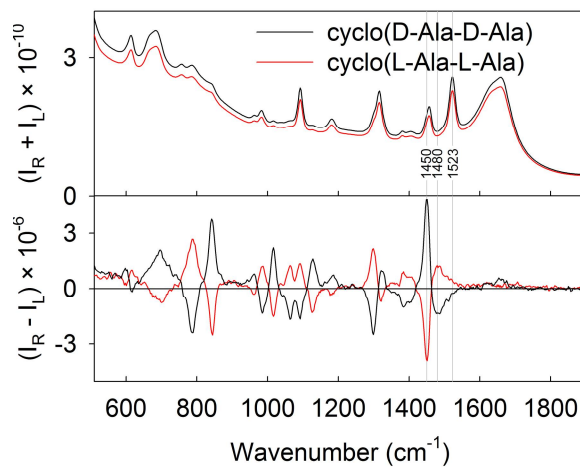
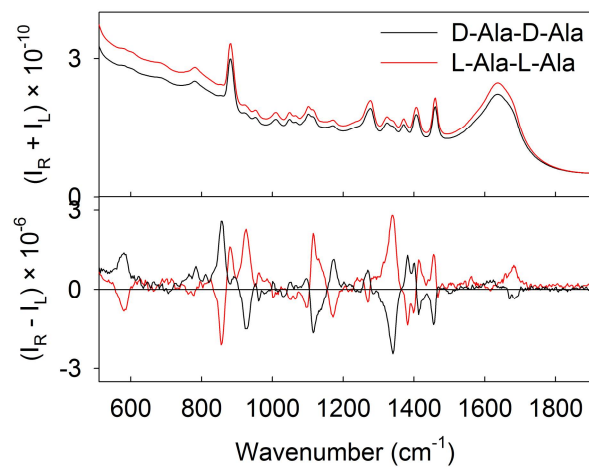
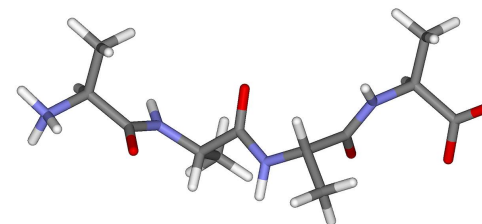
Ala-Ala



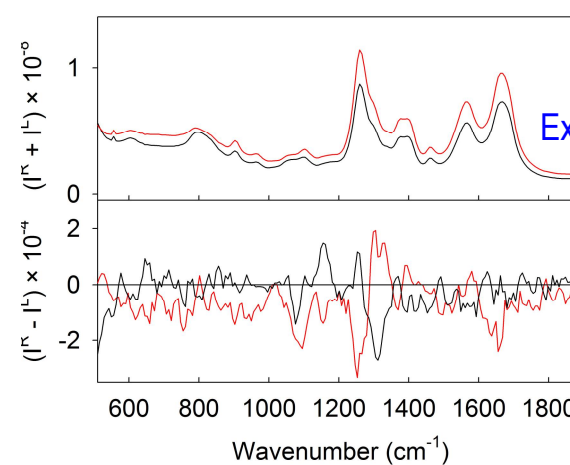
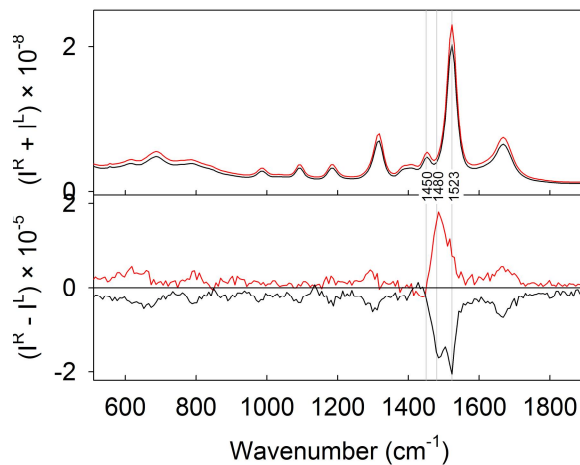
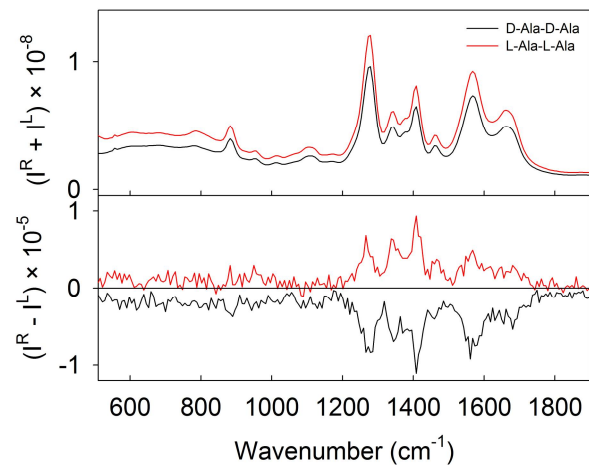
cyclo(Ala-Ala)



Ala-Ala-Ala-Ala

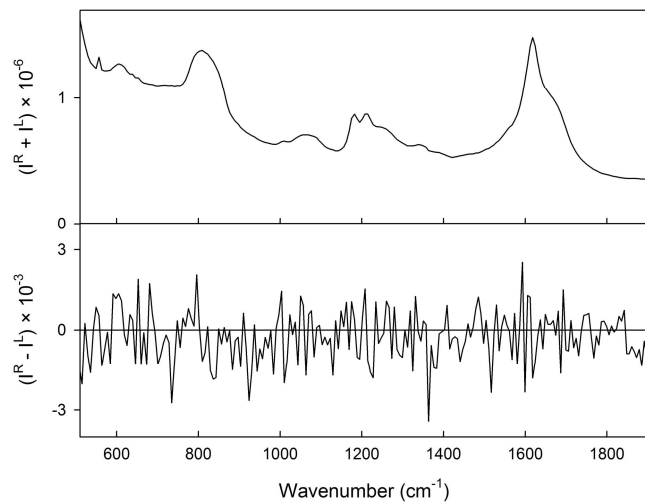


Exc. 532 nm

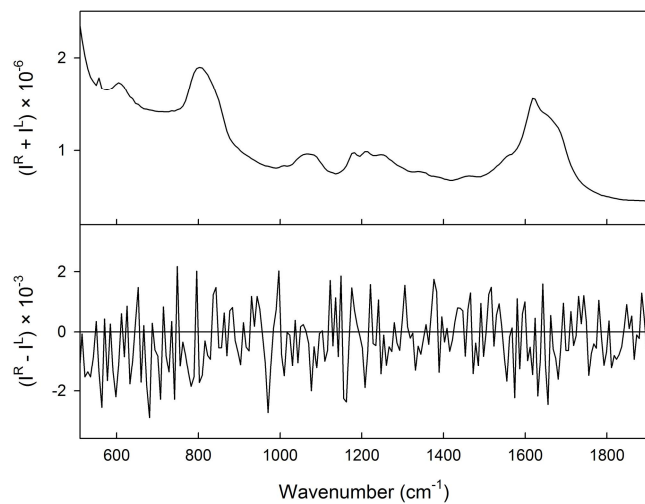


Exc. 244 nm

UV Raman/ROA spectra of proteins



Insulin
pH ~ 3
1.5 mg/mL

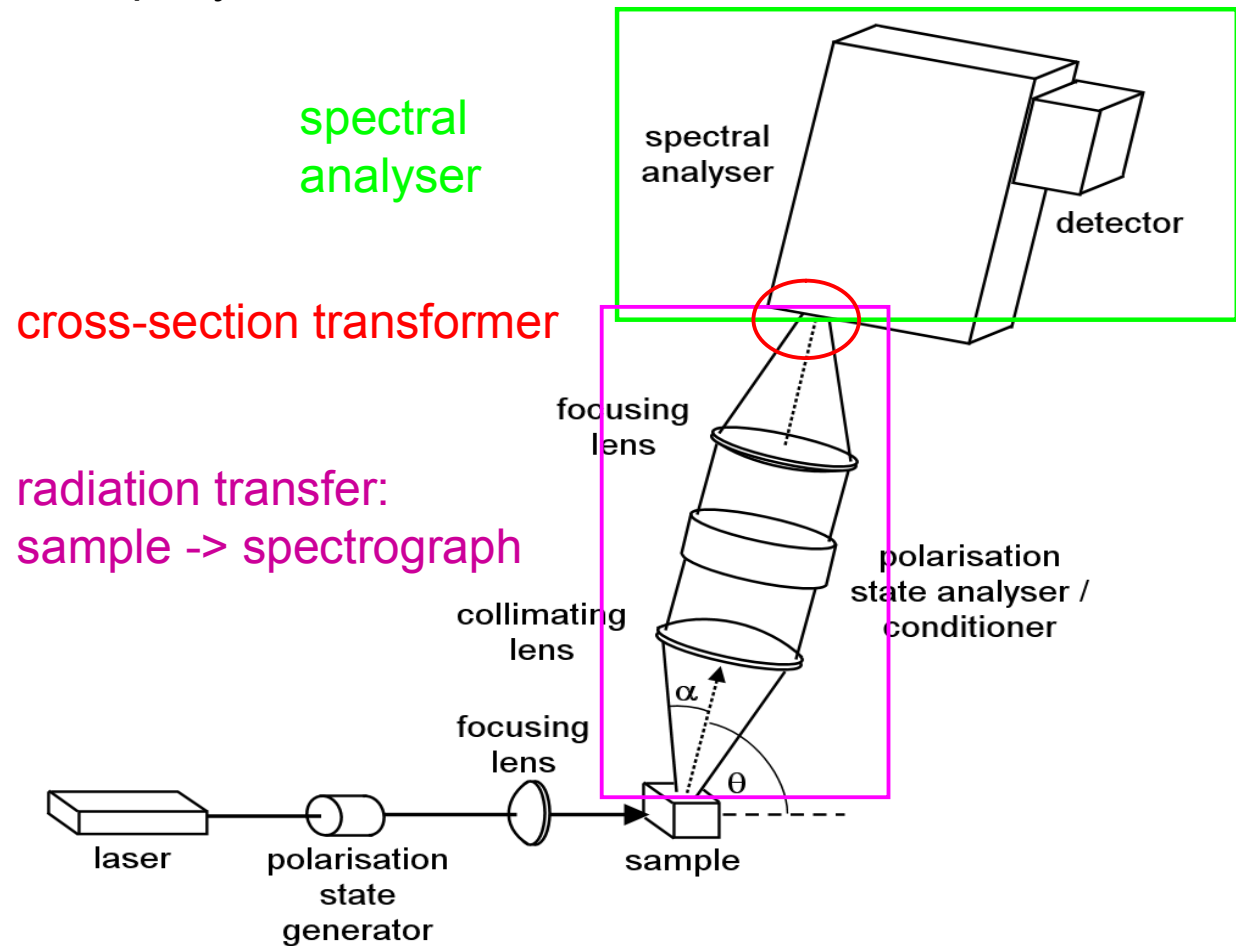


Human serum albumin
pH ~ 7
1.5 mg/mL

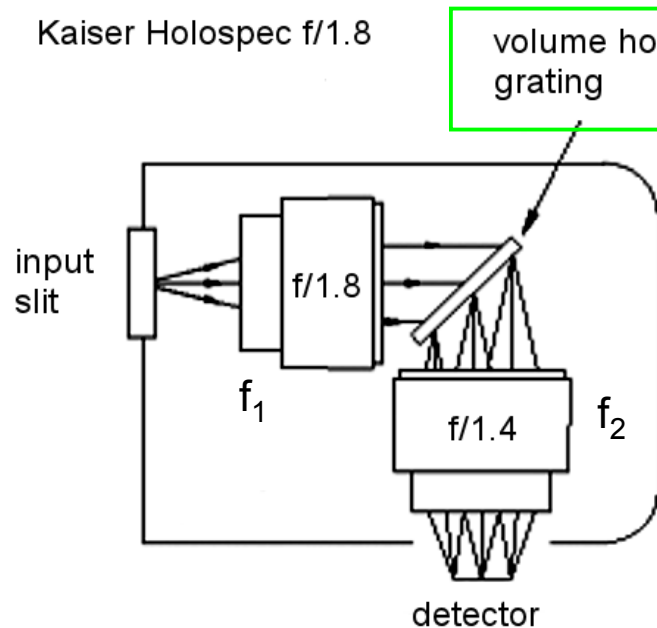
Further development of UV ROA spectrometer

Development of custom made lens-based spectrographs and transfer optics

Collaboration with Meopta company



Spectral analysers utilized in VIS/NIR Raman spectroscopy



$$d\nu = 7 \text{ cm}^{-1}$$

$$\alpha = \beta = 45^\circ$$

$$g = 2400 \text{ mm}^{-1}$$

$$m = 1$$

$$\lambda = 565 \text{ nm}$$

$$y_2 = 6,7 \text{ mm}$$

$$f_1 = f_2 = 85 \text{ mm}$$

$$(f/\#) = 1,8$$

$$G = 0,10 \text{ mm}^2 \cdot \text{sr}$$

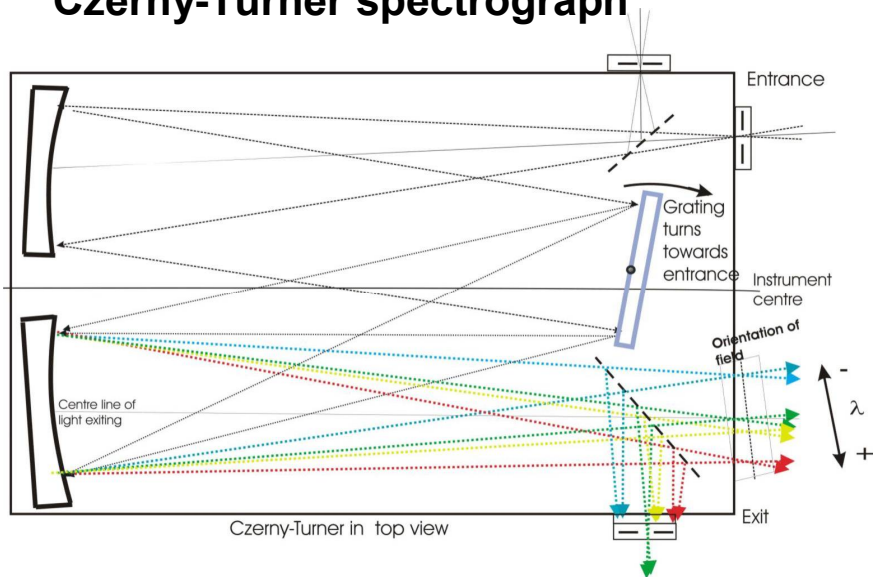
NIR (785 nm)



RoperScientific
Acton

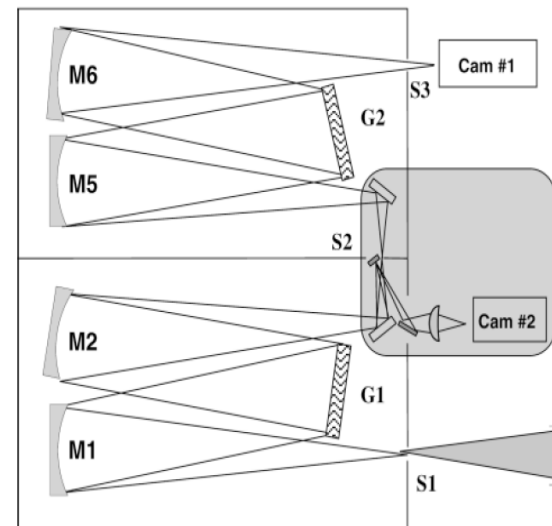
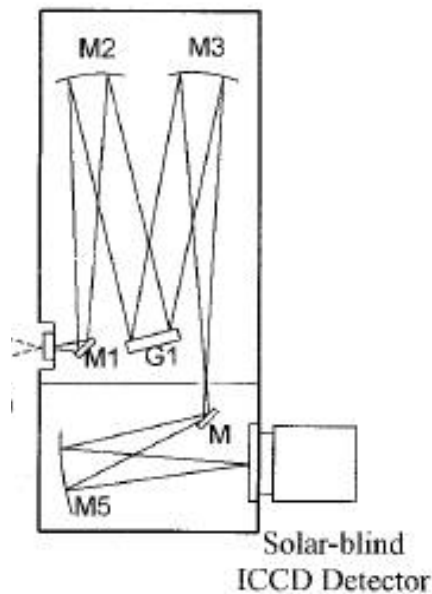
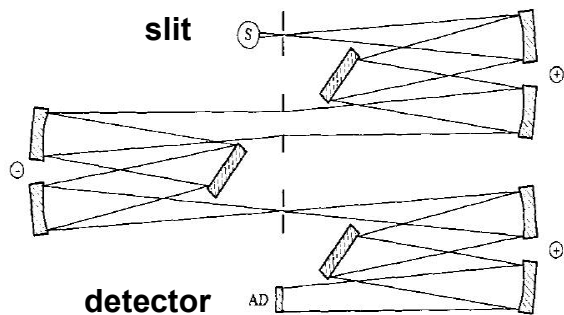
Spectral analysers utilized in UV Raman spectroscopy

Czerny-Turner spectrograph



Advantages:

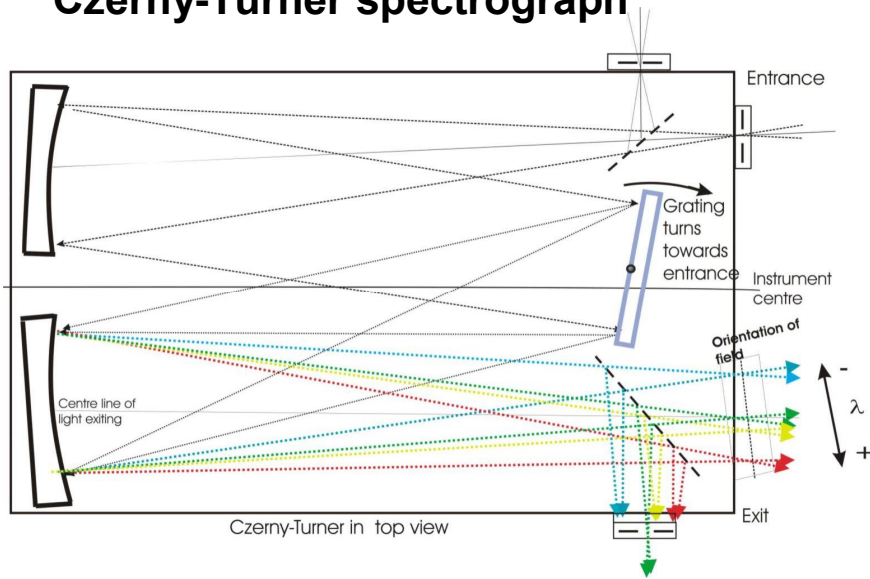
- large reflectivity of mirrors
 - achromatic
 - low level of stray light
- (double monochromator/triple spectrograph)



Bykov, Appl. Spectrosc.
2005, 59, 1541

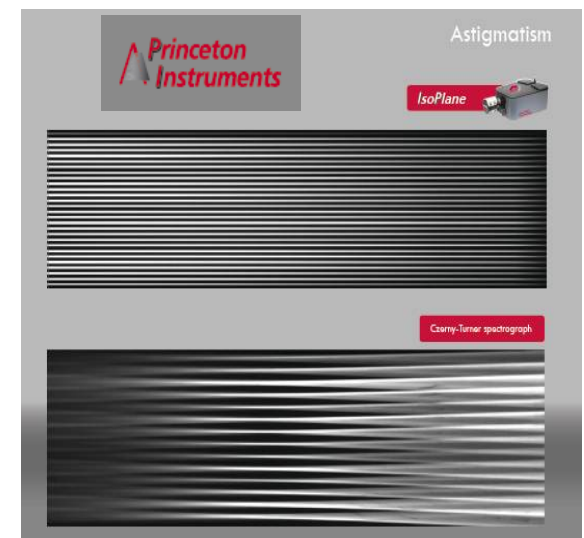
Spectral analysers utilized in **UV** Raman spectroscopy

Czerny-Turner spectrograph



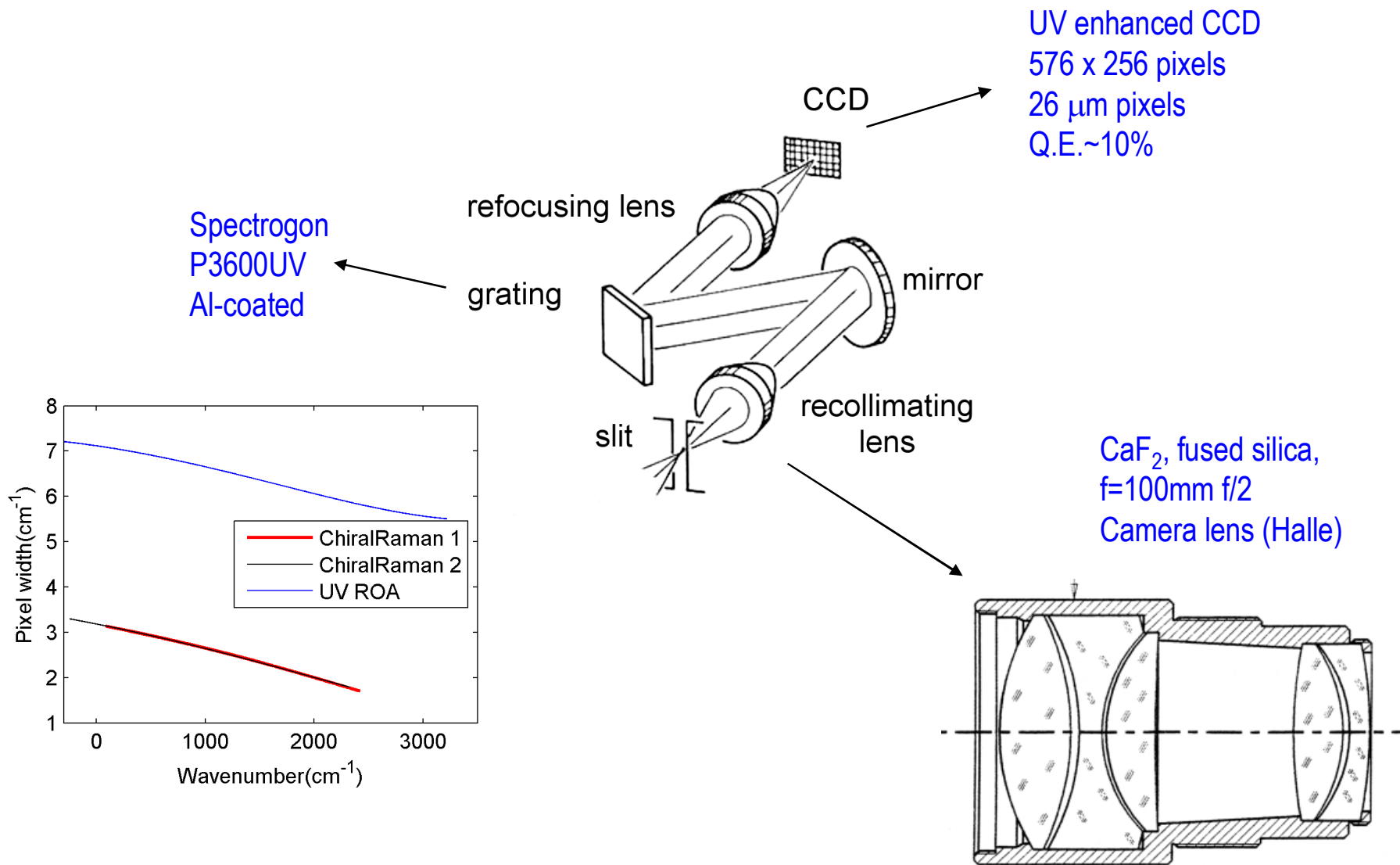
Limiting factors:

- low numerical aperture ($f/\# \sim 4$)
- coma & astigmatism (correction optics needed)



Lens based spectrograph (UV ROA spectroscopy)

Glasgow 2006

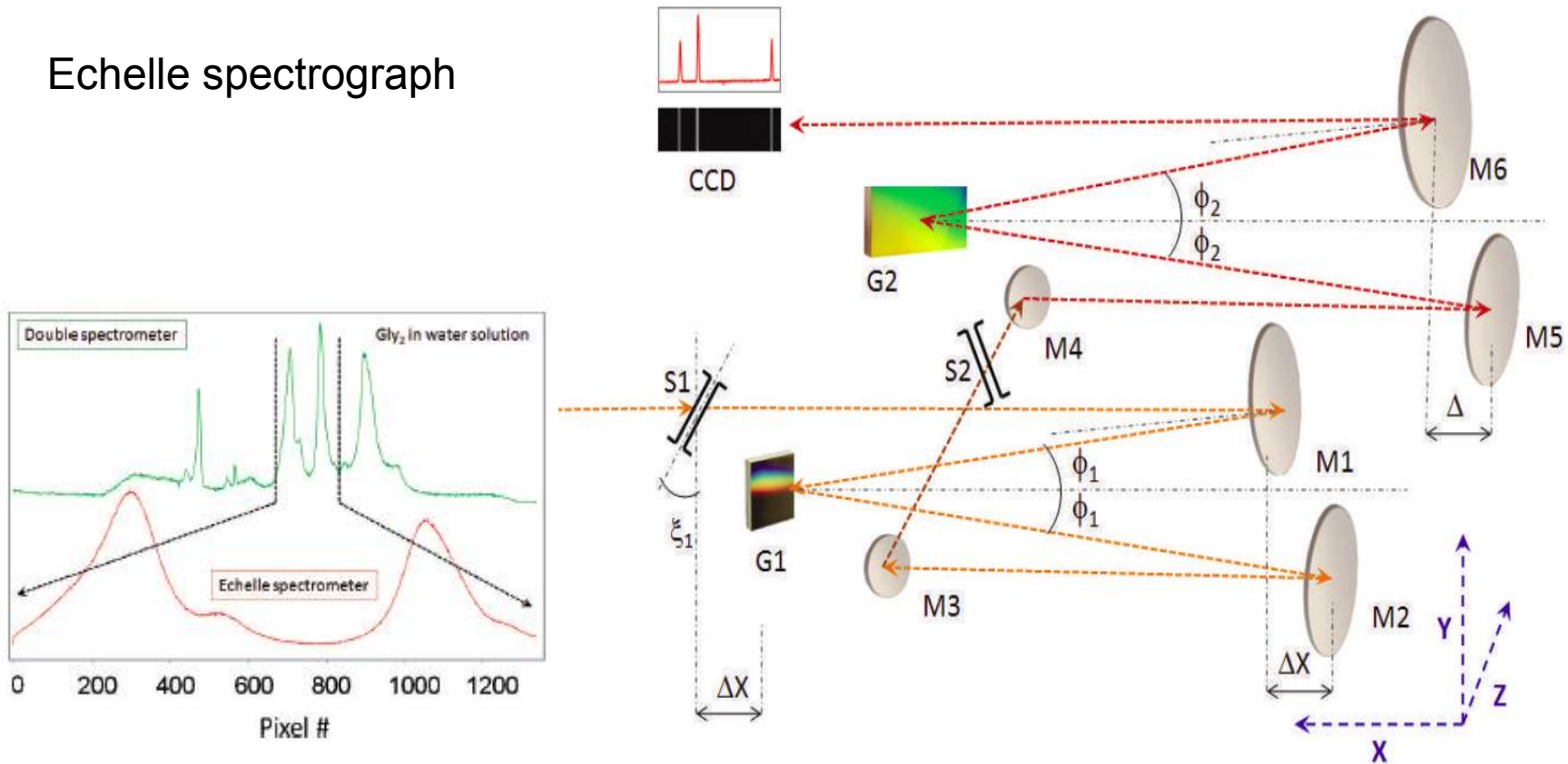


Hecht L et. al.: J. Raman Spectrosc. 2006, 37, 562

Kapitan J. et al.: J. Raman Spectrosc. 2015 46 392

State-of-the-art of spectrographs for the deep UV Raman spectroscopy

Echelle spectrograph



Development of new spectrograph for UV Raman spectroscopy

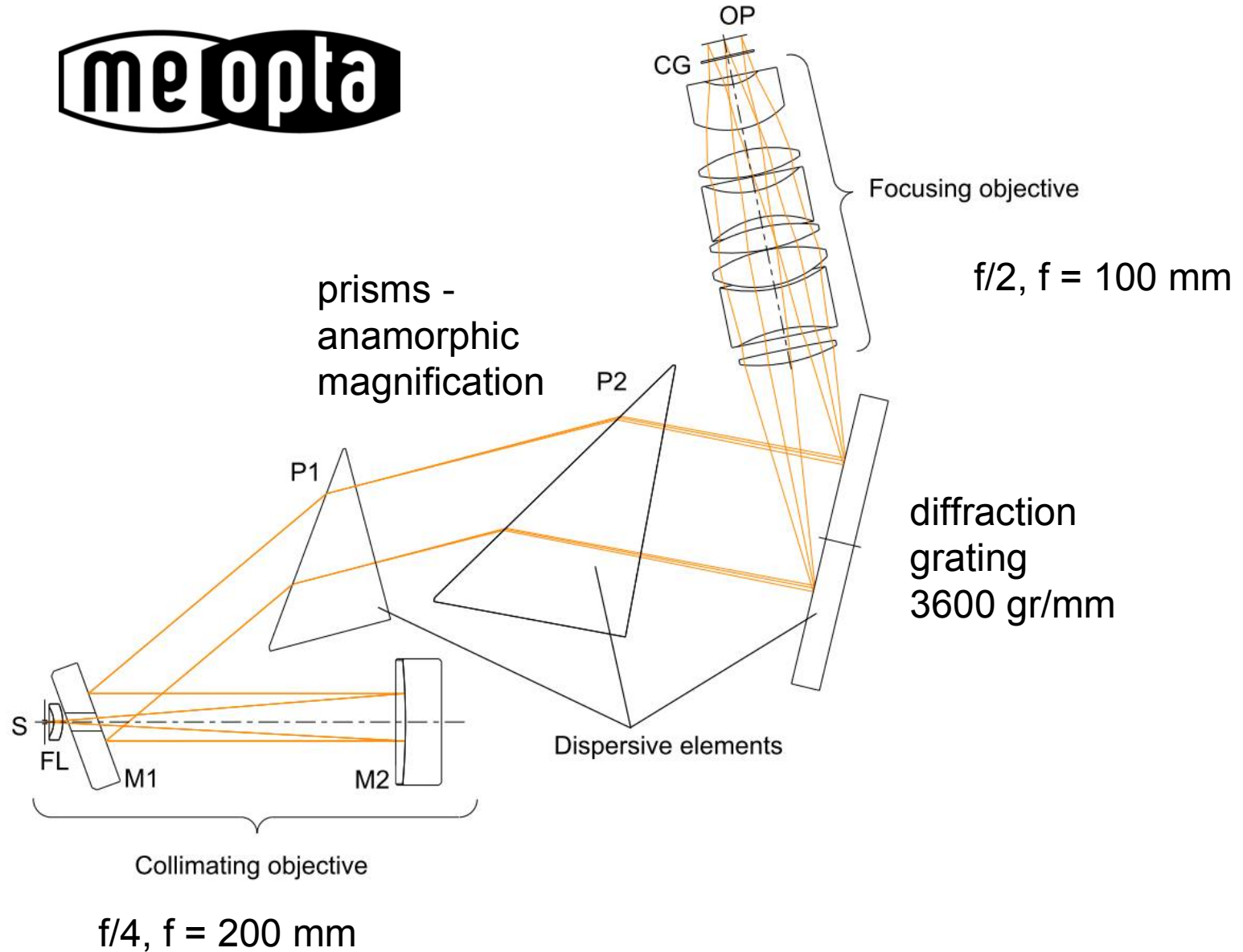
Spectrograph design requirements

Requirement	Value
Spectral resolution	7–15 cm ⁻¹
Spectral region	205–272 nm – see table below
Point spread function (PSF) for 1/e ² criterion	<27 μm (pixel size 13.5 μm)
F-number of focusing objective	2
Focal length of focusing objective	100 mm
Detector size	7 × 26 mm
Diffraction grating	3600 gr/mm, 1. diffraction order

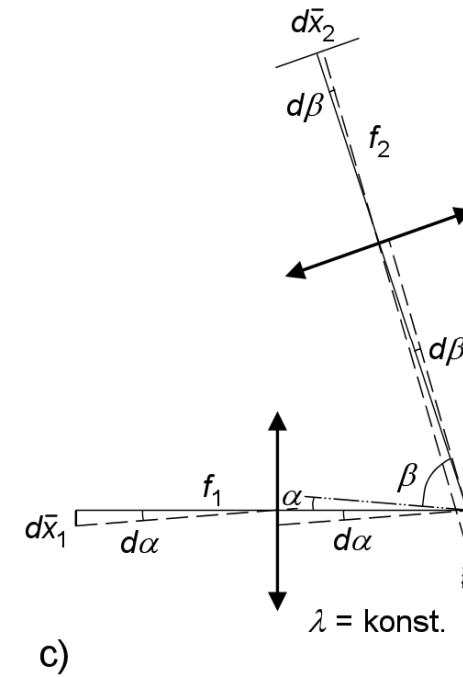
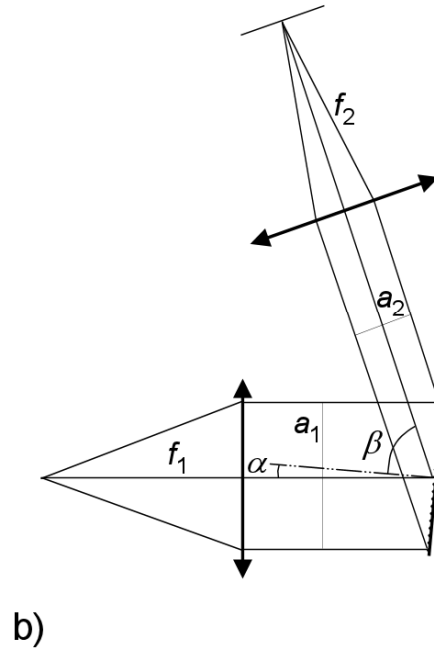
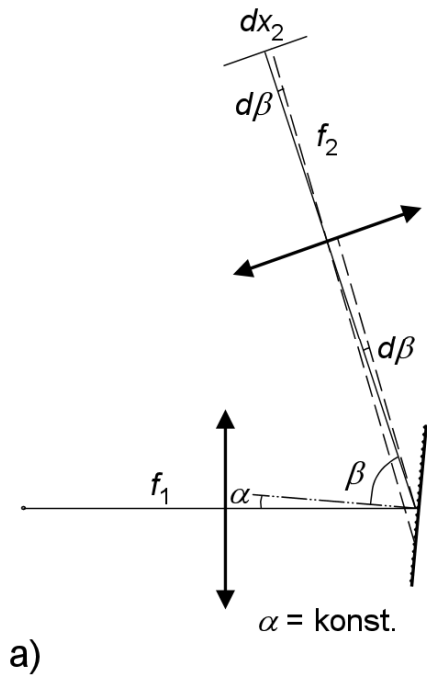
		1	2	3	4	5	6
Weight		0.5	1	1	1	0.5	0.25
Wavenumber shift (cm ⁻¹)		0	500	1150	1800	2400	3200
Wavelength λ (nm)	Conf. 1	250.0	253.2	257.4	261.8	266.0	271.7
	Conf. 2	240.0	242.9	246.8	250.8	254.7	260.0
	Conf. 3	230.0	232.7	236.2	239.9	243.4	248.3
	Conf. 4	218.0	220.4	223.6	226.9	230.0	234.3
	Conf. 5	205.0	207.1	209.9	212.9	215.6	219.4

Excitation wavelengths

Development of spectrograph for UV Raman/ROA spectroscopy



Imaging spectrograph



$$\sin \alpha + \sin \beta = mG\lambda$$

Reciprocal linear dispersion:

$$\frac{d\lambda}{dx_2} = \frac{\cos \beta}{mGf_2}$$

Anamorphic magnification:

$$\frac{a_2}{a_1} = \frac{\cos \beta}{\cos \alpha}$$

$$b_2 = b_1$$

Magnification of slit dimensions:

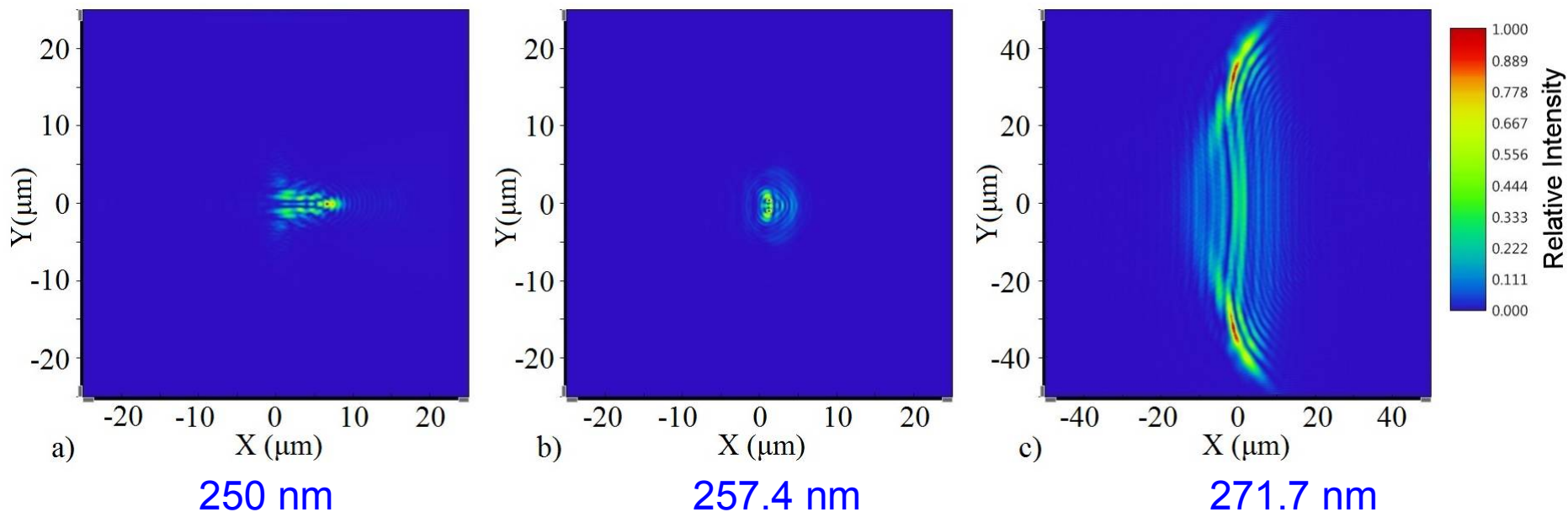
$$\frac{d\bar{x}_2}{dx_1} = -\frac{\cos \alpha}{\cos \beta} \frac{f_2}{f_1}$$

$$\frac{d\bar{y}_2}{dy_1} = -\frac{f_2}{f_1}$$

Development of spectrograph for UV Raman/ROA spectroscopy

Point spread function

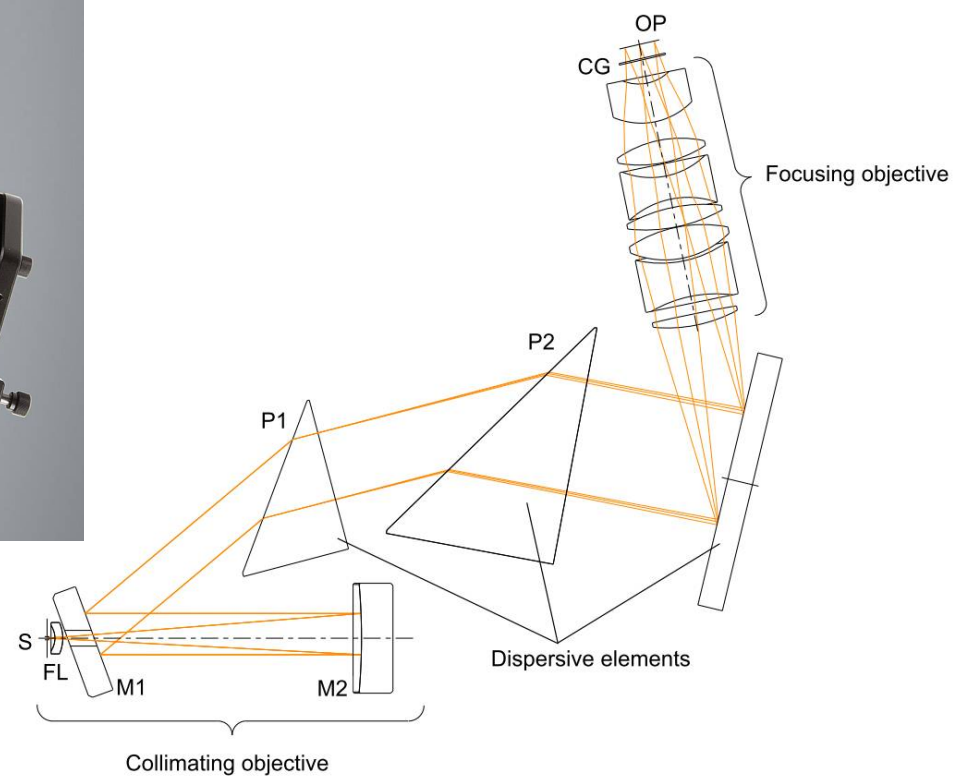
Configuration 1 (worst case)



Spectral resolution: according to geometrical parameters ($2 \times 13.5 \mu\text{m}$ pixels)

Configuration	Exc. wavelength (nm)	Incident angle on diffraction grating (deg)	Spectral resolution (cm^{-1})		
			500 cm^{-1}	1800 cm^{-1}	3200 cm^{-1}
1	250	-1.12	4.4	3.4	3.8
2	240	1.0	4.9	3.9	2.6
3	230	2.9	5.4	4.5	3.3
4	218	5.2	6.2	5.3	4.2
5	205	7.75	7.0	6.2	5.2

Development of spectrograph for UV Raman/ROA spectroscopy

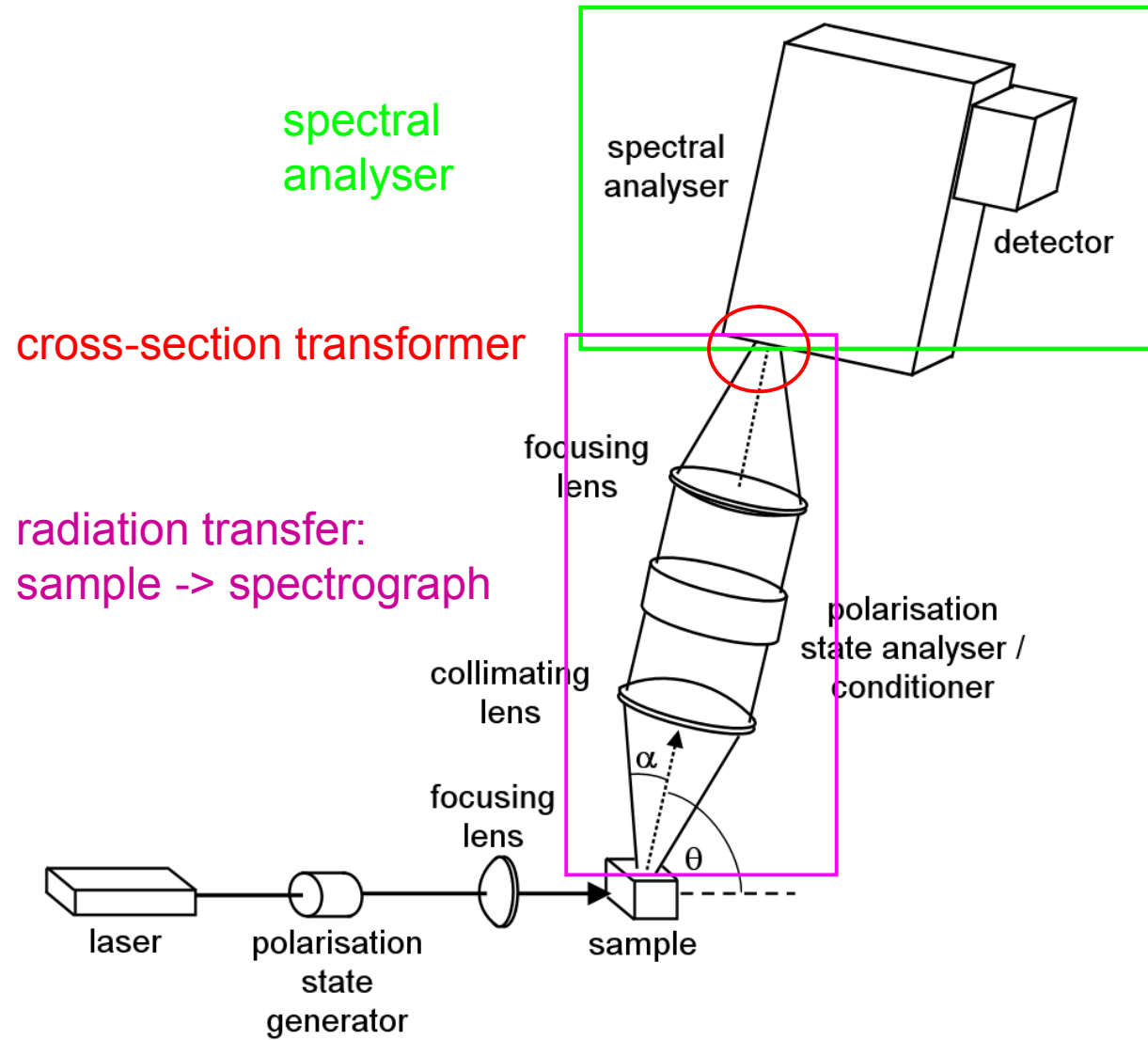


Comparison of “throughput” of the state-of-the-art spectrographs

$$\Phi = \frac{\pi}{4} B_{\lambda} d\lambda \tau \frac{S_{\text{det}}}{(f/\#)^2}$$

$$P = \tau \frac{S_{\text{det}}}{(f/\#)^2}$$

	Transmittance τ	Effective detector area S_{det} (mm ²)	F-number	Total (sr.mm ²)
Meopta UV spectrograph	0.15	6 × 20	2	4.5
triple grating spectrograph	0.05	1 × 26	6.5	0.03
Echelle spectrograph	0.2	6 × 26	6.5	0.73
Corrected Czerny-Turner	0.3	6 × 26	3.8	3.2



Acknowledgement

Laurence D. Barron, Lutz Hecht
Christian Johannessen

Petr Bouř
Jaroslav Šebestík, Ondřej Pačes, Jakub Jungwirth, Jiří Kessler

Vladimír Baumruk

Timothy A. Keiderling

Rina Dukor
Larry Nafie

Werner Hug

Radek Čelechovský
Michal Dudka
Milan Vůjtek

Meopta and Zebr company collaboration